

DETECTION OF URIC ACID IN INFESTED FOOD MATRICES

Thesis Submitted to the Bharathidasan University
for the Award of the Degree of

DOCTOR OF PHILOSOPHY IN BIOTECHNOLOGY

Submitted by

INDUJA C

(ID. No.: 201801DB002)

(Ref. No. 27784-7/Ph.D.K7/Biotechnology/Full time/January 2018 /Date 30.04.2018)

Under the Supervision of

Dr. M.LOGANATHAN,

PROFESSOR & HEAD,

**ACADEMICS AND HUMAN RESOURCE DEVELOPMENT,
NIFTEM-T, MOFPI, GOVERNMENT OF INDIA, THANJAVUR**



**NATIONAL INSTITUTE OF FOOD TECHNOLOGY, ENTREPRENEURSHIP AND
MANAGEMENT- THANJAVUR (NIFTEM-T)**

Formerly Indian Institute of Food Processing Technology (IIFPT)

MINISTRY OF FOOD PROCESSING INDUSTRIES (MOFPI)

GOVERNMENT OF INDIA

THANJAVUR– 613005, TAMIL NADU, INDIA

JUNE – 2022



**NATIONAL INSTITUTE OF FOOD TECHNOLOGY, ENTREPRENEURSHIP
AND MANAGEMENT-THANJAVUR (NIFTEM-T)**
(an Institute of National Importance; formerly Indian Institute of Food Processing Technology - IIFPT)
(Ministry of Food Processing Industries, Govt. of India)
Pudukkottai Road, Thanjavur – 613 005, Tamil Nadu

Dr. M. LOGANATHAN
Dean(i/c) Academics & SW

☎ 04362 – 228155; 09750968410
Email: academic@iifpt.edu.in

CERTIFICATE

This is to certify that the thesis entitled “**Detection of Uric acid in infested food matrices**” submitted in partial fulfilment of the requirements for the award of the degree of **Doctor of Philosophy in Biotechnology** to the Bharathidasan University, Tiruchirappalli is a record of bonafide research work carried out at **National Institute of Food Technology, Entrepreneurship and Management – Thanjavur** (formerly Indian Institute of Food Processing Technology, Thanjavur), Ministry of Food Processing Industries (MoFPI), Government of India by **Ms. Induja C** (ID. No.: 201801DB002; Ref.No.27784-7/Ph.D.K7/Biotechnology/Full time/January 2018 /Date 30.04.2018) under my supervision and guidance and that no part of the thesis has been submitted for the award of any other degree, diploma, fellowship or other similar titles or prizes. However, some part of the research work has been published in peer-reviewed/ reputed scientific journals (copies enclosed).

23/06/22

Dr. M. Loganathan
Research Supervisor

Place : Thanjavur
Date : 23.06.2022



Dean i/c (Academics & Student Welfare)
National Institute of Food Technology,
Entrepreneurship and Management - Thanjavur (NIFTEM-T)
(an Institute of National Importance, Formerly IIFPT)
Pudukkottai Road, Thanjavur - 613005

PLAGIARISM REPORT

Curiginal

Document Information

Analyzed document	C. Induja thesis for plagiarism.docx (D141060445)
Submitted	2022-06-23 10:43:00
Submitted by	Srinivasa ragavan S
Submitter email	bdulib@gmail.com
Similarity	0%
Analysis address	bdulib.bdu@analysis.arkund.com

Sources included in the report

Entire Document

Handwritten signature
23/6/22

Dr. M. Loganathan, M.Sc.(Ag.), Ph.D.
Dean i/c (Academics & Student Welfare)
National Institute of Food Technology,
Entrepreneurship and Management - Thanjavur (NIFTEM-T)
(an Institute of National importance, Formerly IIFPT)
Pudukkottai Road, Thanjavur - 613005

DECLARATION

I hereby declare that the work presented in this thesis entitled “**Detection of Uric acid in infested food matrices**” submitted by me for the award of the degree of **Doctor of Philosophy in Biotechnology** to the **Bharathidasan University, Tiruchirappalli** is a record of the research work I have carried out under the supervision of **Dr. M. Loganathan, Professor & Head, Academics and Human Resource Development, National Institute of Food Technology, Entrepreneurship and Management – Thanjavur (NIFTEM-T) (formerly IIFPT)**. I further declare that this thesis is based on the original work done by me and has not been previously submitted to any other Institution/ University for any degree/diploma by me or any other person. Research materials obtained from other sources have been duly acknowledged in this thesis.

Place : Thanjavur

Date : 23.06.2022



(Induja C)

ACKNOWLEDGEMENT

Gratitude cannot be put in words alone as it has to be felt than shown off. But it is a mysterious thing for me to express my gratitude to the peoples who helped me to complete my PhD work and thesis. First of all, I like to thank God for providing me an opportunity to do PhD and a constant support to finish my research work. I like to express gratitude toward **Bharathidasan University** and **NIFTEM-T** for providing facilities to do my PhD work. I extend my sincere gratitude toward my research supervisor **Dr. M. Loganathan** for continuous support and guidance to finish my research work.

I extend my gratitude to my doctoral committee members, **Dr. S. Shanmugasundaram** and **Dr. C. Anandharamakrishnan** for providing me some ideas and support in my research work. I like to thank the faculties of Department of Academics and Human resource development, **Dr. S. Vignesh, Dr. V. Eyarkai Nambi, Dr. N. Baskaran, Dr. M.R. Bivin, Dr. C. Sukumari** and **Mrs. M. Malathy**. I extend my gratitude to technical and non-technical staffs of A&HRD, **Mrs. R. Durgalakshmi, Mr. U Akash, Smt. V. Uma, Mr. P. Muniyandi, Dr. R. Karthikeyan, Mr. M. Arun kumar, Mr. Anbu kumar** for their support.

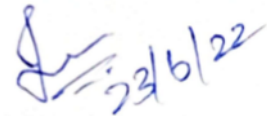
I like to thank **Dr. Seralathan Raju** for performing 16S and ITS sequencing for bacteria and fungi. The PCR was performed for the presence of ABC genes in insect DNA. I extend my gratitude to **Mrs. Shiny Joseph** for performing HPLC analysis to determine the presence of UA in food samples. I like to thank to **Central instrumentation laboratory** at **NIFTEM-T** for analyzing essential oils using GC-MS.

I like to thank my labmates and colleagues **Mr. Barun, Mrs. Lakshmi Praba, Mr. Abhinav Tiwari, Ms. Monisha, Mr. Santhosh, Ms. Karuna** and **Ms. Vidyalakshmi** for helping me in my research work. I like to thank my friends, **Mr. Arun, Ms. Priya, Mr. Anbu, Mr. Hari, Ms. Lakshmi praba, Mrs. Priya, Mrs. Karthika, Mr. Srinivas, Ms. Meena, Mr. Akash, Mr. Mani, Mr. Velan, Ms. Agnes, Ms Vidhya, Mr. Naveen, Ms. Sangeetha** for their motivation.

At the same time, I like to thank my parents, **Mr. I. Chandrasekar** and **Mrs. C. Theivathirumagal** and my two elder brother, **Mr. C. Mohanraj** and **Mr. C. Yuvaraj** for all your patience and support throughout my PhD journey.

Place : Thanjavur

Date : 23.06.2022

A handwritten signature in blue ink, appearing to be 'Induja C', with the date '23/6/22' written below it.

(Induja C)

ABSTRACT

The insect infestation is a major problem during the storage of grains and grain based products. During storage, the grains lead to contamination like uric acid (UA), quinone and presence of insect fragment shows that the product was infested. The major problem during storage of grains and cereals occurs due to the UA contamination. The detection of UA can be measured using some methods such as colorimetric, fluorometric, enzyme based method, HPLC, paper chromatography and enzyme based biosensor was used. The enzyme based methods and HPLC was highly equipped, costly method and takes too much of time for a sample. To overcome this problem, we have developed a simple, rapid method to detect the UA in food samples using UV-Visible spectroscopic and paper based strip.

The preceding method and rapid method were performed using the UV-Visible spectrophotometer. The preceding method shows the R^2 of 0.991 whereas the rapid method showed R^2 of 0.994. The standard error of preceding method (0.000572) and rapid method (0.024806) which shows that the SE was less than 2%.

The CART® regression model was evaluated using the MiniTab software. In preceding method, the absorbance increases with the concentration of UA that shows the optimal R^2 of 0.8803 at 5 terminal node whereas in rapid method the optimal R^2 value of 0.9363 was observed at terminal node 5. The cluster analysis of preceding method shows 40% of similarity level whereas in rapid method showed 50 per cent of similarity.

The paper strip was developed using Whatman filter paper No 40 with width of 20mm and height of 60mm. The extracted filtrate was treated with potassium ferricyanide and after the addition of ferric chloride, blue colour formation was observed. The colour formation was captured using the image processing camera and the images was analyzed using MATLAB software. The linear regression model was performed by XLSTAT software. The R^2 obtained for the paper strip

was 0.993. The CART® regression model shows the colour intensity decreases with increase in concentration of UA with the optimal R^2 of 0.9615 at terminal node 11.

The feed Forward Neural Network (FNN) model was performed to validate the paper strip method using the standard UA and also in control and infested food samples. For standard UA, BFGS Quasi-Newton (BFG- FNN) showed more accuracy with R^2 of 0.9833 than other models.

A DNA based biosensor was developed to determine the UA with the presence of ABC genes that reduces the ATP to ADP and Pi. The developed biosensor was optimized with the DNA immobilization and DNA hybridization. The biosensor showed good response within 1 hour of DNA immobilization. The DNA hybridization was performed upto 40 mins where the biosensor response was better at 40 mins. The linearity, LOD, operational stability, regeneration and reproducibility was performed. The DNA based biosensor showed good linearity with R^2 of 0.9952 and LOD was 97 ppm.

The determination of UA was performed for the real time samples using DNA based biosensor and HPLC method. The RSD value ranges from 6.9 - 9.09% and the recovery ranged from 92-113 per cent.

The UA level in food samples decreases due to the microorganisms that will enhance the activity of uricase and urease enzyme. The bacterial and fungal strains was isolated and identified as *Bacillus amyloliquefaciens* (TM1), *Aspergillus flavus* (FS1), *Candida parapsilosis* (FS2) and *Trichosporon asahii* (FS3) using 16 S and ITS sequencing. The essential oils (EOs) (31) were extracted from various plant sources and the antimicrobial activity was performed against the bacterial and fungal strains. The EOs of thyme, cinnamon, cumin seed, ginger and star anise showed good antimicrobial activity against the bacteria and fungi. The bioactive compounds present in Eos was performed using GC-MS. The chemical compounds present in ginger Eos was cis-alpha-Bergamotene, cedrene and alpha-Farnesene shows the antimicrobial activity against *A. flavus* and *T. asahii*. The anethole in star anise EOs shows antimicrobial activity against *T. asahii*.

The bioactive compounds present in cumin seed EOs such as Cuminal, γ -Terpinene and 1, 4- p – menthadien-7-al showed good antimicrobial activity for *B. amyloliquefaciens*. The major compounds in cinnamon EOs was Cinnamaldehyde, (Z) – 3 – Phenylacrylaldehyde shows the antimicrobial activity against *A. flavus*, *C. parapsilosis* and *B. amyloliquefaciens*. The volatile compounds present in thyme EOs was thymol and phenol 2-methyl-5-(1-methylethyl) - shows antimicrobial activity against the *B. amyloliquefaciens*, *A. flavus* and *C. parapsilosis*.

TABLE OF CONTENT

Chapter no.	Content	Page no.
1	INTRODUCTION	1-14
1.1	Factors and losses affecting stored food products	1
1.2	Method to detect insect infestation	4
1.2.1	Physical methods	4
1.2.1.1	Visual inspection	
1.2.1.2	CO ₂ measurement	
1.2.1.3	Acoustical method	
1.2.1.4	Near- infrared reflectance spectroscopy	
1.2.1.5	X-ray imaging	
1.2.1.6	Electrical conductance	
1.2.2	Chemical methods	8
1.2.2.1	Detection techniques of odor released by insects	
1.2.2.2	Staining techniques	
1.2.2.3	Molecular detection method	
1.3	Contamination in food due to insect infestation	9
1.4	Mechanism of uric acid degradation	12
1.5	Objectives	13
2	REVIEW OF LITERATURE	15-20

2.1	Insect infestation	15
2.2	Detection of insect infestation in foods	16
2.2.1	Colorimetric method	
2.2.2	Level of insect infestation	
2.2.3	Chromatographic techniques	
2.2.4	Odor detection techniques	
2.2.5	Biosensors	
3	MATERIALS AND METHODS	21-41
3.1	To determine the UA levels in samples during storage with rapid method using UV-visible spectroscopy	21-25
3.1.1	Insect culture	21
3.1.2	Infestation of food matrices	21
3.1.3	Extraction of UA	21
3.1.4	Determination of UA with colorimetric method (Preceding method)	22
3.1.4.1	Formation of chromophore based on reaction mechanism in preceding method	22
3.1.5	Rapid spectrophotometric method to determine the UA	23
3.1.5.1	Developing a simple rapid spectrophotometric method to determine UA	23
3.1.5.2	Formation of prussian blue colour based on reaction mechanism (Rapid method)	23

3.1.6	Statistical analysis	24-25
3.1.6.1	Linear regression model	24
3.1.6.2	CART® model	25
3.1.6.3	Cluster analysis	25
3.2	To develop paper based strip to detect UA levels in infested food samples	26-29
3.2.1	Development of paper-based strip to detect UA	26
3.2.2	Evaluation of paper strip method	26
3.2.3	Determination of UA using MATLAB coding	27
3.2.4	Statistical analysis	27
3.2.4.1	Linear regression model	27
3.2.4.2	CART® model	28
3.2.4.3	Cluster analysis	29
3.3	Validation of paper-based strip to detect UA levels in samples	30-31
3.3.1	Neural network	30
3.3.2	Recovery study	31
3.4	FTIR	31
3.5	Development of DNA based biosensor	31-34
3.5.1	Isolation of DNA from T. confusum insect	31
3.5.2	Presence of ABC genes in isolated DNA using PCR	32

	(Polymerase chain reaction)	
3.5.3	Preparation of chitosan mediated silver nanoparticle	32
3.5.4	Development of modified screen printed electrode (SPE)	33
3.5.5	Optimization and performance evaluation of DNA based biosensor	33
3.5.6	Characterization of DNA based biosensor	33-34
3.5.6.1	FTIR	33
3.5.6.2	Scanned electron microscope (SEM)	34
3.5.7	Validation of DNA based biosensor	34
3.6	Isolation and identification of microorganisms from contaminated food samples and its preventive measures	35-39
3.6.1	Isolation of UA degrading microorganisms in infested food samples	35
3.6.2	Identification of microorganisms using molecular techniques	35
3.6.3	Extraction of essential oils (EOs) using hydrodistillation method	36
3.6.4	Antioxidant assay (DPPH radical scavenging assay)	38
3.6.5	Total phenolic content (TPC)	38
3.6.6	Antimicrobial activity	39
3.6.7	GAS chromatography – Mass spectrometry (GC-MS)	39
4	RESULTS AND DISCUSSIONS	40-108

4.1	Validation of UV-visible spectroscopic method to determine UA	40-50
4.1.1	Influence of storage period on UA content in wheat products	40
4.1.2	Comparison of linear regression for preceding and rapid method	41
4.1.3	CART® regression model using Minitab for preceding and rapid method	43
4.1.4	Cluster analysis	48
4.2	To develop paper based strip to detect UA levels in infested food samples	50-56
4.2.1	Color profiling	50
4.2.2	Linear regression model using XLSTAT	51
4.2.3	CART® regression model of paper strip	54
4.3	Validation of paper based strip to detect UA levels in wheat products	57-74
4.3.1	Neural network for standard UA	57
4.3.2	Neural network model for real time samples	60
4.3.3	Recovery study	73
4.4	FTIR	75
4.5	Detection of UA in food samples using DNA based biosensor	76-88
4.5.1	Development of modified SPE	76

4.5.2	Optimization and performance evaluation of DNA based biosensor	78
4.5.2.1	Optimization of DNA based biosensor	78
4.5.2.1.1	Effect of DNA immobilization	78
4.5.2.1.2	Effect of DNA hybridization	79
4.5.2.2	Performance evaluation of DNA based biosensor	80
4.5.2.2.1	Linearity	80
4.5.2.2.2	LOD	81
4.5.2.2.3	Operational stability	81
4.5.2.2.4	Regeneration	82
4.5.2.2.5	Reproducibility	83
4.5.3	Characterization of DNA based biosensor	84
4.5.3.1	FTIR	84
4.5.3.2	SEM analysis	85
4.5.4	Validation of DNA based biosensor using real time samples	86
4.6	Isolation and identification of microorganisms from contaminated food samples and its preventive measures	88-108
4.6.1	Isolation of microorganisms in infested food samples	88
4.6.2	Identification of microorganisms using molecular techniques	91
4.6.3	Extraction of EOs using hydrodistillation method (Clevenger apparatus)	93

4.6.4	Antioxidant assay	94
4.6.5	Total phenolic content (TPC)	95
4.6.7	Antimicrobial activity	97
4.6.8	GC-MS analysis	101
5	Summary and conclusion	109
	References	113
	Annexure	130
	List of publications	134
	Proof for research articles published in journals approved by UGC	135

LIST OF TABLES

S.No	Title	Page No
1	The primers of Abcg2 and Oat genes	32
2	Universal primers used for sequencing of bacteria and fungi	36
3	The plant parts selected for essential oil extraction	37
4	Influence of storage period on uric acid content in wheat products using rapid method	41
5	Validation of preceding and rapid method	43
6	Validation of model parameters that shows Goodness of fit for colour intensity against concentration (ppm)	48
7	Validation of model parameters that shows Goodness of fit for colour intensity against concentration (ppm)	53
8	Validation of paper strip using CART predictive analytics	54
9	Recovery study of known UA added in wheat flour, maida and rava samples	74
10	The correlation of DNA based biosensor and HPLC method to detect UA	87
11	Morphological and biochemical tests for bacterial strain identification	90
12	Yield percentage of essential oils obtained from selected plants	94
13	Antimicrobial activity of TM1 strain (<i>Bacillus amyloliquefaciens</i>)	98
14	Antimicrobial activity of <i>Aspergillus flavus</i> (FS1)	99

15	Antimicrobial activity of <i>Candida parapsilosis</i> (FS2)	100
16	Antimicrobial activity of <i>Trichosporon asahii</i> (FS3)	100
17	Phytochemical compounds present in ginger essential oil	102
18	Phytochemical compounds present in star anise essential oil	104
19	Bioactive compounds in Cumin seed EO	104
20	Phytochemical compounds in Cinnamon EO	106
21	Bioactive compounds in thyme EO	107

LIST OF FIGURES

S.No	Title	Page. No
1	Factors affecting stored food grains	2
2	Losses due to insect infestation in food grains	3
3	Types of food grain storage structures	4
4	Different methods to detect insect infestation in food grains	7
5	Degradation of uric acid to ammonia by purine breakdown pathway	13
6	The oxidation reaction of uric acid to allantoin	23
7	The mechanism of Prussian blue colour formation	24
8	Schematic diagram of paper based strip	26
9	Flowchart of extraction of uric acid and Prussian blue colour formation	27
10	Schematic diagram of neural network	30
11	Insect DNA isolation by Spin column method	31
12	Schematic diagram of DNA based biosensor	33
13	Extraction of essential oils using Hydrodistillation method (Clevenger apparatus)	38
14	Calibration curve of the preceding method	42
15	Calibration curve of the rapid method	42
16	Regression tree diagram of UA (preceding method) of CART regression model	45

17	Regression tree diagram of UA (rapid method) of CART regression model	46
18	R ² versus terminal node plot A) preceding method and B) Rapid method	47
19	Scatterplot of response fit Vs actual values A) preceding method and B) Rapid method	47
20	Dendrogram of preceding (A) and rapid method (B) to determine UA	49
21	Color chart of different concentration of standard uric acid	51
22	Regression plot of colour intensity by concentration (ppm)	52
23	Regression tree diagram of UA (paper strip) of CART regression model	55
24	R ² versus terminal node plot of paper strip	55
25	Scatterplot between the real value of the colour intensity and the predicted values of the colour intensity observed in paper-strip for the training data set and the test data	56
26	Performance plot of standard uric acid using BFG-FNN algorithm	57
27	Regression plot of standard uric acid using BFG-FNN algorithm	58
28	Training state of standard uric acid using BFG-FNN algorithm	59
29	Regression plot of uninfested maida sample using LM-FNN algorithm	61
30	Performance plot of uninfested maida sample using LM-FNN algorithm	62
31	Training state of uninfested maida sample using LM-FNN algorithm	62

32	Regression plot of infested maida sample using LM-FNN algorithm	63
33	Performance plot of infested maida sample using LM-FNN algorithm	64
34	Training state of infested maida sample using LM-FNN algorithm	64
35	Performance plot of uninfested rava using LM-FNN algorithm	65
36	Regression plot of uninfested rava using LM-FNN algorithm	66
37	Training state of uninfested rava using LM-FNN algorithm	66
38	Regression plot of infested rava sample using LM-FNN algorithm	67
39	Performance plot of infested rava sample using LM-FNN algorithm	68
40	Training state of infested rava sample using LM-FNN algorithm	68
41	Regression plot of uninfested wheat flour sample using BFG-FNN algorithm	69
42	Performance plot of uninfested wheat flour using BFG-FNN algorithm	70
43	Training state of uninfested wheat flour sample using BFG-FNN algorithm	70
44	Regression plot of infested wheat flour sample using RP-FNN algorithm	71
45	Performance plot of infested wheat flour sample using RP-FNN algorithm	72
46	Training state of infested wheat flour sample using RP-FNN algorithm	72
47	FTIR spectra of standard UA	75

48	FTIR spectra of spiked wheat flour sample	76
49	Cyclic voltammogram of bare and immobilized electrode	77
50	Cyclic voltammogram of different concentration of UA	77
51	Linear relationship of peak current and scan rate	78
52	Effect of DNA immobilization	79
53	Effect of DNA hybridization	79
54	Calibration curve of standard UA that shows the linearity of DNA based biosensor	80
55	Operational stability of DNA based biosensor	82
56	Regeneration cycle of DNA based biosensor	83
57	Reproducibility of DNA based biosensor	84
58	FTIR analysis of DNA based biosensor, bare electrode (dark blue), AgNPs coated electrode (orange), DNA immobilized electrode (red) and substrate immobilized electrode (light blue)	85
59	SEM analysis of SPE, bare (A), AgNPs (B), DNA (C) and UA immobilized electrode (D)	86
60	The correlation of DNA based biosensor with HPLC method	87
61	Pure isolates of bacteria (TM1) (a) and fungal strains (FS1, FS2 and FS3) (b)	88
62	Observation of uric acid crystals	88
63	Gram staining of bacterial strain (TM1)	89
64	Lacto phenol cotton blue staining for fungal strain (FS1, FS2 and FS3)	89
65	Phylogenetic tree of bacterial and fungal strains	91

66	Calibration curve of ascorbic acid	95
67	Antioxidant content of essential oils	95
68	Standard curve of Gallic acid	96
69	TPA content of essential oils	97
70	Chromatogram of essential oil extracted from ginger	102
71	Chromatogram of star anise essential oil	103
72	Chromatogram of Cumin seed EO	104
73	Chromatogram of Cinnamon EO	105
74	Chromatogram of thyme EO	107

SYMBOLS AND ABBREVIATIONS

Units	Symbols
%	Percentage
Hrs	Hours
Nm	Nanometer
nM	Nanomolar
μ M	Micromolar
G	Gram
°C	Degree Celsius
Mg	Milligram
μ g	Microgram
Ppm	Parts per million
Min	Minute
mL	Milliliter
Rpm	Revolution per minute
M	Molar
Mm	Millimeter
mM	Millimolar
Bp	Basepairs
m/z	Mass to charge ratio

V/s	Volt per second
eV	Energy of electrons
CFU/ml	Colony forming unit per milliliter

Abbreviations

NIR	Near-Infrared reflectance spectroscopy
CO ₂	Carbon oxide
GC-MS	Gas chromatography-Mass spectroscopy
SPME	Solid phase micro extraction
DHS	Dynamic headspace sampling
e-nose	Electrical nose
UV	Ultraviolet
DNA	Deoxyribonucleic acid
RT-PCR	Real time-Polymerase chain reaction
q-PCR	Quantitative-Polymerase chain reaction
ZnO	Zinc oxide
LOD	Limit of detection
TLC	Thin layer chromatography
HPLC	High performance liquid chromatography
FLD	Fluorescence detector
DAD	Diode array detector
MS	Mass spectrometer
UPLC	Ultra performance liquid chromatography
ELISA	Enzyme linked immunoassay
UA	Uric acid
NaOH	Sodium hydroxide
HCl	Hydrochloric acid

ISPT	Isoproterenol
Ph	Potential of hydrogen
Pt	Platinum
AuNPs-GO	Gold nanoparticle mediated graphene conjugates
DW	Durbin-Watson
SE	Standard error
CART	Classification and regression tree
MSE	Mean square error
RMSE	Root mean square error
AIC	Akaike's information criterion
MAPE	Mean absolute percentage error
C _p	Mallow's C _p criterion
SBC	Schwarz's Bayesian criterion
APC	Amemiya's prediction criterion
FNN	Feed forward neural network
LM	Levenberg-marquardt
RP	Resilent backpropagation
BFG	BFGS quasi-newton
SCG	Scaled conjugate gradient
FTIR	Fourier transform infrared spectroscopy
ATR	Attenuated total reflection
Ag	Silver

SPE	Screen printed electrode
SEM	Scanned electron microscopy
ITS	Internal transcribed spacer
EDTA	Ethylenediaminetetraacetic acid
dNTPs	Deoxynucleoside triphosphate
ddNTPs	Dideoxynucleotide triphosphate
Na ₂ SO ₄	Sodium sulphate
Eos	Essential oils
DPPH	2, 2-diphenyl 1-picrylhydrazyl
NA-UA	Nutrient agar- Uric acid
RBA-UA	Rose Bengal agar- Uric acid
MAD	Mean absolute deviation
RSD	Relative standard deviation
RSM	Response surface methodology
TPC	Total phenolic compound
TPC	Total phenolic content
TMB	Tetramethylbenzidine
H ₂ O ₂	Hydrogen peroxide
RGB	Red, Green, Blue
rRNA	Ribosomal ribonucleic acid
OFSP	Orange fleshed sweet potato
NEO	Neomycin
NYS	Nystatin

TA	Triamcinolone
CLV	Clavulanic acid
AMX	Amoxicillin
RBF	Radial basis function
FLU	Fluticasone
SMT	Salmeterol
GDA	Gaussian discriminant analysis
TS	Tensile strength
DT	Disintegration time
PCA	Principal component analysis
MRA	Multiple regression analysis
CV	Cyclic voltammetry
GNS	Graphene nanospheres
PBA	Pyrene butyric acid
cDNA	Complementary deoxyribonucleic acid
PAA	Poly acrylic acid
PVI	Poly 1-vinyl imidazole
PPy	Polypyrrole
PGEs	Pencil graphite electrodes
G6PD	Glucose-6-phosphate dehydrogenase
CaMV	Cauliflower mosaic virus
dsDNA	Double stranded deoxyribonucleic acid

GPO	Glycerol-3-phosphate oxidase
GK	Glycerol kinase
SD	Standard deviation
GA	Glutaraldehyde
SiNS	Silica nanospheres
APTES	3- aminopropyl triethoxysilane
GM	Genetically modified
BLASTN	Nucleotide Basic Local alignment search tool
NCBI	National center for Biotechnology Information
MIC	Minimum inhibitory concentration

CHAPTER 1

INTRODUCTION

In developing nations, cereals play a key role to satisfy the worldwide food demand of growing population. The cereal-based production system is the major source of nourishment and calorie consumption. Wheat (*Triticum aestivum L.*) is one of principal cereal crops grown worldwide and one of most staples of 2.5 billion of global population. The major crop which provides most of all calories in North Africa and West and Central Asia. Wheat found to be one of important sources of protein in least established countries and middle-income nations. India is the second major producer of wheat in worldwide. One of cheapest sources of energy which affords majorly of protein (20%) and consumption of calories (19%) (Ramadas, Kiran Kumar, and Pratap Singh 2020).

1.1 Factors and losses affecting stored food products

The cereals and other food products have to be stored for a shorter and longer period depends on the requirement and condition of the products. There are possibilities of quality and quantity deterioration of food material during storage by biotic and abiotic factors (Jayas 2012). The damage of food grains occurs due to the biotic factors like insects, mites, rodents, birds and microorganisms (Fig.1). The loss of stored grains is associated with the storage condition and other biotic factors. Among these biotic factors, the significant problem that reduce the quality of grains during storage is insect infestation. Insect infestation is the most vital problem in the storage of grains and flours. The one third of grains are lost during storage period over world per year (Jayas 2012).

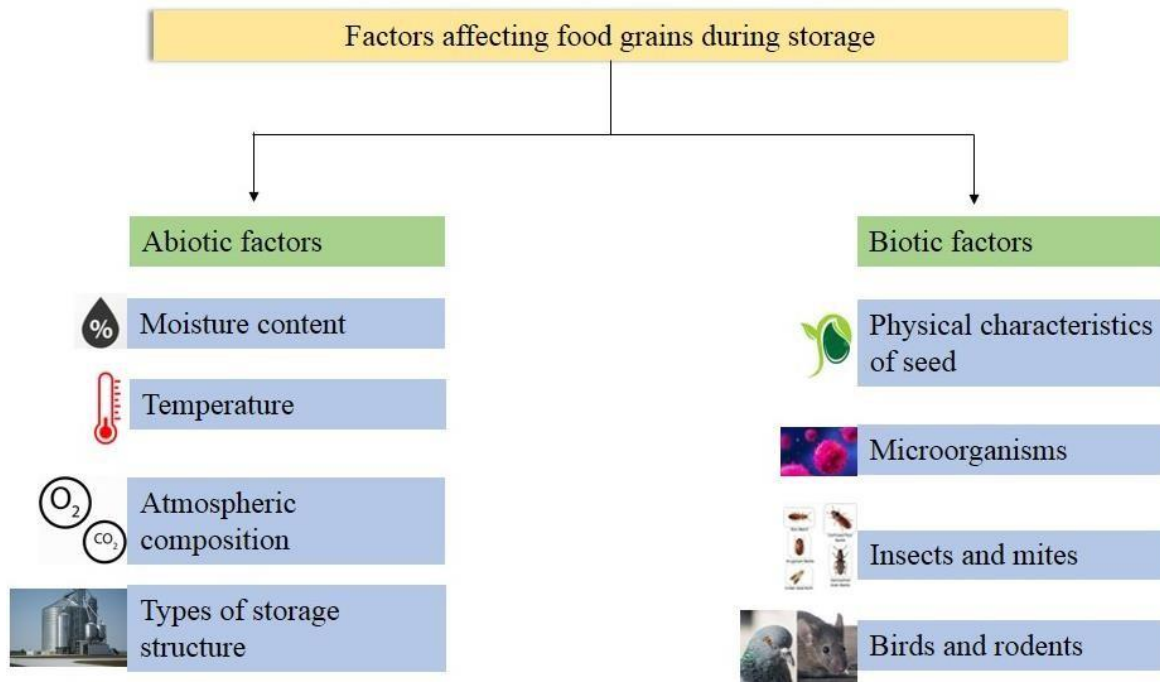


Fig 1. Factors affecting stored food grains

The stored food products are affected by around 600 species of beetles and 70 species of moths. The overall post-harvest losses in global ranges from 10 to 20 per cent because of pests (Singh *et al.* 2009). The insect infestation has a negative impact on human health issues, viability of grains and commercial value and loss of nutritional value in food grains. This leads to an unpleasant odor and also damages the storage structures. The health problems like carcinogenic quinines, allergies, ulcerative colitis are created by the infested grains (Rajendran 2015).

The losses due to insect infestation in food grains are quantitative loss, nutritional value, qualitative loss, commercial values, seed viability and loss of storage structures (Fig 2). The quantitative loss is caused by direct feeding by insect live stages. Both organic and inorganic matters degrade the quality of food grains. The toxins and chemical residues are the contaminants that affect the quality of store food grains. The biochemical value of grains is also affected due to insect infestation. There is a loss in nutritional values such as carbohydrates, proteins, fiber, moisture, weight loss of the kernel in food grains. The loss of

germination is referred as losing seed viability. The germination is an index of quality in grain market. The loss of financial value is defined as the loss of commercial values. This leads to moderate the trade and market value of products (Rajendran 2005).

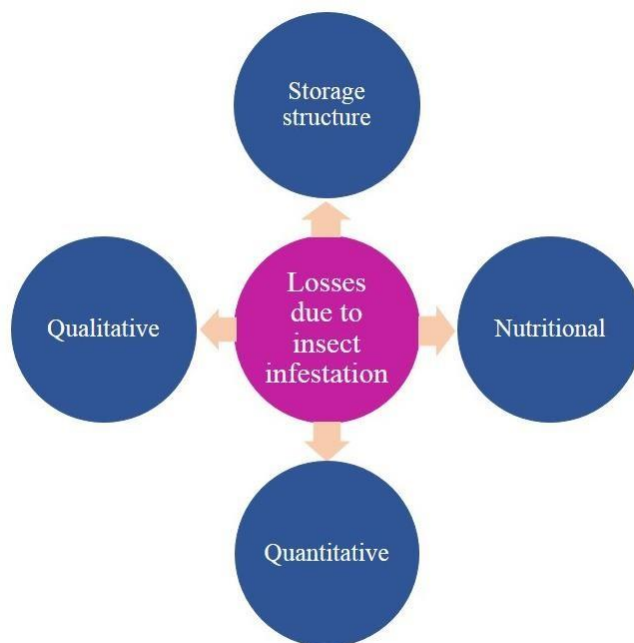


Fig 2. Losses due to insect infestation in food grains

The traditional, improved and modern forms of storage structures are shown in Fig 3. In traditional storage, the food grains are stored in bulk quantity. These structures have the capacities of 1-50 tonnes. There are some improvements done in the traditional storage structures, and it is termed as improved storage structures. These kind of storage structures have high storage capacity for long-term storage of food grains. The capacity of storage structure is about 1.5-150 tonnes. In India, the large volume of food grains is stored in horizontal sheds (godowns) designed for bag storage and modern silos. Based on quality and cost considerations, the modern storage structures are found to be suitable. The spillage of food grains also responsible for infestation in various storage structures (Vimala Bharathi *et al.*, 2017).

Types of storage structures

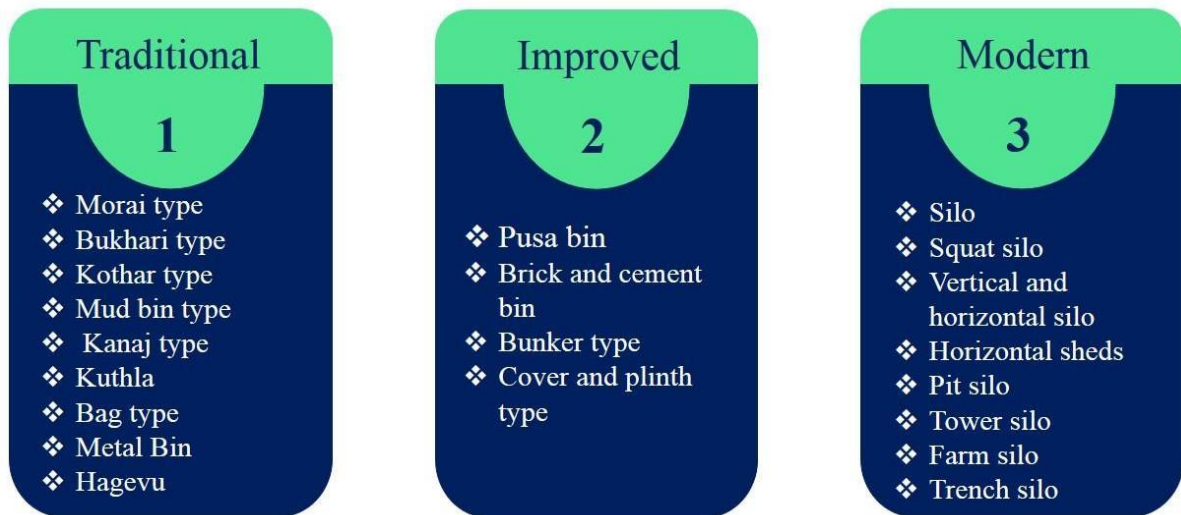


Fig 3. Types of food grain storage structures.

1.2 Methods to detect insect infestation

There are physical and chemical methods to determine the insect infestation on stored food grains (Fig 4). The hidden infestation can be detected by X-ray imaging, breeding out, specific gravity, insect fragment count, staining techniques, nuclear magnetic resonance and NIR techniques (Neethirajan *et al.* 2007). The external infestation can be detected by acoustic methods, visual inspection, sampling and sieving, grain probes and insect traps and heat extraction methods.

1.2.1 Physical methods

1.2.1.1 Visual inspection

Visual inspection is one of the detection method to monitor insect infestation in stored foods. It is also qualitative, independent and uniform method to detect insects in stored food materials. The presence of adults, eggs and infested grains can be examined by naked eyes (Banga *et al.* 2018). It is also used as a usual method for evaluation of quantitative loss.

1.2.1.2 CO₂ measurement

The occurrence of internal infestation in food grains can be identified using the amount of CO₂ formed in grains owed to inhalation of insects in 24hrs. The CO₂ estimation is one of acceptable method to detect insect infestation in food grains (Rajendran 2005). In uninfested grain, the acceptable CO₂ level should be less than 0.25% with moisture content of 14 per cent (Mehmood *et al.* 2018). The CO₂ measurement act as an indicator of stored grain condition that increases attention due to its reliability and sensitivity. The changes in CO₂ level will occur due to the insect and fungal activities with stored grains. The CO₂ level occur due to insect infestation will reduce the grain-quality control and measurement and also expands protection processes against insects and fungal activity (Neethirajan *et al.* 2007, Abalone *et al.* 2011). This method is less sensitive at low level of insect infestation, time consuming and it is not applicable to the grains with more than 14 per cent of moisture content.

1.2.1.3 Acoustical method

An insect-feeding sounds are used to monitor both internal and external grain feeding insects by using the acoustical methods. The hidden insects present inside the kernels can be detected by the amplification and based on filtering their movement and feeding sounds. The insects can be detected in grains based on the requirement of physical and biological factors that affect sound production, insect distribution, and detection. The intensity, duration, spectral

characterization of sound at the source, distance to receive, the receiver spectral sensitivity and background noise are the physical factors that affect detection of hidden insects in grain samples. The unfavorable environment, insect behavior and insect inactivity are biological factors affecting presence of insects in food samples. The acoustic method is not suitable to detect the dead insect and also early larval stage infestation in grains (Thanushree *et.al.*, 2018).

1.2.1.4 Near-Infrared reflectance (NIR) spectroscopy

The NIR spectroscopy is a fast, reliable, accurate and economical technique available for the compositional analysis of grains. The both qualitative and quantitative analysis can be done using NIR techniques (Kim *et al.* 2003). The information based on the reflectance properties of different substances present in the food product are provided by this technique. The NIR is based on the absorption of electromagnetic wavelength of 750-2500nm. The classical absorption spectroscopy can be used to determine the concentration of constituents such as water, protein and carbohydrates. The NIR is used as a method to detect the presence of both live and death rice weevil in single kernel with various life stage in wheat (Elizabeth B. Maghirang *etal.* 2013). An accuracy of 94, 92, 84 and 62 per cent were found in the sound kernel and kernel containing pupae, large larvae, medium-sized larva and small larva respectively. This technique is also used to detect the parasitized weevil in wheat kernel (Dowell *et al.* 1999) and to detect internal and external insect infestation in wheat grains (Floyd E. Dowell *et al.*, 1998; Ghaedian & Wehling, 1997; Ridgway & Chambers, 1998).

The NIR system is a rapid method which takes one minute per sample and do not require sample preparation (Perez-Mendoza *et al.* 2003). This method may not suitable to detect the low levels of insect infestation in bulk samples (Dowell *et al.* 1999). The moisture content of the sample is very sensitive in the NIR method. The images of infested samples can be captured by the NIR vidicon camera. A comparison of both NIR and X-rays images concluded that the NIR images can detect insects in wheat grains by the composition of kernel

as a result of insect infestation. But, Ridgway and Chambers (1998) reported that the NIR imaging method is an indirect method and it cannot detect the larvae because of the movement of larvae is due to heat generated from lightening.

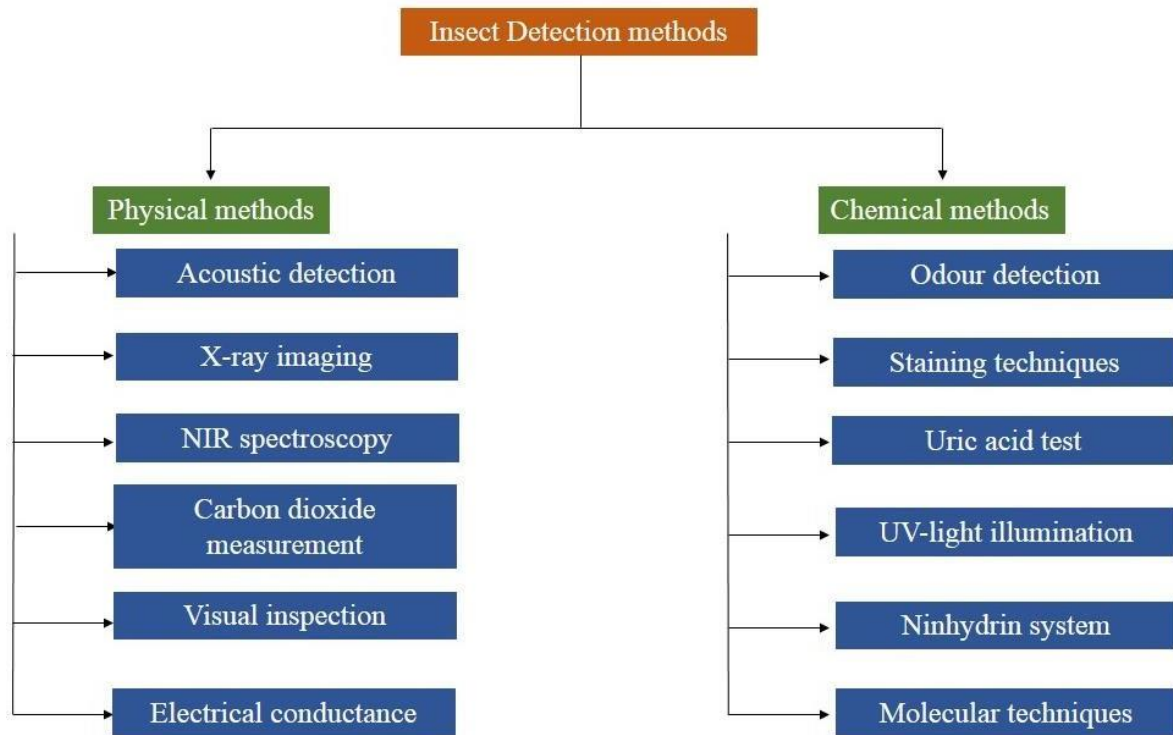


Fig 4. Different methods to detect insect infestation in food grains.

1.2.1.5 X-ray imaging

A soft X-ray is the direct method and only non-destructive method that can be used to detect the insect infestation in grain kernel (Milner, Lee & Katz, 1952; Haff & Slaughter, 2013). This system consists of fluoroscope operated at 15kV potential and 65 μ A that produce real-time images. A single wheat kernel has to be placed on plastic wrap on platform between X-ray tube and detection system which will scan the grain. A detection screen with the images were captured by CCD black and white camera computed by the digital video creator. The digital images have to be processed to detect the insect-infested kernels. This method is a non-destructive and time-saving technique. The mechanical damage in grains can also be identified by the soft X-rays. It is difficult to distinguish from the denser portion of grain with the

presence of small larvae and weevil eggs by using soft X-ray technique (Karunakaran *et al.*, 2003)

1.2.1.6 Electrical conductance

The electrical conductance can detect the hidden internal insect infestation in wheat kernels (Pearson *et al.*, 2003). The grain kernel weight, moisture content, diameter and hardness can be measured using the single kernel characterization system. The principle of electrical conductance and compression of force exists as a base work of this system. This system comprise of voltage-divider circuit and two resistors in which one resistor act as a kernel. The voltage across the kernel can be monitored and measured using the electrical conductance. The presence of live insects inside the kernel leads to large downward slope in the conductance signals. The infested kernel can be differentiated from the sound kernel based on the signal characteristics, and the range of voltage levels in the conductance signal. This method is in-expensive and the inspection of a single kernel is time-consuming. A kernel with the presence of eggs and young larva cannot be detected because of the low moisture content. A kernel with dead insects cannot be detected by this method. The insect detection rate was low in this method when compared to inspection by the soft X-rays. Pearson *et al.* (2003) reported that this method is suitable for single kernel only.

1.2.2 Chemical methods

1.2.2.1 Detection techniques of odor released by insects

The odor detection techniques are used to identify volatile compounds released by insects that lets to detect infestation during the storage period (Olsson *et al.*, 2002). It possesses moderate sensitivity and high accuracy with a workable cost of operation. The extraction of odors can be done by distillation and headspace techniques and detected by using gas chromatography or GC- mass spectroscopy. Some of the headspace techniques are dynamic

headspace, solid phase micro-extraction, and E-nose which can detect the insect infestation. The headspace method is a non-destructive method which involves the adsorption of volatile compounds on suitable adsorbents like Tenax and coated silica in DHS and SPME and then detected by GC or GC-MS. A collection of chemical arrays containing in e-nose to detect odor compounds from the infested samples (Paolesse *et al.*, 2006).

1.2.2.2 Staining techniques

1.2.2.2.1 Egg-plug stain

Some of the insects will deposit the eggs inside the grains. The grains will be stained with 0.5% acid fuchsin to identify the egg-plug present in stored grains. The egg-plugs appear in cherry red in colour (Rajendran 1999). Similarly, the grains treated with 1% gentian violet will show the eggs in purple colour (Negi *et al.* 2021). The grains was soaked in 20ppm concentration of berberine sulphate aqueous solution for a minute and the egg-plug was stained, which flame greenish yellow in colour and observed under UV light with wavelength of 366nm (Rajendran 2005). The number of egg-plug will show the level of insect infestation occurred in stored grains. This method will be applicable only for weevils. The damaged parts of grains will also get stained during the process in these methods and hence it is not popular.

1.2.2.2.2 Molecular detection method

A DNA-based approach such as DNA bar-coding, species-specific polymerase chain reaction and RT-PCR techniques to detect the hidden infestation in food grains. All stages of insect can be recognized and counted by using q-PCR method by its DNA sequences at maximum reliable and quick way. Multiplex PCR technique are high accuracy with less time to detect insect infestation and also used to detect all stages of insect infestation in food grains (Thanushree *et.al.*, 2018).

1.3 Contamination in food due to insect infestation

The contamination of food materials with uric acid, quinone and mycotoxins may occur due to insect infestation and fungal infection.

1.3.1 Uric acid

The major nitrogenous waste of birds, reptiles and also in most of the insects which lacks the uricase, and allantoinase activity is known as uric acid. The uric acid can serve as a good index of infestation and unhygienic conditions in infested food grains (Cooper *et al.* 2006). ZnO has an excellent uric acid and dopamine sensing properties. The zinc oxide microsphere was synthesized using rapid microwave method and by alteration of urea ratio to enhance the biosensing properties of microparticles (Kogularasu *et al.* 2019). This study was carried out in foods (meat and wheat flour) and also biological samples. They reported that wheat flour possesses a wide linear range of 100nM-145 μ M with LOD of 35.4 nM (± 0.139) and the calculated sensitivity was 1.4057 μ A μ M⁻¹ cm².

The two glucose biosensors had been developed based on poly (3,4-ethylenedioxythiophene) and polyacrylic acid treated with poly (4-lithium styrenesulfonic acid) (Paweł Krzyczmonik & Sławomira Skrzypek, 2018). An amperometric measurement was used to determine the glucose level in phosphate buffer. The glucose concentration can be determined using biosensors by ascorbic and uric acid that act as interfering agent. Hence, this method applied for beverage and food samples such as grape juice and honey.

Wehling and Wetzel (2020) used liquid chromatography to measure the uric acid content of wheat internally infested by various growth stages of granary weevil (*Sitophilus granarius*), rice weevil (*Sitophilus oryzae*), and lesser grain borer (*Rhyzopertha Dominica*). They reported that correlation exists between number of insects and uric acid content of grain infested by a stage of an internally infesting stored product insect, with correlation coefficients ranging from 0.970 to 0.998. They also found that a detection limit for the analytical procedure

of less than 1.0 ppm uric acid allows detection of infestation level as low as one kernel per 100 g grain for late instar granary weevil larvae. But it is difficult to analyze many samples in these methods in a shorter period.

1.3.2 Mycotoxins

The toxic secondary metabolites produced by the filamentous fungi are mycotoxins. An ongoing problem of world is mycotoxins contamination. It is also considered as unavoidable and unpredictable problem during storage of food grains (Alshannaq and Yu 2017). All over world, 25% of harvested crops are contaminated by mycotoxins / year and leads to both agricultural and industrial losses (Hubert *et al.* 2018). Many methods can detect mycotoxins in food grains like thin layer chromatography (TLC), HPLC coupled with FLD, UV, DAD or MS, GC-MS, UPLC, ELISA and rapid screening test (Mahato *et al.* 2019). But there are some drawbacks to detect a low level of mycotoxins contamination and also too complicated extraction process of mycotoxins contamination.

1.3.3 Quinone contamination

Red flour beetle, *Tribolium castaneum* contaminate the flour samples and releases unpleasant odor, and the samples color gets pinkish. This beetle can produce the benzoquinone from the prothoracic and abdominal glands (Yezerki, Gilmor, and Stevens 2004). The *T. castaneum* can produce three benzoquinone namely methyl 1, 4-benzoquinone, ethyl 1, 4-benzoquinone and methoxy 1, 4-benzoquinone, whereas *T. confusum* produce methyl 1, 4-benzoquinone and ethyl 1, 4-benzoquinone (Pappas and Morrison 1995). Benzoquinone are highly reactive, and it's difficult for identification and quantification of benzoquinones. The quinones can also be detected using some analytical techniques such as UV-visible spectroscopy, HPLC and RP-HPLC (El-Desouky *et al.*, 2018).

1.4 Mechanism of uric acid degradation

Uricase is an enzyme which catalyzes the oxidation of uric acid with the presence of oxygen to allantoin and hydrogen peroxide in purine breakdown pathway. The uric acid is less soluble in water compared with allantoin (Hafez, Abdel-Rahman, and Naguib 2017).

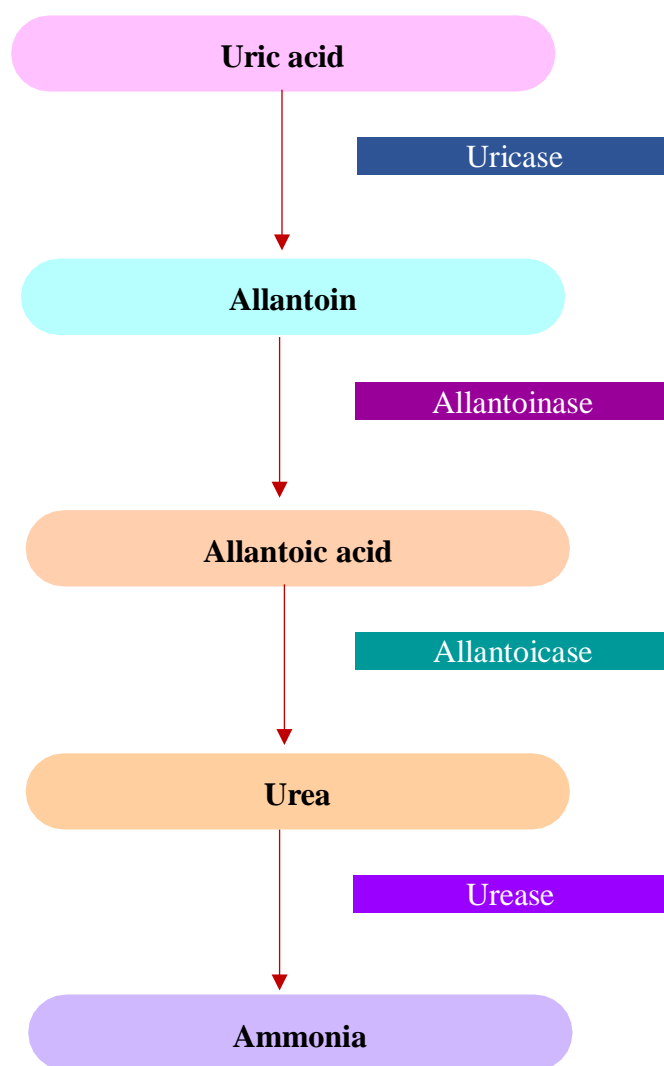


Fig 5. Degradation of uric acid to ammonia by purine breakdown pathway

1.5 Objectives

Based on this review, most of the detection methods required high tech equipment and consumes more time. Hence, there is a need to develop a rapid method to detect the uric acid in a shorter time. So, the study was planned with the following objectives,

- ❖ To determine the uric acid levels in food samples during storage with rapid method using UV – visible spectroscopy
- ❖ To develop paper based strip to detect UA levels in infested food samples
- ❖ Validation of paper based strip to detect UA levels in infested food samples

DNA based biosensor is also planned to develop to detect the uric acid. An attempt is also planned to control the growth of uric acid degrading microbes by using some essential oils obtained from medicinal plants

CHAPTER 2

REVIEW OF LITERATURE

2.1 Insect infestation

The major food source for human and domesticated animals over worldwide are cereals, oilseeds and legumes. The food commodities have to be stored for a shorter and longer period depends on the requirement and condition of the product. There are possibilities of quality and quantity deterioration of food material during storage by biotic and abiotic factors. The damage of food grains occurs due to the insects, mites, rodents, birds and microorganisms (Vimala Bharathi *et al.* 2017). The primary quality consideration of food products is insect infestation by various insect species. A severe loss may happen to processors by the contamination of food product with the presence of live insects, webbing, protective secretions, feces, cast skins (Indumathi *et al.* 2021). There are possibilities of reduction in profitable value of food products and returns of product occurs due to the presence of live insects that reduces the consumer confidence because of insect infestation (Johnson, 2013).

Insect infestation was the most vital problem in the storage of grains and flours. The insect infestation in the food products leads to a loss in quantity and quality of the food products. It will result in contamination of uric acid and exuviae in stored food materials. These contaminations reduce the quality of the product and its market value. The feeding of the larva and adults causes damage to food products and direct loss to the quantity. The metabolic by-products of the insect and body fragments will contaminate the food materials during the developmental stages and also by the adult insects. The heat and moisture content may increase in food products through the metabolic activities during the growth of insects which lead to microbial growth. The infested grains are unhealthy for kernel and its products, become unfit for human consumption (Induja and Loganathan, 2022).

2.2 Detection of insect infestation in foods

The periodical monitoring of infestation will help to assess the quality of the grains and flours and to take necessary control measures. The infestation can be monitored by visual inspection but the contamination in grains has to be detected by insect fragment counts and uric acid estimation. The invisible insect fragments and uric acid present in the food products have been detected by several methods. The floatation, radiographic techniques, acoustic techniques, uric acid measurement, nuclear magnetic resonance imaging, immunoassays and staining of kernels to detect the entrance holes for eggs are the techniques developed to detect the insect infestation (Induja and Loganathan, 2021).

The presence of insects has to be identified in the early stage to safeguard the food materials. There are physical and chemical methods to determine the insect infestation in stored food grains. The hidden infestation can be detected by X-ray imaging, specific gravity, insect fragment count, staining techniques, NMR and NIR techniques. The external infestation can be detected by acoustic methods, visual inspection, sampling and sieving, grain probes, insect traps and heat extraction methods (Thanushree et.al, 2018).

It was reported that the analytical methods were used to detect uric acid contamination using spectrophotometer, high-performance liquid chromatography, various sensors and capillary electrophoresis. Some of the techniques are very difficult to use for fast detection, required trained manpower, and are laborious for real-time. Most of these techniques have not been found suitable to implement in food inspection systems because of their cost, inconstant, and variation in the results. Earlier researcher reviewed the advantages and limitations of various insect detection method including uric acid analysis and the advantages of one technique over the other. Most of the methods of uric acid detection were based on chemicals, enzymatic, fluorescence and biosensors. The important structural components of insect cuticle

are chitin, but it cannot be used as a sign of infestation or contamination. The presence of fungi in stored food products may also indicate insect infestation. But the microbial growth will occur only when the grain or flour stored with high moisture content. It was reported that the major end product of nitrogen metabolism in insect is uric acid and 80 per cent of nitrogen from faeces was released by insects. Hence measuring uric acid with accurate and quick method will help to follow disinfestation method in the food storage system (Induja and Loganathan, 2021).

2.2.1 Colorimetric method

A colorimetric method was used to measure the uric acid content in infested food samples. A large number of food samples can be analyzed by this colorimetric method using phosphotungstic acid. The turbidity in food samples (flours and grains) can be avoided by using phosphotungstic acid. It was reported that the method based on arsenophosphotungstic acid gave a practically good correlation between uric acid concentration and insect number exists in the grain samples. It had been enhanced by a fusion of uricase enzyme and by use of paper chromatography. An enzyme-based colorimetric method was simpler than an enzymatic-ultraviolet method to determine uric acid in flour. This method is more susceptible and uricase enzyme action can be destroyed by adding hydrochloric acid to the sample, it applies to a variety of cereal products. This procedure had not been widely used because of the time required for analysis is too long. In infested wheat flour, the UA can be detected by paper chromatographic method and it can be estimated by using Benedict's UA reagent. The results obtained by direct colorimetric method reveal that the UA content steadily increases. There is no presence of UA in uninfested wheat flour. The extraction of protein free aqueous solution of uninfested wheat flour showed the presence of some other substances other than UA which get reacted with Benedict's reagent and showed an apparent yield of UA (Franke 1922).

The UA level in food samples can be determined by the semiautomated differential colorimetric method. The samples were treated with HCl, incubated in water bath at 55-60°C and neutralized using NaOH. The extraction of UA was carried using sodium acetate and was determined using phosphotungstic acid (colour reagent). The UA was destroyed by uricase enzyme and the reaction specificity and immobilization of uricase enzyme in nylon coil contribute reliability of this method. Based on this method, the UA level can be detected for 30 samples / hr. The analysis of actual samples and the recovery studies showed that UA can serve as an chemical index of infestation in different food samples (Cox *et al.*, 1976).

2.2.2 Level of insect infestation

The total protein, non-protein nitrogen, total nitrogen and UA level in wheat, sorghum and maize with 75, 50 and 25 per cent of insect infestation has been recorded that there was an increase in all those samples. The insect infestation was caused by *R. dominica* and *Trogoderma granarium* in mixed population and also separately. Significantly, the protein content of three grains at 75% of insect infestation showed a reduction in these content whereas there is a non-significant decrease at 25 and 50% of infestation. The UA content produced by both the insect species showed 10mg/100g which above the acceptance level at 50% of insect infestation in all grain varieties (Pixton,1965).

2.2.3 Chromatographic techniques

The UA level is an index of insect infestation or contamination was found to be non satisfactory. The method was not sensitive. Based on insect population level, the quantity of UA can be determined. During wheat milling, the rate of UA was determined by inoculating wheat kernels with larvae of rice weevil. The inoculated samples had the presence of UA (25µg/g of wheat). All samples were milled using Buhler mill that produce three reduction flours, two millfeed flour and three break flours. The UA content of all individual milled flours

was quantified using reverse phase high performance liquid chromatography (RP-HPLC) attached with UV detector. About 90% of UA content was found in wheat flour, 50% of UA in first break fraction and 10% of UA was present in millfeed fraction (Randy L Wehling, David L Wetzel 1984).

The liquid chromatography was also to measure the uric acid content of wheat internally infested by various growth stages of granary weevil (*S. granarius*), rice weevil (*S. oryzae*), and lesser grain borer (*R. dominica*). It was reported that correlation exists between number of insects and uric acid content of grain infested by a given stage of an internally infesting stored product insect, with correlation coefficients ranging from 0.970 to 0.998. They also found that a detection limit for the analytical procedure of less than 1.0 ppm uric acid allows detection of infestation level as low as one kernel per 100 g of grain for late instar granary weevil larvae. But it is difficult to analyse large number of samples in these methods in a shorter period.

2.2.4 Odor detection technique

The odor detection techniques are used to detect insect infestation during the storage of food material by way of identifying volatile compounds released by the insects (Olsson *et al.*, 2002). The compounds at lower concentration have to be extracted by distillation and headspace techniques and can be detected by using GC- mass spectroscopy. The E-nose can also be used to detect the insect infestation. A collection of chemical arrays containing in e-nose is used to detect odor compounds from the infested samples (Paolesse *et al.*, 2006).

2.2.5 Biosensors

The determination of isoproterenol (ISPT) in presence of UA was performed using p-chloranil carbon nanotubes paste electrode. The suitability of p-chloranil as a mediator for the electrocatalytic oxidation of ISPT (pH = 10.5) was investigated using the chronoamperometric,

cyclic voltammetry and electrochemical impedance spectroscopic methods. The UA and ISPT were measured with the potential difference of 360mV using the differential pulse voltammetry. The linearity of electrocatalytic current with ISPT and UA ranged from 0.015-100 mol⁻¹ and 3.0-310 mol⁻¹ respectively. The LOD of UA and ISPT was equal to 2.3 and 0.009 mol⁻¹ (Jirakunakorn et.al. 2020).

The enzyme based biosensor was developed to detect UA in human serum by using conductivity meter by Ibupoto *et al.* (2011). A nata de coco membrane – Pt electrode act as a working electrode and uricase enzyme isolated from *Candida utilis* was immobilized on the working electrode. The linearity of enzyme based biosensor ranges from 1-6 ppm and this biosensor shows good selectivity properties. The operational stability of enzyme based biosensor was less than three days and the relative standard error was less than about 10 per cent.

Based on the peroxidase enzyme activity in colorimetric method, a paper based device was developed to detect UA in blood serum samples using AuNPs-GO (gold nanoparticle mediated graphene conjugates). The paper (Whatman filter paper No 1) was treated with the AuNPs-GO solution and 3, 3', 5, 5' tetramethylbenzidine – hydrogen peroxide (TMB-H₂O₂) was dipped on the surface of paper with the presence of UA. The colour changes were measured, when UA interact with AuNPs-GO. The blue colour formation disappears within 5 minutes to white colour due to the peroxidase enzyme activity. The LOD (4 ppm) for the detection of UA was observed on paper visualization. The paper based device showed good selectivity for UA. The paper based device provides rapid, real-time and easy to use platform for the detection of UA as reported by Martinez *et al.* (2008).

CHAPTER 3

MATERIAL AND METHODS

Objective 1- To determine the uric acid levels in food samples during storage with rapid method using UV – visible spectroscopy

A simple rapid method for uric acid determination was developed using standard uric acid at different concentrations and compared with the colorimetric method (Preceding method). The rapid method was validated statistically.

3.1.1 Insect culture

The confused flour beetle, *T. confusum* was cultured in the wide mouth glass container with wheat flour as food. The freshly emerged adults of *T. confusum* (50 numbers) were collected from the stock culture, released in the glass container containing 300g of wheat flour and covered with the muslin cloth. It was kept at ambient temperature ($34\pm 2^{\circ}\text{C}$) for the egg laying. The adults were removed after 24 hrs of egg laying. The eggs grown into larvae, pupae and emerged as uniform aged adults which were used for further studies (Induja and Loganathan, 2021).

3.1.2 Infestation of food matrices

The freshly emerged adults of *T. confusum* were separated from culture and released 20 adults each in seven sets of glass containers containing the wheat flour, maida, and rava for infestation and covered with the muslin cloth. The infested food materials were kept at ambient temperature ($34\pm 2^{\circ}\text{C}$) for four weeks. The larvae release the uric acid during their growth and leads to uric acid contamination in the infested food material. The infested wheat flour, maida, and rava were subjected to extraction of uric acid every week and the quantity of uric acid was estimated (Induja and Loganathan, 2021).

3.1.3 Extraction of Uric acid

One gram of infested product (wheat flour, rava, maida) with 7mL of sodium borate was taken in centrifuge tubes, mixed well in vortex and adjusted the pH to 8.7 with 0.01N HCl. The samples were centrifuged (REMI: model: C-30BL) at 5000rpm for 15 minutes. The supernatant was collected, filtered using Whatman No.1 filter paper and stored the filtrate in vials for further spectrophotometric analysis (Induja and Loganathan, 2021).

3.1.4 Determination of uric acid with colorimetric method (Preceding Method)

The different concentrations of uric acid and filtrate of infested food samples (1mL) were taken in boiling tubes. Then, 5mL of distilled water and 1mL of NaOH (0.05M) were added in each boiling tube. They were mixed well using a vortex (DLab; MX-S60HZ) and kept in a water bath at 100°C for 7 minutes. The tubes were cooled with water and adjusted the pH to 2.16 with 0.05M HCl. Then, 1 mL of phenylhydrazine hydrochloride (0.023 M) was added and mixed using vortex. The tubes were again kept in a water bath at 100°C for 7 minutes and immersed it immediately into an icy alcohol bath (40% NaOH) for 7 minutes. Then 3 mL of concentrated HCl and 1 mL of potassium ferricyanide (0.05M) were added and kept for 20 minutes. The colour developed was recorded at 522 nm in a UV-visible spectrophotometer (Shimadzu; UV-1800) (Induja C, Loganathan M 2022).

3.1.4.1 Formation of chromophore based on reaction mechanism in preceding method

In the preceding method, uric acid was hydrolyzed using weak alkaline (NaOH, 0.05M) at 100°C. The hydrolysed uric acid changed into allantoinic acid by the activity of allantoinase enzyme. The allantoinic acid degrades into urea and glyoxylic acid in acid solution (HCl, 0.05M). The phenyl hydrazine hydrochloride reacts with glyoxylic acid to form phenyl hydrazone. The potassium ferricyanide reacts with phenyl hydrazone to form an unstable chromophore (Fig.6) (Induja and Loganathan, 2022).

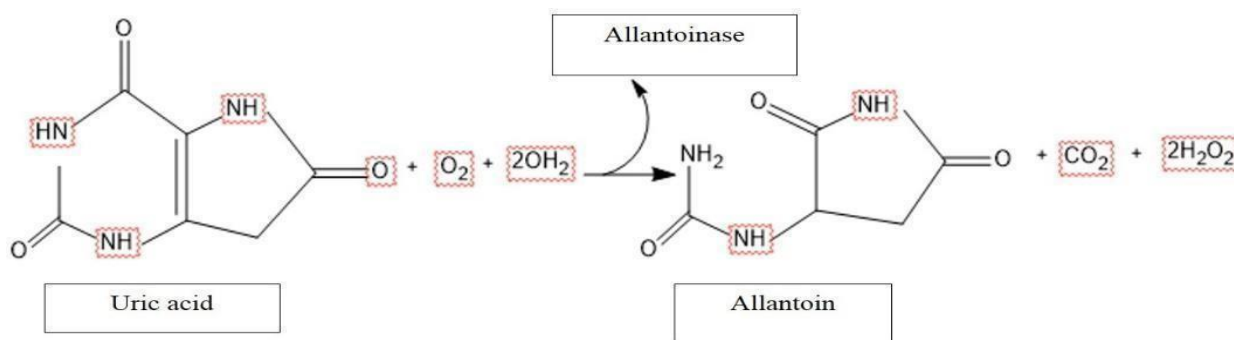


Fig.6.The oxidation reaction of uric acid to allantoin

3.1.5 Rapid spectrophotometric method to determine the uric acid

3.1.5.1 Developing a simple rapid spectrophotometric method to determine the uric acid

A rapid method was developed to reduce the duration of analysis and also to get accuracy. In this method, filtrate of infested food samples (1mL) and different concentrations (1mL) of uric acid was diluted five times with distilled water. Then 1mL of potassium ferricyanide and ferric chloride (1mL) were added. It was mixed well and kept for 5 minutes. The spectrophotometric readings were taken in a UV-visible spectrophotometer (Shimadzu; model: UV-1800) at the absorbance of 520 nm (Induja and Loganathan, 2022).

3.1.5.2 Formation of Prussian blue colour based on reaction mechanism (Rapid method)

The reaction mechanism of uric acid was studied for the simple rapid method to determine the uric acid content using UV-visible spectroscopy. The potassium ferricyanide reacts with the uric acid in infested samples and converts into potassium ferrocyanide (Fig.7).

Ferric chloride reacts with potassium ferrocyanide to produce Prussian blue color. The principle of the present rapid method was based on the formation of Prussian blue. The potassium ferricyanide reacts with the ferric or ferrous solution to form Prussian blue. The thermal equilibrium occurs between the two solutions and the colour intensity will increase based on the heating process at 25°C (Induja and Loganathan 2022) .

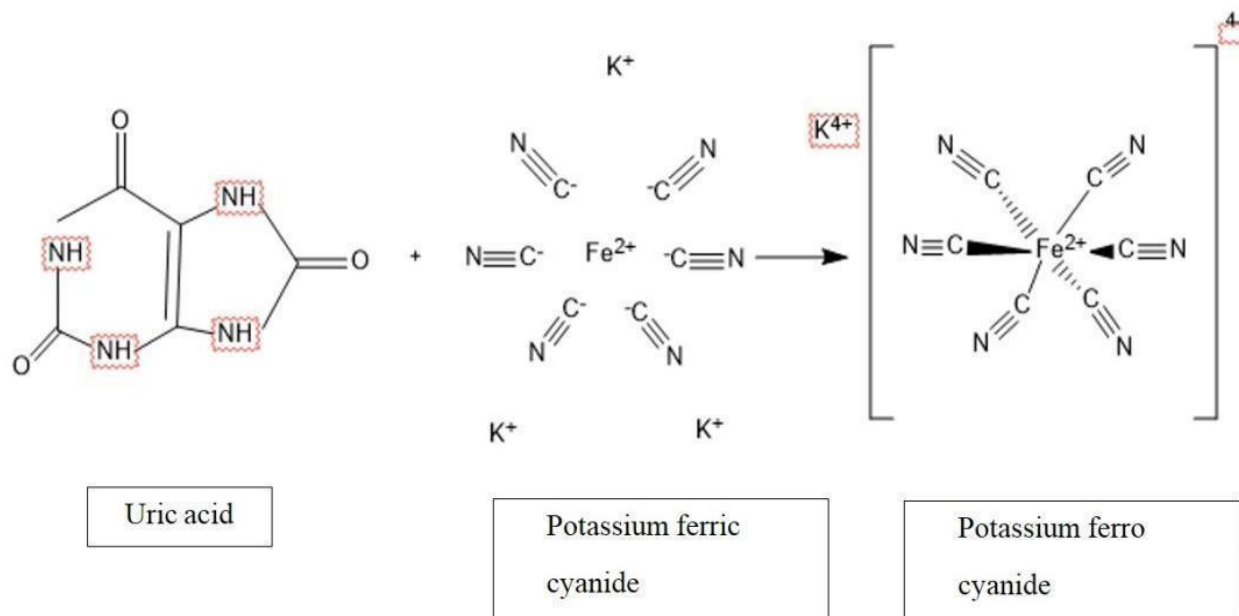


Fig.7. Mechanism of Prussian blue colour formation

3.1.6 Statistical analysis

3.1.6.1 Linear regression model

A multiple linear regression involves fitting a model for a dependent variable involving more than one independent variable, which is linear in its parameters. The model summary describes R , R^2 , Adjusted R^2 and standard error of dependent value (OD) of both the methods. The R value is considered as a measure of quality of prediction of dependent variable (OD). The R^2 ranges from 0 to 1 that represents the proportion of variation in the dependent variable that can be explained by the model explanatory variable (Oswald, 2012). The R^2 represents the coefficient of correlation between dependent and independent variables in the linear regression. The R^2 increases whereas the model is better. The adjusted R^2 is the correction for the number of x variables involved in the predictive model. The adjusted R^2 is close to 1 that indicates the large proportion of variability in the dependent variable that has been explained by the regression model. The adjusted R^2 number which is nearer to 0 indicates that it did not showed much variations in the dependent variable. The Durbin-Watson (DW) test was used to test the hypothesis with autocorrelation. If the DW value lies from 0 to 2, it indicates positive

autocorrelation. The standard error (SE) represents the average distance that the observed values fall in the regression line. The smaller value of SE indicates that the observation is closer to the fitted line. Both preceding and rapid methods were evaluated based on parameters of the regression model (Induja and Loganathan, 2022).

3.1.6.2 CART[®] model

The Classification and Regression Tree (CART) was constructed and performed by using MATLAB R2019a software. The concentration of standard, concentration of infested and uninfested food samples were used as dependent variables and the absorbance of standard and absorbance of infested and uninfested samples obtained were act as independent variable in CART analysis. The k-fold cross validation function was used to evaluate the accuracy of the regression tree (Hameed and Kim, 2021).

3.1.6.3 Cluster analysis

In hierarchical cluster, the average and maximum distance from centroid is the measure of variability within each cluster. Based on Euclidean distance and complete linkage was used to draw dendrogram that showed similarity between the concentration and absorbance of uric acid by UV-visible spectroscopy method (preceding and rapid method) (Fatih *et al.* 2021).

Objective 2. To develop paper-based strip to detect UA levels in infested food samples

3.2.1 Development of the paper-based strip to detect uric acid

The paper strip was prepared using Whatman filter paper No.40 as base material with 20 mm of width and 60 mm of height (Fig 8). Then, ferric chloride ($30\mu\text{l}$, 0.02M) was added to the surface of the paper strip and dried in shade.

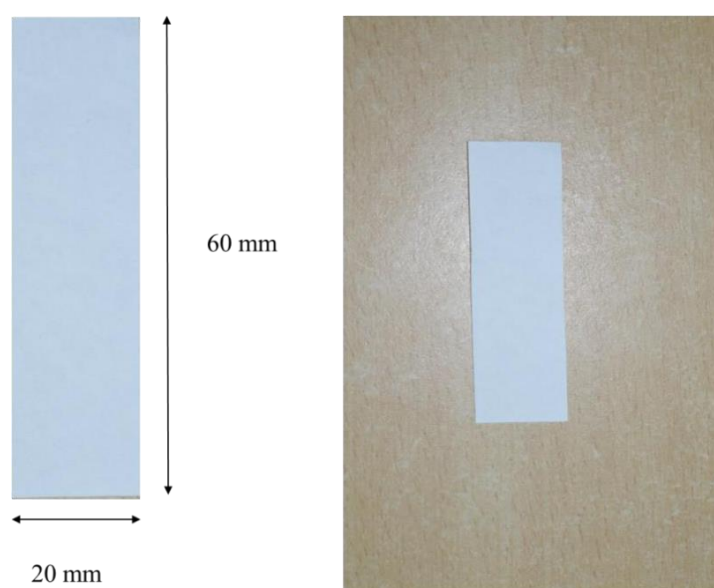


Fig 8. Schematic diagram of paper based strip

3.2.2 Evaluation of paper strip method

The different concentrations of standard uric acid and extracted filtrate from all wheat products were treated with potassium ferricyanide ($30\mu\text{l}$, 0.02M) where the uric acid present in the filtrate will react with potassium ferricyanide to form potassium ferrocyanide. When potassium ferrocyanide react with ferric chloride leads to formation of Prussian blue colour (Fig. 9). The colour formation was captured by a GigE vision area scan camera (C1600, Genie color series, DALSA) fitted with a magnifying lens (Zoom 7000, 9mm, Navitar). The captured images were analyzed using Matlab software. The MATLAB code was generated to determine the uric acid present in infested food samples as described by Khan and Garnier (2014).

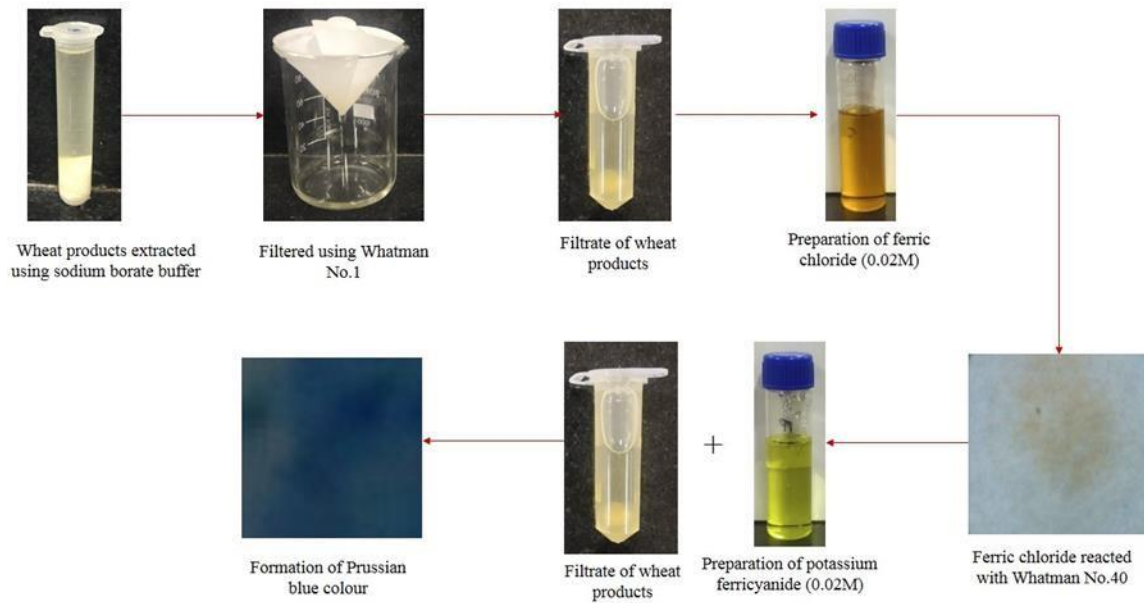


Fig 9. Flowchart of extraction of uric acid and Prussian blue colour formation

3.2.3 Determination of uric acid using MATLAB coding

The uric acid was determined using the Matlab R2019a software. Initially, the RGB values (three-dimensional matrix) were converted into gray (Black & white) values which was denoted as (b). The total pixel value (c) and color intensity (d) were calculated as mentioned in Matlab coding. The mean value (m) was calculated from the resulted matrix. The color signal was developed for different concentrations of standard uric acid (Islam *et al.* 2018). The color intensity of different uric acid concentrations was calculated by Matlab code as mentioned below.

Close all;

Clear all;

```
a=imread('samm7.png');
```

```
b=rgb2gray(a);
```

```
imshow(b)
```

```
Min(min(b))
```

```

Max (max (b))
c=sum (b (:))
d=c/sum ((b (:)> 0))
m= (b<255&b>122);
y=b (m)
x=mean(y)
Min (min(y))
Max (max(y))
PPM=(x-min (min(y))/m)

```

3.2.4 Statistical analysis

3.2.4.1 Linear regression model

A linear regression is defined as a statistical analysis applied to a set of data to describe and quantify the relationship between the dependent and independent variables. The regression analysis allows to predict the values of dependent variables based on one independent variable values. In correlation analysis, “r” is a dimensionless number where the value falls from -1 to 1. If the r value falls in -1 indicates that negative relationship whereas it falls in +1 range indicates positive relationship. The linear regression analysis uses an equation ($y = mx+c$) that defines the best fit of line for the relationship between dependent and independent variables. The mean squared error (MSE) measures the average of square deviation between predicted and actual data. The square root of variance of residuals is defined as root mean squared error (RMSE).

The R^2 indicates the degree of variability of dependent variables due to independent variables. The adjusted R^2 gives the percentage of variations explained by the independent variable that affect the dependent variable. The Akaike’s Information Criterion (AIC) indicates

by adding more parameters in model that expands the goodness of fit but also increases the penalty imposed by adding more parameters. The measure of quality of predictions made by regression model is known as MAPE (Mean Absolute Percentage Error). The DW (Durbin-Watson statistics) that denotes the autocorrelation coefficients of residual series.

The measure of influence of individual cases in a set of data on linear regression fit is equally impressive is defined as Mallows's C_p criterion (C_p). The Schwarz's Bayesian Criterion (SBC) is used to test and locate the changes of variances in normal distribution. The Amemiya's Prediction Criterion (APC) was proposed by Amemiya in 1980 and is used like adjusted R^2 to take account of parsimony of the model (Induja and Loganathan, 2022).

3.2.4.2 CART[®] model

The Classification and Regression Tree (CART) was constructed and performed by using MATLAB R2019a software as described in the section 3.1.6.2. The concentrations of standard, infested and uninfested food samples were used as dependent variables and the absorbance of standard and absorbance of infested and uninfested samples obtained from paper strip were used as independent variables in CART analysis. The k-fold cross validation function was used to evaluate the accuracy of the regression tree (Fike *et al.*, 2021).

3.2.4.3 Cluster analysis

In hierarchical cluster, the average and maximum distance from centroid is the measure of variability within each cluster. Based on Euclidean distance and complete linkage was used to draw dendrogram that showed similarity between the concentration and colour intensity of uric acid achieved by paper strip method (Achmad and Fernandes, 2021).

Objective 3. Validation of paper-based strip to detect UA levels in samples

The level of uric acid in uninfested and infested wheat products has been studied for seven weeks of storage period. The formation of Prussian blue colour of infested and uninfested food samples in paper-based strip has been captured by image processing camera and using MATLAB coding to find the concentration with colour intensity of captured images. The neural network was carried out to validate the data.

3.3.1 Neural network

Neural network is an interrelated group of nodes, which is related to vast neurons in brain. Each node represents an artificial neuron and arrow represents the connection of one neuron from output to another neuron from input. The neural network consists of three type of layer, input layer, hidden layer and output layer. The connection between input and output layer is known as hidden layer (Fig. 10). In the present study, Feedforward Neural Network (FNN) model has been used to evaluate the data sets and input variable will be concentration of uric acid and colour intensity will be the output variable in neural network. Four algorithms have been used in FNN namely Levenberg-Marquardt (LM-FNN), BFGS Quasi-Newton (BFG-FNN), Resilient Backpropagation (RP-FNN) and Scaled Conjugate Gradient (SCG-FNN) algorithm (Toboc and Lavric 2012).

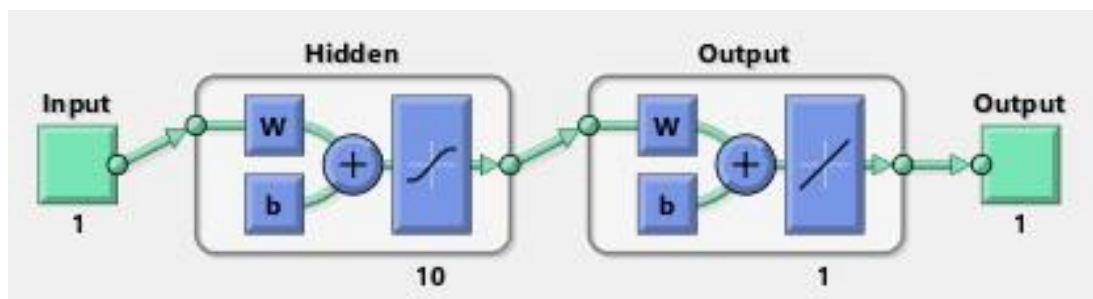


Fig 10. Schematic diagram of neural network

3.3.2 Recovery study

The known different concentrations (8-96 mg/100g) of uric acid has been added to the uninfested wheat products (wheat flour, rava and maida). In this study, recovery percentage of wheat products and relative standard deviation has been calculated (Jen *et al.*, 2002).

3.4 FTIR

In order to obtain the IR spectra of UA in wheat flour, the standard UA with different concentrations (20, 40, 60, 80 and 100 mg) and spiked wheat flour were mixed with anhydrous KBr, pelletized and analyzed using FTIR ATR spectrometer with the range from 4000 to 400cm⁻¹ (Asyana *et al.* 2016).

3.5 Development of DNA based biosensor to detect uric acid in food samples

3.5.1 Isolation of DNA from *T. confusum* insect

About 50g of *T. confusum* adult was freeze dried at -80°C for 15 minutes and 50mg of freeze dried sample was used for DNA isolation. The DNA was isolated from adult using HiPurA™ Insect DNA purification kit (MB529) as per manufacturer's instruction. The isolated DNA of insect was eluted by 200µL of elution buffer (10mM Tris Cl, pH-8.5) and centrifuged at 10,000 rpm for 1 minute (Fig. 11). The agarose gel electrophoresis was used to check the integrity and efficiency of isolated DNA. The purity of isolated DNA was analyzed using UV-Visible spectrophotometer by measuring the absorbance at 280 and 260nm (Oppert *et al.* 2019).

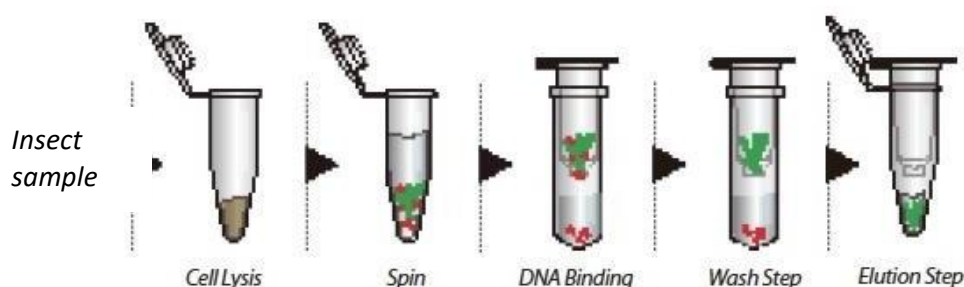


Fig 11. Insect DNA isolation by Spin column method

3.5.2 Presence of ABC genes in isolated DNA using PCR (Polymerase chain reaction)

The amplification of genes was carried out for the DNA sample using gene specific forward and reverse primers (Table 1)s (Cleophas *et al.* 2017). The initial denaturation was done at 95°C for 5 mins followed by 40 cycles with denaturation at 95°C for 30 second, annealing at 60°C for 30 sec, extension at 72°C for 30 sec and final extension at 72°C for 5mins. The PCR-generated amplicon was confirmed and purified using GeneJET PCR purification kit (Thermo Scientific, EU-Lithuania) to remove primer dimer and other contaminations. The quality of the PCR product was assessed using 2% agarose gel along with 100bp DNA ladder as size standard (Annexure 1).

Table 1. The primers of Abcg2 and Oat genes

Primers used	Sequence (5' to 3')	Amplicon size (cDNA size as per reference)
Oat3 F	CTGAAGGAGATGGCCCAGTC	105
Oat3 R	CCAGGTCAGGATAGGCTTGC	
Abcg2 F	CCGGAAAACAGCTGAGAAAG	181
Abcg2 R	GAAATTGGCAGGTTGAGGTG	

3.5.2 Preparation of chitosan mediated Silver nanoparticles

The chitosan (2.0g) was weighted and dissolved in 1% glacial acetic acid (100ml) solution, stirred continuously for 30 minutes. The solution was filtered to remove the impurities. The 1M NaOH (100µl) and 0.1M silver nitrate solution was prepared freshly, added on the filtered chitosan solution (50ml). The mixture was mixed and stirred for 10hrs at 60°C (Badawy *et al.*, 2019).

3.5.3 Development of modified Screen Printed Electrode (SPE)

The SPE was developed with three electrodes that consist of working electrode (glassy carbon), reference and counter electrode was Ag/AgCl. The chitosan (1%) mediated silver nanoparticle (5 μ l) was added to the working electrode. After that, 3 μ L of insect DNA was added on the working area. Before the complete drying of insect DNA, 5 μ L of 1% Glutaraldehyde was added to react with the protein present in insect DNA. After immobilization and hybridization, 90 μ L of 10mM Tris-Cl buffer (pH-8.5) was spread to surface of modified working, counter and reference electrode. The parameter used for cyclic voltammetry was 0.05 V/s scan rate from -0.09 to 0.09 V (Ulianas *et al.*, 2014).

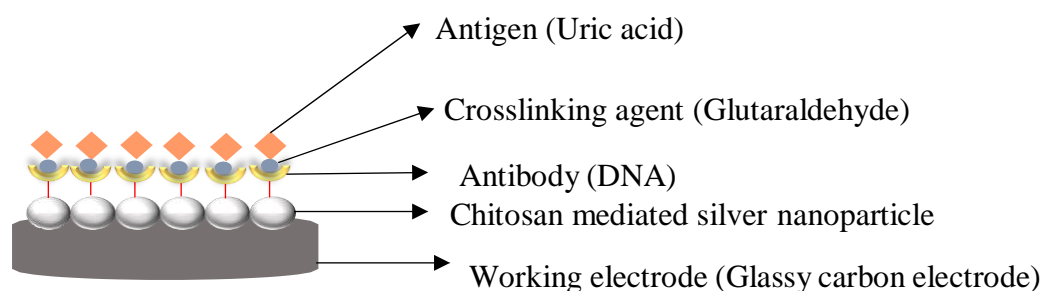


Fig 12. Schematic diagram of DNA based biosensor

3.5.4 Optimization and performance evaluation of DNA based biosensor

The DNA immobilization duration in the modified SPE by varying the DNA immobilization between 1 to 3 hours, whereas the DNA hybridization time was examined by increasing the DNA hybridization period from 20 to 40 minutes and the response was observed. The performance evaluation of DNA based biosensor was carried out by regeneration, linearity range, LOD (Limit of detection) and storage stability (Ebrahimi *et al.*, 2011).

3.5.5 Characterization of DNA based biosensor

3.5.5.1 FTIR

The functional groups was identified using the Fourier Transform Infrared spectroscopy (FTIR, Shimadzu & IR Affinity-1S, A22135901136) with wavelength range from 400 to 4700 cm^{-1} (Dayakar *et al.*, 2017).

3.5.5.2 Scanned electron microscope (SEM)

The SEM analysis was performed to observe the surface morphological characteristics of modified and uric acid (substrate) immobilized working electrode using the CAREL ZEISS, EVO 18 SEM was operated with voltage of 10 kV. The SEM micrographs of modified and substrate immobilized was analyzed at 5.00 kx magnification (Ramesh *et al.*, 2015).

3.5.6 Validation of DNA based biosensor

Sample preparation and HPLC method

The control and sample were spiked with different concentrations of UA (25, 50, 75 and 100 ppm). The spiked sample (2.5 g) was weighted in 50ml of centrifuge tube and 10ml of 0.5N HCl was added. The mixture was vortexed for 2 minutes and 20ml of Methanol: Acetonitrile: Water (1:1:1), vortexed for 5 minutes. The extract was neutralized using 3N NaOH (1ml) and shaken vigorously for 5 minutes using shaker. The mixture was centrifuged at 8000rpm for 10 minutes and the supernatant was added in 50ml volumetric flask. The supernatant was made up using Methanol: Acetonitrile: Water (1:1:1) and filtered using 0.45 μm syringe. The filtrate was injected in HPLC. The Chromatography was performed by HPLC (Agilent Technologies 1200 Series, USA), attached with autosampler, degasser, DAD detector, column thermostat and quaternary gradient pump. The column C18 (250 \times 4.6 mm, I.D., 5 μm) (Thermo Scientific, USA) at 25 $^{\circ}\text{C}$. Mobile phase consist of phosphate buffer (0.05M) with pH of 7.0 and its flow rate was 1 ml/min. The sample injection volume was 10 μl . The wavelength of DAD used for detection of uric acid was 290 nm (Ghadimloozadeh, Sohrabi, and Fard 2021).

3.6 Isolation and identification of microorganisms from contaminated food samples and its preventive measures

3.6.1 Isolation of uric acid microorganisms in infested food samples

The infested wheat flour (1 g) was added in 50ml of double distilled water at 250 rpm for one hour. The debris was settled down and the supernatant was inoculated in enrichment media which contains 0.3% UA. It was allowed to grow at 250rpm for 24 hours in incubator shaker. The culture was grown overnight, serial dilution was carried out and spread plate was done using nutrient agar for identification of microbes. The serial diluted samples of 10^{-5} and 10^{-6} were used for bacterial identification and 10^{-3} and 10^{-4} dilutions were used for fungal identification using Rose Bengal agar. Based on colony morphology, the bacterial and fungal strains was maintained separately and the plates were incubated at 37°C for 72 hours.

The screening of bacteria and fungi was performed by monitoring the presence of zone of clearance. The morphological characterization of bacteria was identified using gram staining and fungal strains morphology was identified using Lacto phenol Cotton Blue staining. The biochemical tests such as catalase, oxidase, starch hydrolysis, Indole, Methyl Red, Voges-Proskauer, Citrate utilization, nitrate reduction, Gelatin liquefaction and carbohydrate fermentation tests were performed to identify the bacterial strains (Atty and Joseph, 2016).

3.6.2 Identification of microorganisms using molecular techniques

The bacterial and fungal strains were used to extract the genomic DNA using MagGenome Xpress DNA isolation kit as per manufacturer instructions. The quantity of genomic DNA was assessed using UV-Visible spectrophotometer (Labman, LMSP-UV1200). The quality of DNA was good enough to carry on to PCR. The amplification of 16S rRNA genes and ITS region of bacterial and fungal strains was carried out using forward and reverse primers which is mentioned in Table 2. The expected band was amplified in all samples. The

PCR generated amplicon was confirmed and purified using GeneJET PCR purification kit (Thermo Scientific, EU-Lithuania) to remove the primer dimer and all other contaminations. The quality of the product was evaluated using 2% agarose gel with 100bp DNA ladder as standard and the product was found to be good for sequencing.

Table 2. Universal primers used for sequencing of bacteria and fungi

Primer for bacterial strain	Primer for fungal strain
27 f: AGAGTTTGATCMTGGCTCAG	ITS 5: GGAAGTAAAAGTCGTAACAAGG
1492 R: TACGGYTACCTTGTTACGACTT	ITS 4: TCCTCCGCTTATTGATATGC

The amplified PCR products was purified and cycle sequencing was done using the Big Dye® Terminator 3.1 sequence kit (Applied Biosystems, Foster City, California, USA). After the cycle sequencing, the products were purified using Ethanol-EDTA purification protocol to remove the un-incorporated dNTP's, ddNTP's and primer dimer. The purified cycle sequenced products were dissolved in 12µl Hi-Di formamide and the samples were subjected for denaturation at 95°C for 5 minutes. The denatured products were subjected for sequencing in forward and reverse direction using Genetic Analyzer 3500 (Life Technologies Corporation, Applied Biosystems®, California 94404, USA) as per manufacture's instruction. The sequence was aligned using MEGA 11 software to confirm the bacterial and fungal species (Atty and Joseph, 2016).

3.6.3 Extraction of essential oil using hydrodistillation method

The dried parts of various plants (Table 3) were collected in 1000ml round bottom flask and 100 g of samples was added to 500 ml of distilled water in a Clevenger - apparatus until oil distillation ceased after 5 h. The essential oil was collected in the glass vials, dried using anhydrous Na₂SO₄ (Palacios *et al.* 2009) and kept in the freezer for further studies.

Table 3. The plant parts selected for essential oil extraction

Common name	Scientific name
Orange peel	<i>Citrus sinensis</i>
Lemon	<i>Citrus limon</i>
Lemongrass	<i>Cymbopogon</i>
Rosemary	<i>Salvia rosmarinus</i>
Cinnamon	<i>Cinnamomum verum</i>
Clove	<i>Syzygium aromaticum</i>
Star anise	<i>Illicium verum</i>
Cumin seed	<i>Cuminum cyminum</i>
Caradamon	<i>Elettaria cardamomum</i>
Ginger	<i>Zingiber officinale</i>
Fennel seed	<i>Foeniculum vulgare</i>
Java plum	<i>Syzygium cumini</i>
Juniper seed	<i>Juniperus monosperma</i>
Black pepper	<i>Piper nigrum</i>
Nutmeg	<i>Myristica fragrans</i>
Mint	<i>Mentha piperita L</i>
Guava leaf	<i>Psidium guajava</i>
Black cumin seed	<i>Nigella sativa</i>
Curry leaf	<i>Murraya koenigii</i>
Tumeric	<i>Curcuma longa</i>
Thyme	<i>Thymus vulgaris</i>
Sweet marjorum	<i>Origanum majoranta</i>
Basil	<i>Ocimum tenuiflorum</i>
Sage	<i>Salvia officinalis</i>
Mosambi	<i>Citrus limetta</i>
Eucalyptus	<i>Eucalyptus globulus</i>
Mace	<i>Myristica fragrans</i>
Citron	<i>Citrus medica</i>
Orange peel and fruit	<i>Citrus × sinensis</i>
Coriander	<i>Coriandrum sativum</i>
Betel leaf	<i>Piper betle</i>

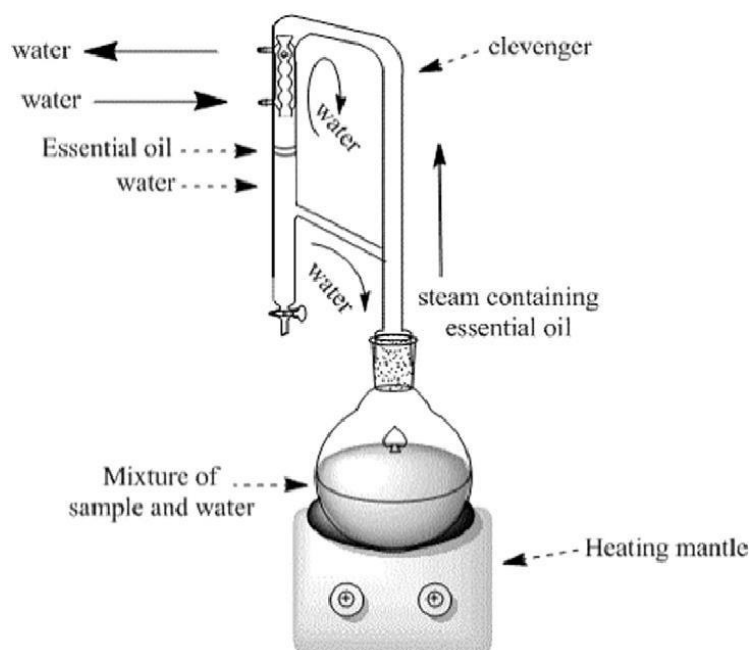


Fig 13. Extraction of essential oils using Hydrodistillation method (Clevenger apparatus)

3.6.4 Antioxidant assay (DPPH radical scavenging assay)

The DPPH (2, 2-diphenyl 1-picrylhydrazyl) was dissolved in 10ml methanol to get 200 μ M concentration. The 10 μ l of essential oil was diluted in 15 μ l of methanol and 175 μ l of DPPH solution was added. The sample was mixed well and after 20 minutes of incubation in dark, the absorbance was measured at 515 nm (Haliloglu *et al.*, 2017).

3.6.5 Total phenolic content

The total phenolic content was determined using UV-visible spectrophotometer using Folin-Ciocalteu's method. The 100 μ l of essential oil was diluted with 100 μ l of methanol, 2.5ml of 10% Folin-Ciocalteu's reagent was added. The mixture was covered and incubated for 2 minutes in dark condition. After incubation, 2ml of 7.5% sodium carbonate in water was added. The mixture was incubated for 1 hour at ambient temperature. The absorbance was measured at 765nm against blank (methanol) (Mak *et al.*, 2013).

3.6.6 Antimicrobial activity

The antimicrobial activity of essential oils was carried out by one bacterial and three fungal strains was evaluated by the disc diffusion method, with the presence of zone of inhibition, using nutrient agar (NA) for bacteria and Rose Bengal agar (RBA) for fungi. The 50 μ l of essential oil was added in sterile discs and the zone of inhibition (mm) was measured after 48 hours of incubation for bacteria (37°C) and fungi (27°C). The negative control for antimicrobial activity was used as acetone and the positive control was vanomycin (20 μ g/disc) was used to determine the microbial sensitivity (Binimeliz *et al.*, 2020).

3.6.7 Gas chromatography - Mass spectrometry (GC-MS) analysis

The GC-MS analysis of the essential oils (thyme, cinnamon, cumin seed, clove, star anise and ginger) which showed good antimicrobial activity was selected for GC system (Agilent 8890GC, USA) as earlier reported. The split/ splitless injector was equipped in this instrument. The capillary column Rtx-5MS (5% Diphenyl / 95% Dimethyl poly siloxane, 30m x 0.25mm ID 0.25mm thickness) was attached with the auto sampler and fitted along with Mass detector (Agilent 5977B series, USA). The carrier gas (Helium) was used with the flow rate of 1ml/min. The split ratio was maintained at 10:1 with injector temperature (280°C) and temperature of detector was 290°C. The column temperature was set at 110°C for 3.50 mins and the linear programming was performed from 110-280°C (at 5°C/min) for 12 mins. The inlet line temperature was kept at 280°C and mass spectra was acquired with the scan mode (70 eV) in range of 50-550 m/z . The 2 μ l of 1ml/l oil sample was diluted using hexane was injected. The compounds present in oils were obtained by chromatogram and it was used to compare the mass spectra with National Institute of Standards and Technology (NIST, 2020) libraries (Dev *et al.* 2010).

CHAPTER 4

RESULT AND DISCUSSION

Objective 1- To determine the uric acid levels in food samples during storage with rapid method using UV – visible spectroscopy

4.1 Validation of UV-Visible spectroscopic method to determine uric acid

4.1.1 Influence of storage period on uric acid content in wheat products

The uric acid content in insect infested wheat flour, maida, and rava were extracted and estimated using spectrophotometric methods (rapid and preceding) at weekly interval for 7 weeks. It was observed that the larvae contaminated the food material with uric acid ranged from 25 to 74 ppm within four weeks. The results showed a gradual significant increase in uric acid content in all wheat products. But the uric acid concentration decreases on 28th day due to the pupal stage which will not excrete the uric acid in that stage and at the same time uricase degrading microorganisms may act on uric acid (Atty and JosepH 2016). It was also observed that the uric acid level gets increases after 30th days (Table 4) due to second generation of *T. confusum* adults which will excrete uric acid (Gin Farn, 1963).

The increase in uric acid (UA) content may be due to increase in UA release by the larval stage as reported by Holmes (1980). But the UA level was comparatively less in rava throughout the period when compared to maida and wheat flour which may be due to the variation in preference of food products by *T. confusum* beetle. Similarly, the results showed that there was an increase in uric acid in all wheat products as the storage days' increases. The uric acid concentration of all wheat products showed significant difference from each other ($p < 0.05$) still 4th weeks of storage.

Table 4. Influence of storage period on uric acid content in wheat products using rapid method

Storage period (days)	Uric acid concentration (ppm)*		
	Rava	Maida flour	Wheat flour
0	0 ^h	0 ^h	0 ^h
7	25 ^g	27 ^f	35 ^f
14	46 ^f	46 ^d	50 ^d
21	53 ^c	63 ^c	68 ^c
28	61 ^b	66 ^b	71 ^b
35	66 ^a	69 ^a	74 ^a
42	49 ^d	20 ^g	30 ^g
49	48 ^e	37 ^e	40 ^e

* Values with different letters in the same column differ significantly ($p < 0.05$)

4.1.2 Comparison of linear regression for preceding and rapid method

The linear regression is normally used for the comparison of analytical methods. It was reported that aromatic characteristics of 2-cyano-N-(3-cyano-7-tetrahydrobenzo[b]thiophen-2-yl)-acetamide using multiple linear regression models showed an R value of 0.754 (Papa, Pilutti, and Gramatica 2008). Whereas present research work, the model outline of linear regression describes about the R value of 0.996 and 0.997 for preceding and rapid method respectively which showed the R value of both methods indicates good sign of prediction in regression model. The purine derivatives against c-Src tyrosine kinase showed best fit with R² of 0.802 was explained by earlier workers (Kissinger *et al.*, 1974). Similarly, the present study showed the R² of 0.991 and 0.994 for preceding and rapid method respectively (Fig 14 and 15). These results revealed that the R² value of 0.994 is more accurate and the rapid method is more

fit in the regression model. The adjusted R^2 of preceding and rapid method were 0.990 and 0.994 respectively.

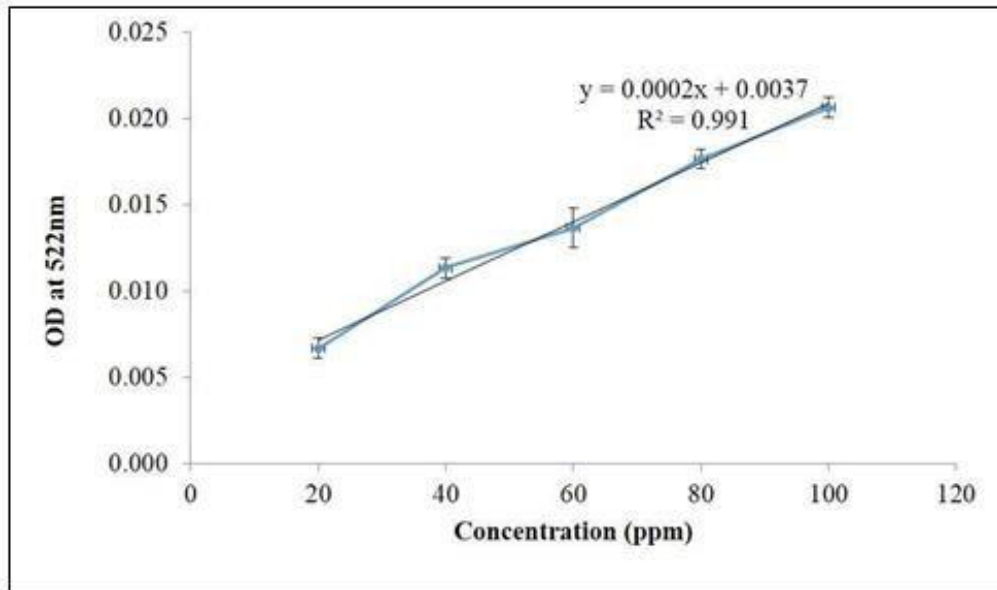


Fig 14. Calibration curve of the preceding method

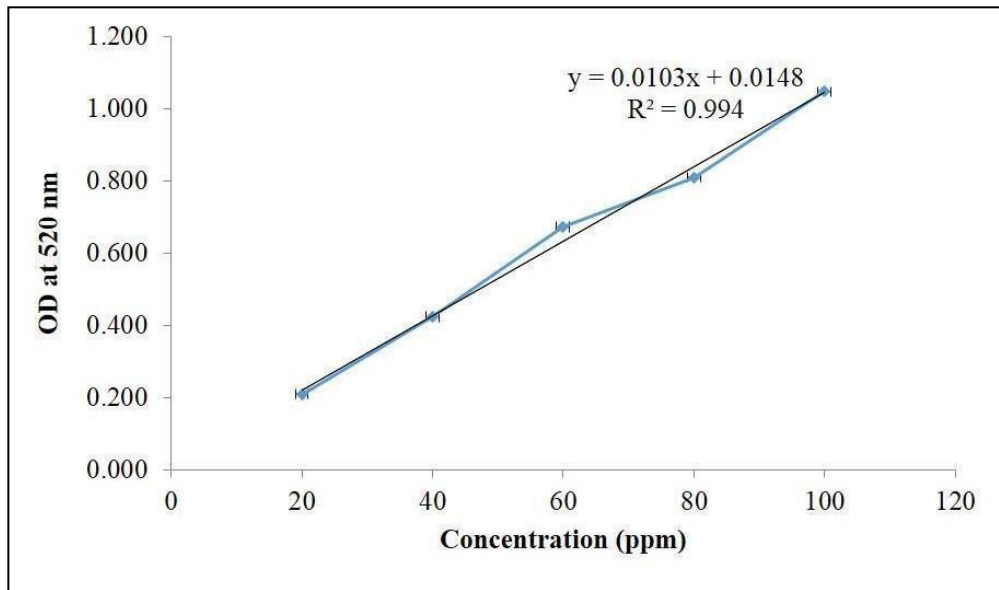


Fig 15. Calibration curve of the rapid method

The SE of model fit is a measure of precision. The SE of preceding and rapid method are 0.000572 and 0.024806 which are less than 2 as reported earlier by Dhakal (2019). The DW test indicated the autocorrelation of preceding and rapid method were 1.103 and 1.713 respectively which are less than 2 (Table 5).

Table 5. Validation of preceding and rapid method

Parameters	Preceding method	Rapid method*
R	0.996	0.997
R ²	0.991	0.997
Adjusted R ²	0.990	0.994
SE of the estimate	0.000572	0.024806
DW test	1.103	1.713
Time required per sample (min)	40	20

*Rapid method showed good fit with lesser time for each sample

The accuracy of the methods were predicted using multiple linear regression model with R, R² and SE in the present study which is similar to that the prediction of imidazo[1,2-a]pyrazine derivatives against cancer cell lines Log HepG-2 using multiple linear regression model with the terms of R, R², SE value (Chtita *et al.*, 2007). The results of the present study support the earlier report of Zakladnoy and Yaitskikh (2020), uric acid detection which can be used as an index of insect infestation. It also demonstrated a positive linear correlation between the amount of uric acid and the density of rice weevil, *S. oryzae* in wheat grain.

4.1.3 CART® regression model using MiniTab for preceding and rapid method

The CART® regression is to create decision tree for continuous variable with categorical and continuous predictor variables. In preceding method, the regression tree (Fig 16) showed that the terminal node 1 have mean of absorbance of 0.0063 while in terminal node 5 showed the mean of absorbance as 0.0192 whereas in rapid method, the tree at the terminal node 1 showed absorbance mean as -0.0016 and the mean value of absorbance as 0.9977 at terminal node 5. In preceding method (Fig 17), the results showed that absorbance increases with concentration of uric acid at terminal node 5 showed optimal R² value of 0.8803 (Fig 18A) while in rapid method, at terminal node 5 showed that the absorbance and concentration of uric

acid increases with the optimal R^2 value of 0.9363 (Fig 18B). The scatterplot of actual response value on x-axis and predicted response value on y-axis. The quality of actual and predicted values was represented in the green line. The accuracy of prediction is very high, when the actual and predicted values are identical in case of rapid method (Fig 19B) but in case of preceding method, the actual and predicted values are not identical (Fig 19A) that reveals the prediction is less accurate compared with rapid method.

The input data for regression tree model was the concentration of ground deposition at different distances that will obtain the pattern of accident and to establish prediction model. The actual response value was represented on X-axis whereas predicted response value was represented on Y-axis in scatterplot. The equality of actual and predicted values was represented in green line. The predicted and actual values are similar that shows more prediction accuracy. The training and test data points shows similarity whereas the performance of tree on training data is close to the performance of tree on test data. The R^2 for training and test data was 0.998 and 0.994. This showed better linear relationship between the original data and predicted data. In training and test data showed the mean absolute percentage error (MAPE) with range from 26.9 to 28.1 per cent as observed by Hameed and Kim, (2021).

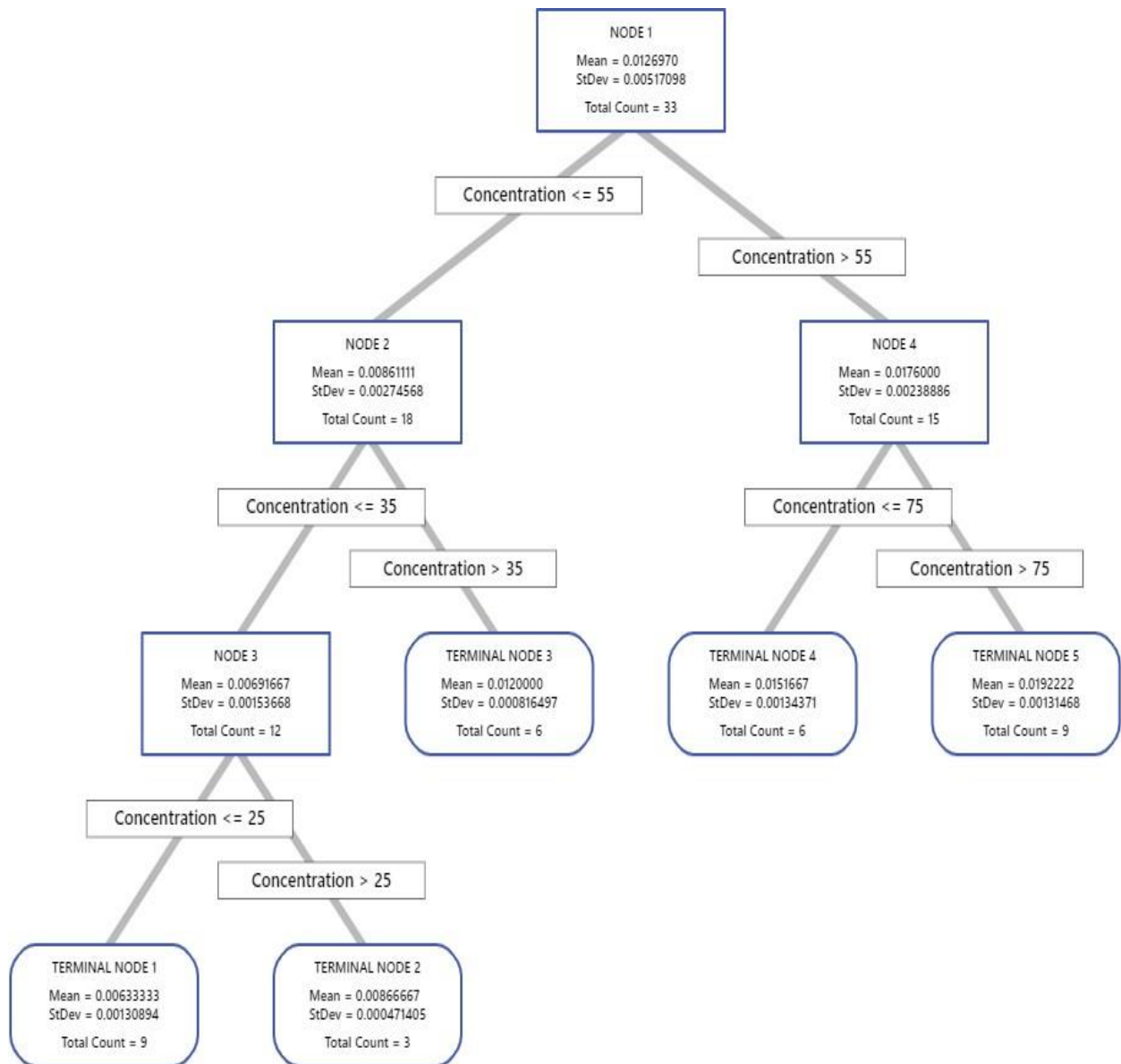


Fig 16. Regression tree diagram of UA (preceding method) of CART regression model

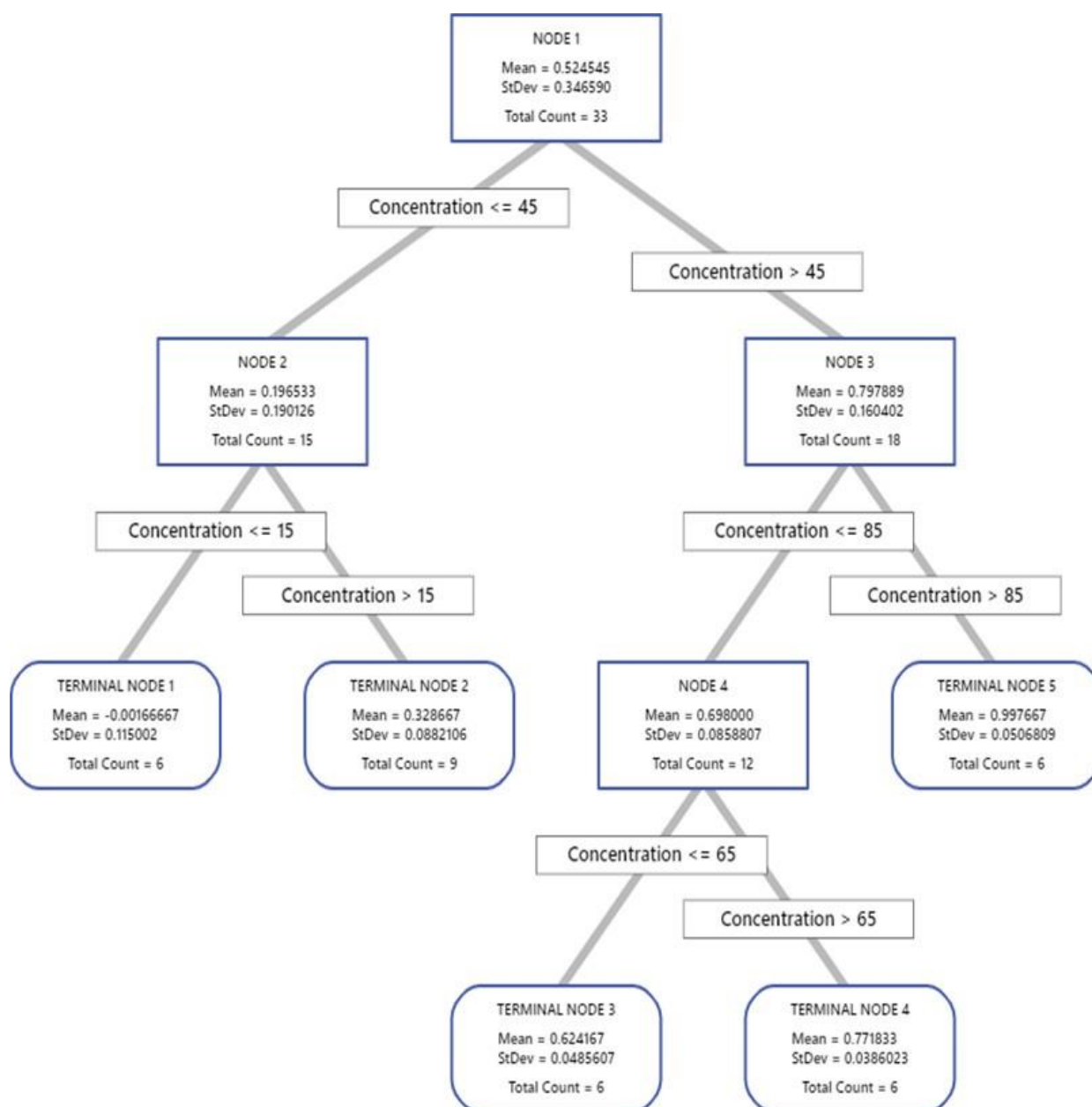


Fig 17. Regression tree diagram of UA (rapid method) of CART regression model

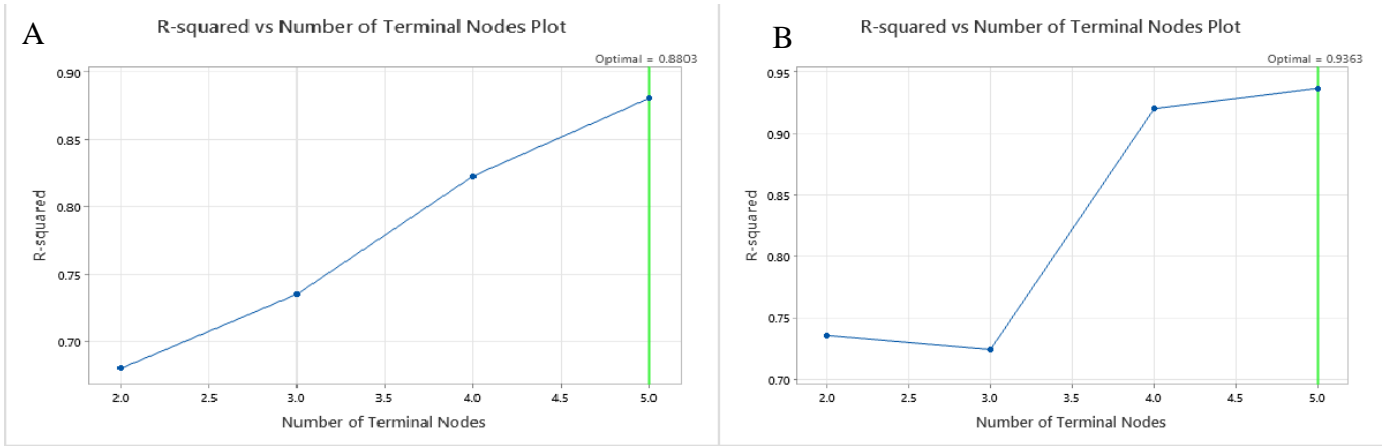


Fig 18. R^2 versus terminal node plot A) preceding method and B) Rapid method

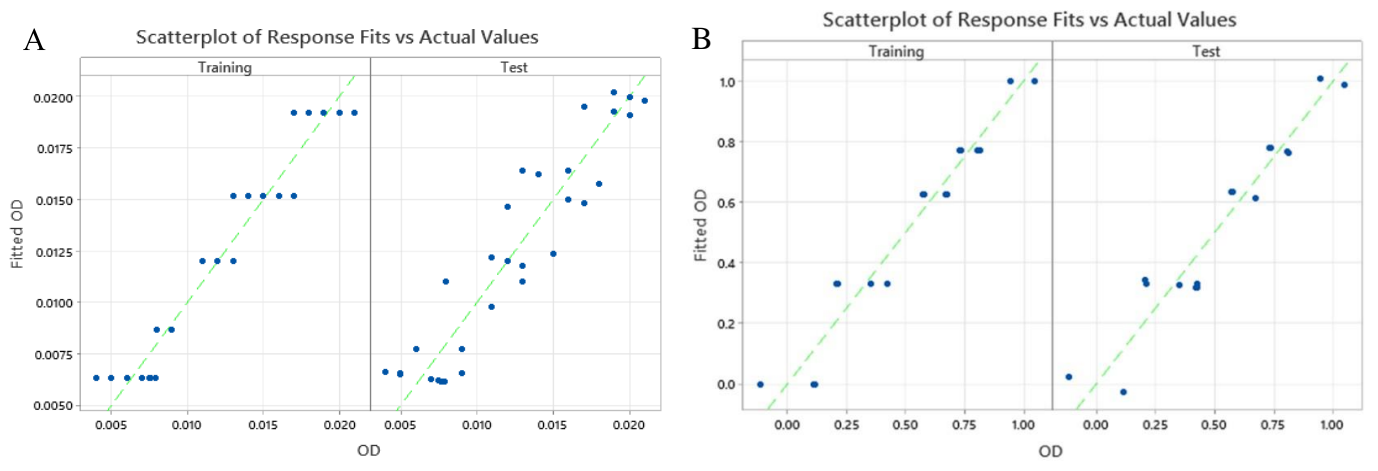


Fig 19. Scatterplot of response fit Vs actual values A) preceding method and B) Rapid method

Table 6. Validation of model parameters that shows Goodness of fit for colour intensity against concentration (ppm)

Statistics	Preceding method		Rapid method	
	Training	Test	Training	Test
R ²	0.947	0.880	0.953	0.936
RMSE	0.001	0.002	0.076	0.088
MSE	0.000	0.000	0.006	0.008
MAD	0.001	0.002	0.067	0.078
MAPE	0.103	0.160	0.291	0.34

In preceding method, the RMSE, MSE, MAD and MAPE value of training model showed 0.001, 0.000, 0.001 and 0.103 respectively whereas test model showed 0.002, 0.000, 0.002 and 0.160 respectively. In rapid method, RMSE, MSE, MAD and MAPE values of training model showed 0.076, 0.006, 0.067 and 0.291 respectively whereas test model showed 0.088, 0.008, 0.078 and 0.34 respectively. The RMSE, MSE, MAD and MAPE value were within the range of 0.2-0.5 which shows that the model is predicted accurately. The CART[®] regression for rapid method that the R² of training and test data (0.953 and 0.936) showed better accuracy than the preceding method with R² of training and test data were 0.947 and 0.880 (Table 6). In food samples, the maida flour showed more accuracy compared to rava and wheat flour in rapid method.

4.1.4 Cluster analysis

In hierarchical cluster, the average and maximum distance from centroid is the measure of variability within each cluster. The dendrogram showed the formation of two clusters in preceding and rapid method to determine UA (Fig. 20). The similarity level of

preceding method showed 40 per cent whereas rapid method showed 50 per cent. The similarity level showed more accurate in rapid method than the preceding method.

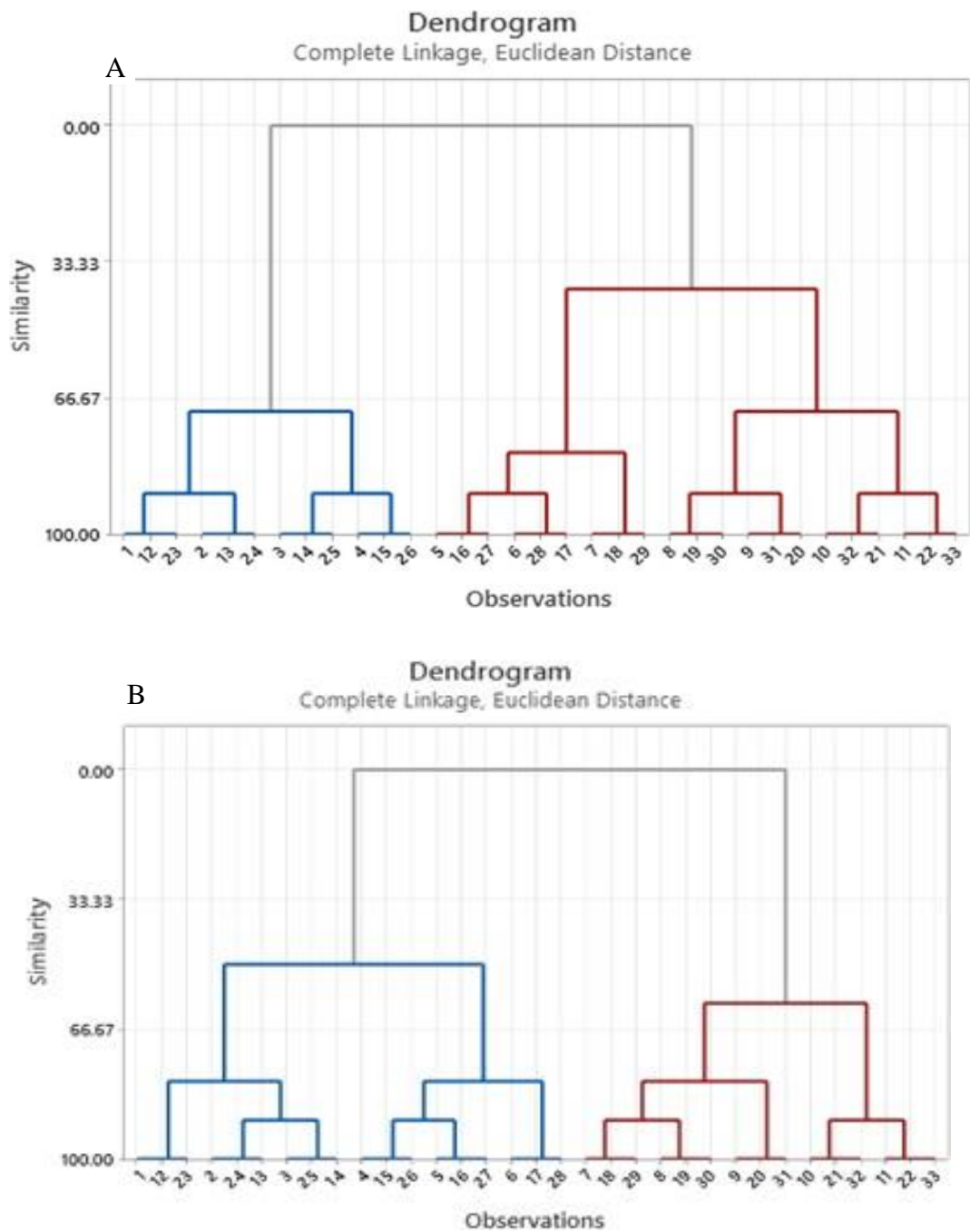


Fig 20. Dendrogram of preceding (A) and rapid method (B) to determine UA

Kebeya *et al.*,(2021) carried out the cluster analysis for mozzarella cheese enriched with orange fleshed sweet potato (OFSP) with sensory attributes. The influence of the sensory characteristics to the overall acceptability of the cheese products enriched with OFSP was

found into three group of clusters: cluster 1 has colour only, cluster 2 has aroma, texture and fibrousness, but cluster 3 has taste and acidity.

The cluster analysis was performed and dendrogram was prepared for the *Phyllanthus niruri* from 15 locations. It has been divided into 5 group of clusters. The samples of *P.niruri* was grouped in different cluster due to different quality and chemical content. The development of five clusters of *P.niruri* sample was assessed due to the terrestrial condition of sample source. The grouping of clusters of *P.niruri* samples was due to impact of altitude and some other factors (Kartini *et al.*, 2021).

Objective 2. To develop paper-based strip to detect UA levels in infested food samples

4.2.1 Color profiling

The paper strip has been developed using Whatman filter paper No.40 as base material with 20 mm of width and 60 mm of height (Fig. 8). Then, ferric chloride (30 μ l, 0.02M) was added to the surface of the paper strip. The different concentration of standard uric acid and extracted filtrate from all wheat products was treated with potassium ferricyanide (30 μ l, 0.02M) where the uric acid present in the filtrate will react with potassium ferricyanide to form potassium ferrocyanide. When potassium ferrocyanide react with ferric chloride leads to Prussian blue colour formation. The colour formation was captured by a GigE vision area scan camera (C1600, Genie color series, DALSA) fitted with a magnifying lens (Zoom 7000, 9mm, Navitar). The captured images were analyzed using Matlab software. The MATLAB code was generated to determine the uric acid present in wheat flour.

The MATLAB coding was developed to determine the concentration and colour intensity of UA. The colour chart of different concentrations of UA that showed the colour intensity decreases when the concentration increases (Fig. 21).

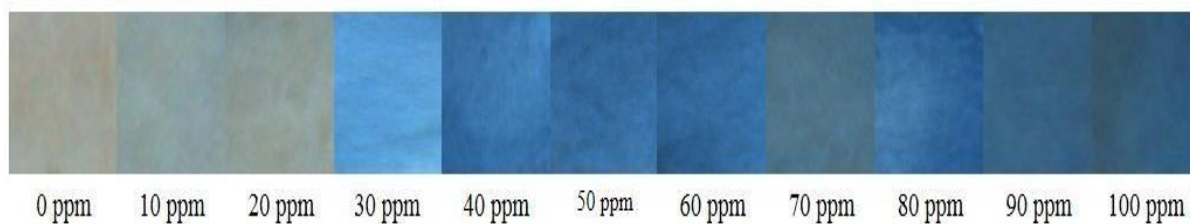


Fig 21. Color chart of different concentration of standard uric acid

Islam *et al.* (2018) has highlighted the development of paper based diagnostic method to quantitative and qualitative detection of uric acid in human urine samples. The determination of uric acid in human urine samples using MATLAB coding was revealed as use of software application and diagnostics. The paper based diagnostic device was suitable for detection of uric acid in human urine samples and also other biofluids. This technique was cheap, biocompatible, and biodegradable and gives results within few seconds. Similar attempt was made in the present study and gave good results.

4.2.2 Linear regression model using XLSTAT

The multiple linear regression of colour intensity can be validated in terms of R^2 , MSE, RSME, MAPE, DW, Cp, AIC, SBC and PC values that refers to goodness of fit of colour intensity as validated. The data obtained in the present method were analyzed and presented the values of R^2 , MSE, RSME, MAPE, DW, Cp, AIC, SBC and PC (Table 7).

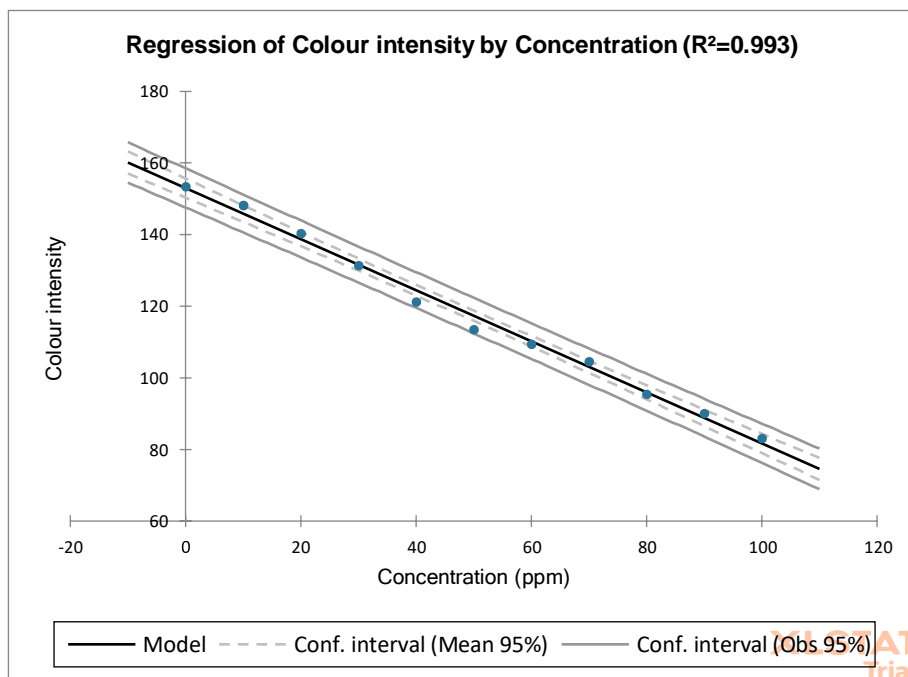


Fig 22. Regression plot of colour intensity by concentration (ppm)

In general, the R^2 reveals 60 per cent of variance is acceptable to consider that the model is fitted. In this method, the R^2 showed 99.3 per cent of variances in colour intensity is accounted by linear regression with the concentration (ppm) and showed that the model of fit test (Fig.22). The adjusted R square (adj. R^2) is used instead of R^2 by adding uneventual independent variables to model to raise the R^2 . In this analysis, adj. R^2 of 99.2 per cent variation in colour intensity can be attributed to the concentration (ppm) that showed it is an excellent model. In linear regression, the RMSE showed the accuracy of the model which is fit or unfit. The RMSE value less than 7 is acceptable value for the scientifically community. In our cases, the RMSE is about 2.102 for colour intensity showed that the model is accurate and fit.

Table 7. Validation of model parameters that shows Goodness of fit for colour intensity against concentration (ppm)

Comments	Colour intensity
Equation of model	$y=153.045-0.713*x$
R Squared	0.993
Adjusted R Squared	0.992
MSE	4.420
RMSE	2.102
MAPE	1.358
DW	0.934
CP	2.000
AIC	18.140
SBC	18.935
APC	0.010

MAPE is an average of absolute percentage error. MAPE value less than 20 per cent is acceptable for the model. MAPE value of colour intensity was 1.358 per cent which showed the accuracy of the model. The DW is a test for autocorrelation in the residuals from a regression analysis. The DW value less than 2.0 indicates positive autocorrelation. The DW value of 0.934 of colour intensity in the present study showed positive autocorrelation that achieves the consistency of β increases with the intensity with autocorrelation (Table 6). Similarly, AIC and SBC showed that the results were accurate as reported by Kumari and Yadav (2018). Hence, the paper based method of uric acid estimation found to be the accurate method.

4.2.3 CART[®] regression model of paper strip

In CART[®] regression, the regression tree showed that the terminal node 1 have mean of colour intensity as 153.507 while in terminal node 11 showed the mean of colour intensity as 83.174 (Fig 23). The results showed that colour intensity decreases with increase in concentration and at terminal node 11 showed optimal R² value of 0.9615 (Fig 24).

Table 8. Validation of paper strip using CART predictive analytics

Statistics	Paper strip	
	Training	Test
R ²	0.967	0.962
RMSE	4.158	4.521
MSE	17.288	20.436
MAD	3.095	3.351
MAPE	0.026	0.028

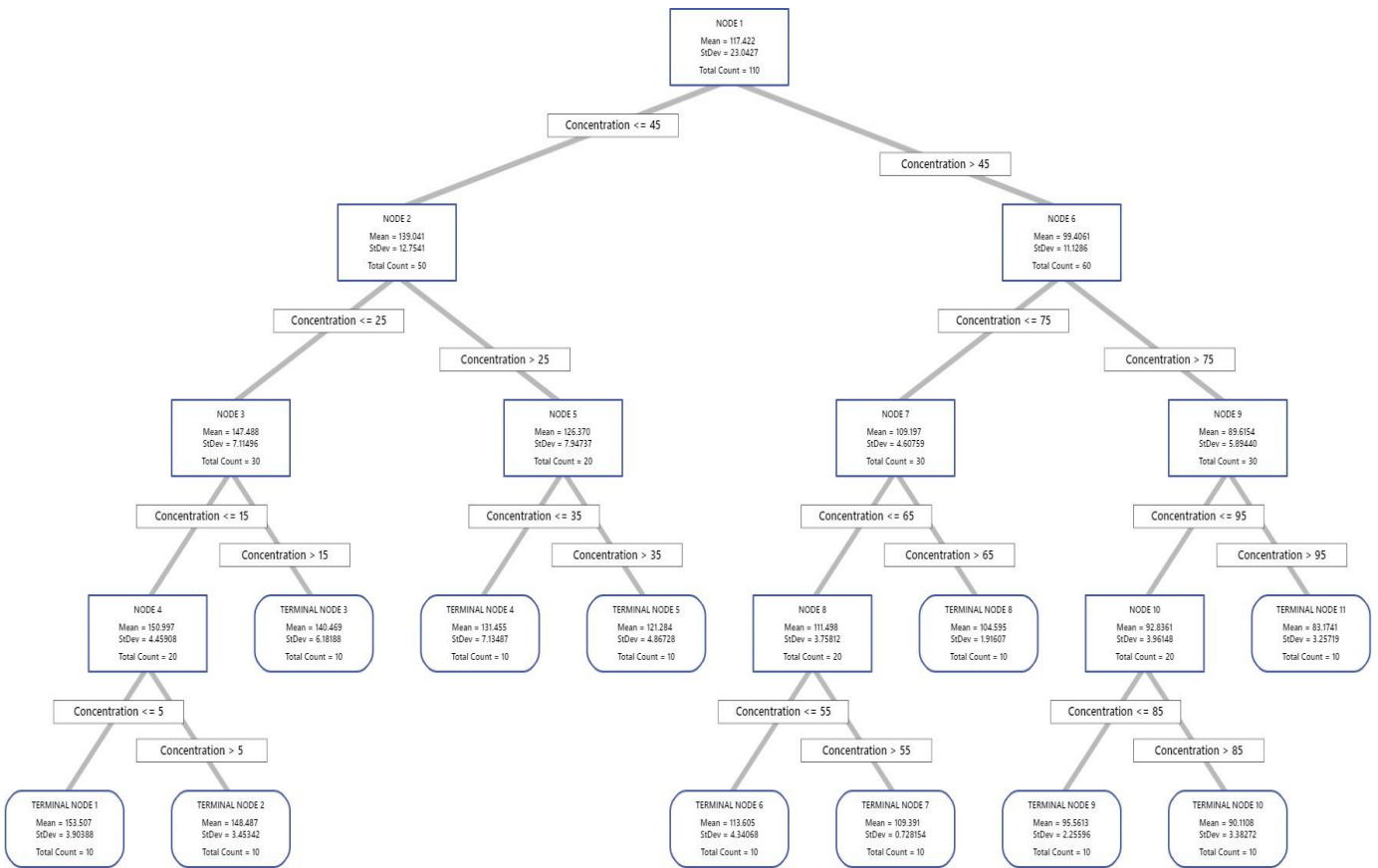


Fig 23. Regression tree diagram of UA (paper strip) of CART regression model

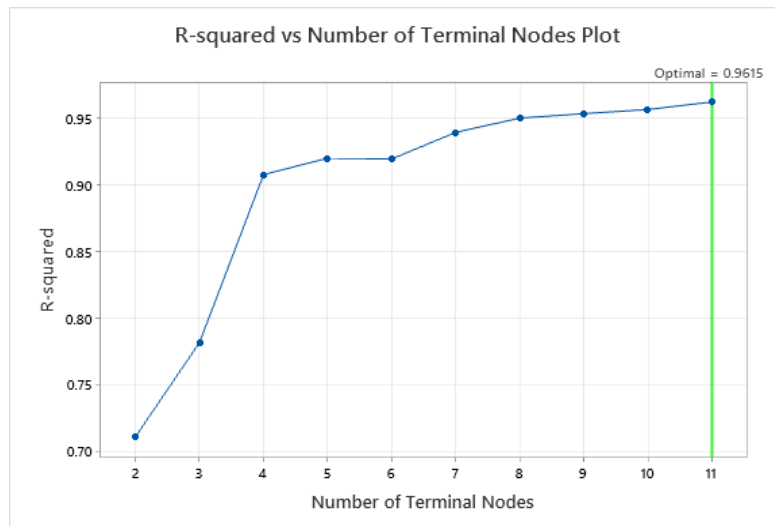


Fig 24. R^2 versus terminal node plot of paper strip

The scatter plot of actual response value on x-axis and predicted response value on y-axis were presented in Fig.25. The quality of actual and predicted values was represented in the green line. The accuracy of prediction is very high, when the actual and predicted values

are identical. The training and test data set points are almost in similar pattern. The performance of tree on test data is close to the performance of tree on training data. The R^2 of training data (0.967) and test data (0.962) showed significant positive linear relationship between the actual and predicted values. The mean absolute percentage error (MAPE) is 0.026 for training data and 0.028 for test data set (Table 8). The paper strip method showed good accuracy with low MSE, MAPE where the uric acid content decreases within month due to flour based wheat products that will observe moisture easily, when compared with whole grains.

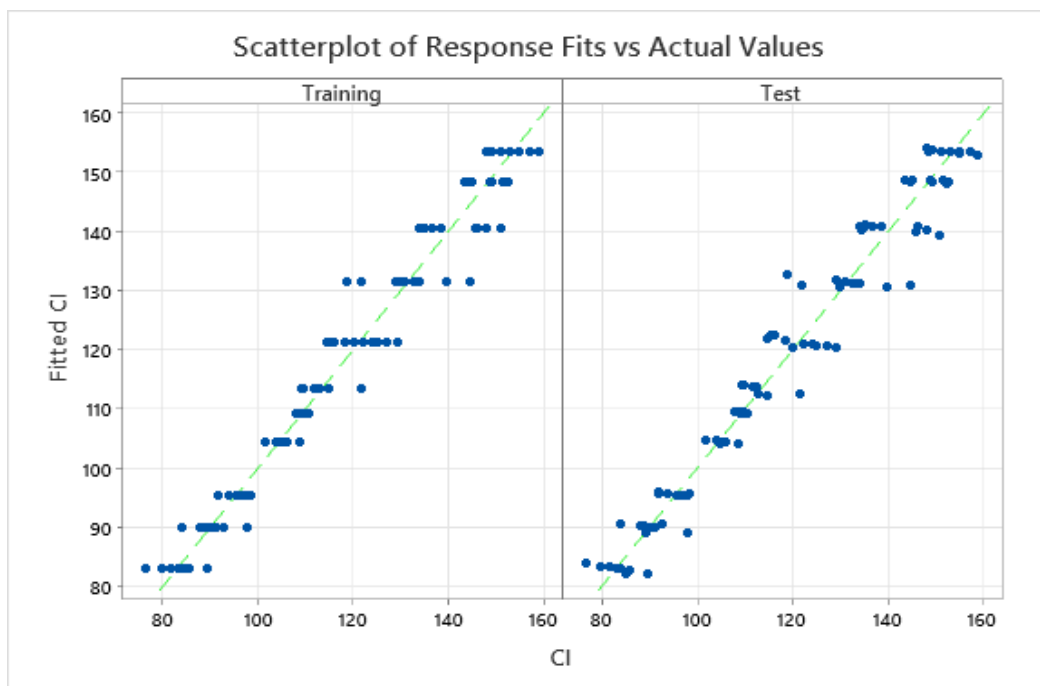


Fig 25. Scatterplot between the real value of the colour intensity and the predicted values of the colour intensity observed in paper-strip for the training data set and the test data

Objective 3. Validation of paper-based strip to detect UA levels in wheat products

4.3.1 Neural network for standard uric acid

The BFG-FNN showed overall R^2 of 0.9833 which was more accurate than LM-FNN, RP-FNN and SCG-FNN. The Mean Squared Error (MSE) is equal to 15.839 at 688 training iteration that showed the best performance of validation than LM-FNN, RP-FNN and SCG-FNN for standard uric acid. In BFG-FNN, the gradient value increases at 694th iteration with the value of 0.108 and the validation fail due to validation check at 694th iteration with the value of 6. This showed that among these four algorithms, BFG-FNN found more accuracy than other three algorithms for standard uric acid (Fig 26-28).

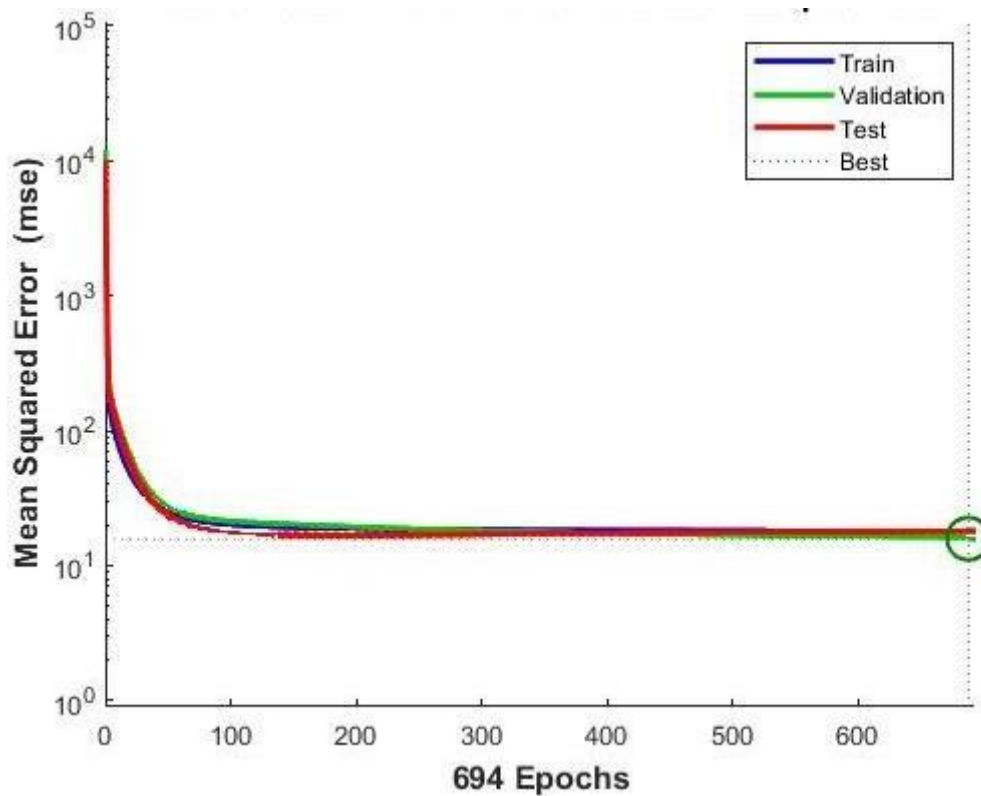


Fig 26. Performance plot of standard uric acid using BFG-FNN algorithm

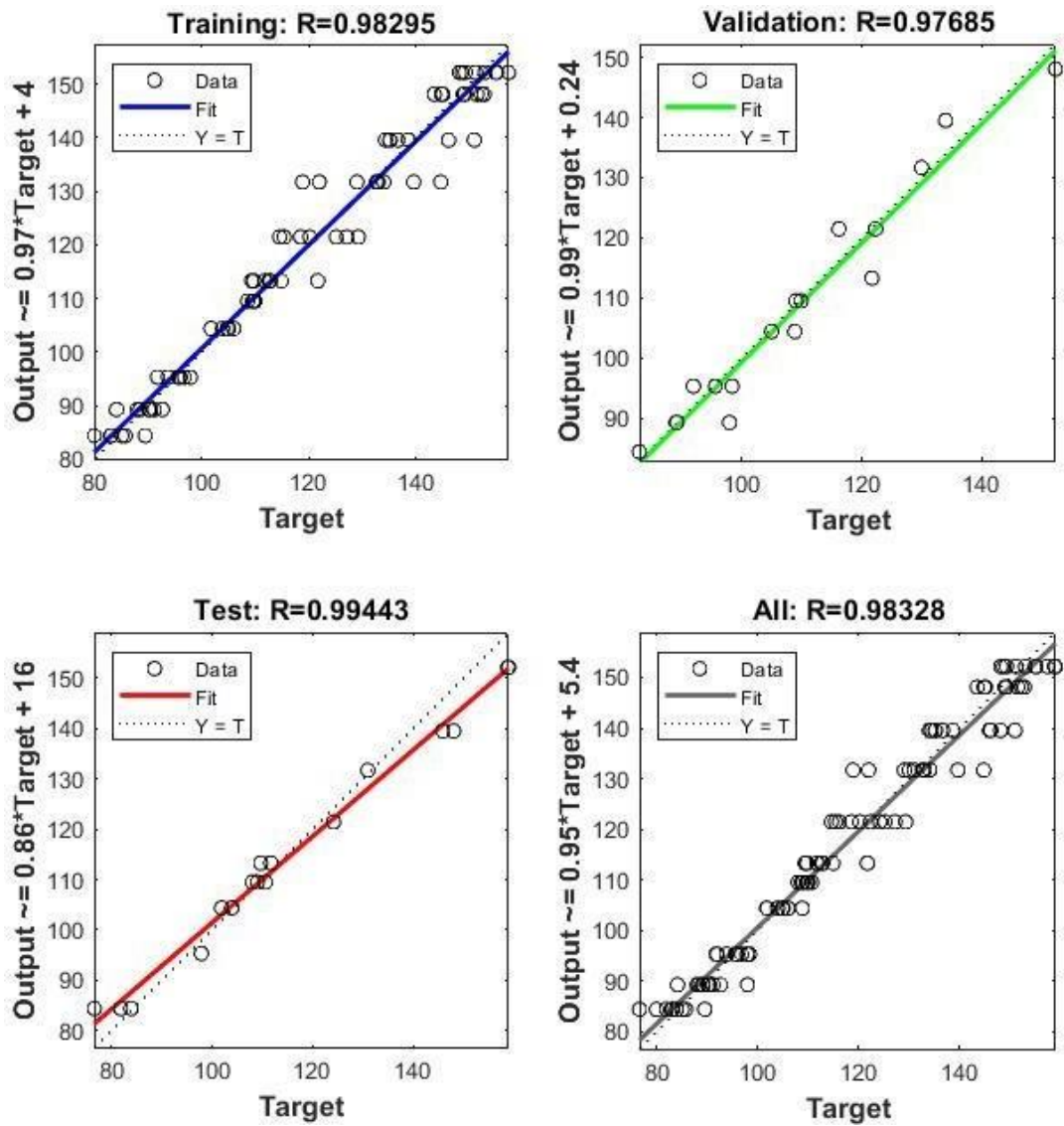


Fig 27. Regression plot of standard uric acid using BFG-FNN algorithm

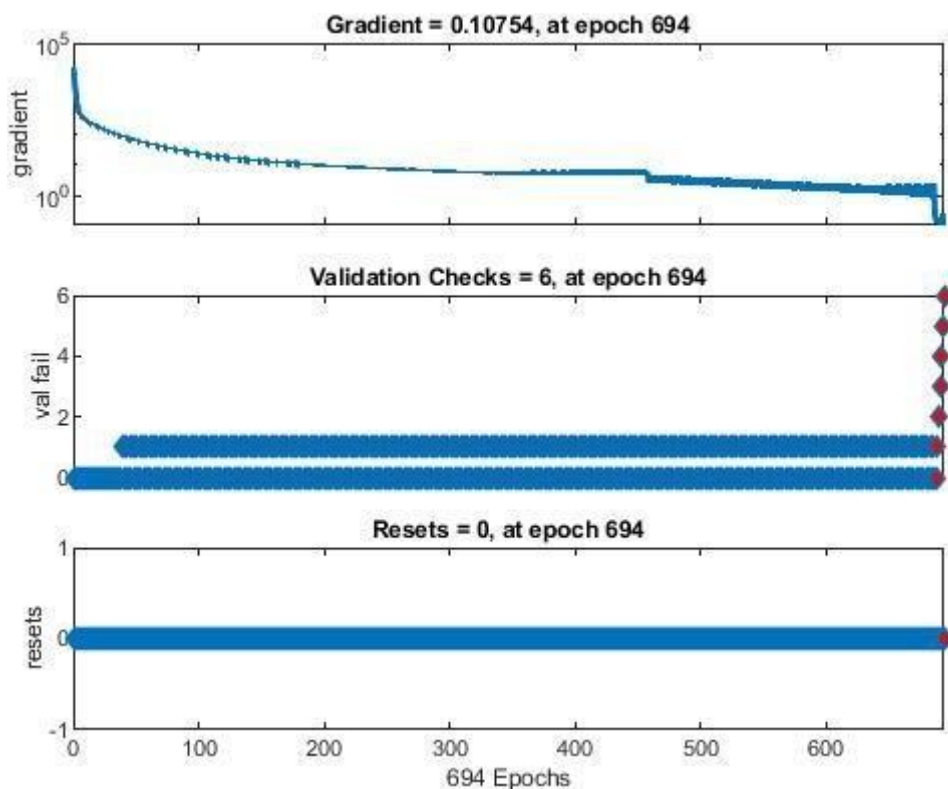


Fig 28. Training state of standard uric acid using BFG-FNN algorithm

Similarly, the eugenol percentage yield by batch experimental data was predicted by the neural network model development (Ghanta et. al., 2022). The model output showed the best prediction and the neural network was designed with 5 input variables and 8 neurons within the single hidden layer. The minimum MSE value of training data was 0.0011 and maximum R^2 value was 0.9990. The parameters of neural network model indicated good agreement among the experimental and predicted yield of eugenol.

The antioxidant activity and phenolic compounds was extracted from *Musa acuminata* (unripe) peel waste using microwave-assisted extraction and also studied the correlation between the response surface methodology (RSM) and artificial neural network (ANN) (Saidet.al., 2020). Both RSM and ANN has showed better prediction for antioxidant and total phenolic compound (TPC). The ANN model showed higher prediction due to its coefficient of determination (R^2) for ANN was 0.9803 and RSM was 0.9742, Root mean square error

(RMSE) for ANN was 2.69 whereas RSM was 3.07 observed for both antioxidant and TPC (Saidet.al., 2020).

4.3.2 Neural network model for real time samples

The neural network model has been carried on for the control and infested wheat products (Maida, Rava and wheat flour). The overall R^2 of 0.7011 and the MSE of 359.651 were showed in uninfested maida at 5th iteration among 11th iterations and the gradient value decreased at 11th iteration with 9.619 value and mu value also decreased at 11th iteration with value of 1 in LM-FNN algorithm. The LM-FNN showed more accuracy than other three algorithms for uninfested maida (Fig 29-31). Abasi *et al.* (2021) has studied the measurement of neomycin (NEO), nystatin (NYS) and triamcinolone (TA) using the Levenberg-Marquardt (LM) and Scaled conjugate gradient (SCG) algorithm with feed forward back propagation neural network (FFBP-NN) which was used in this analysis. The LM algorithm showed least mean square error (MSE) for NEO = 3.20×10^{-28} , NYS = 2.18×10^{-29} and TA = 1.62×10^{-28} . The RMSE of LS-SVM for NEO = 0.488, NYS = 0.350 and TA = 0.409. The LM algorithm showed better accuracy than other algorithm.

The authors (Amin *et al.*, 2013) has highlighted that the data mining was one of the method to predict and clinical decision support system to diagnosis the various heart diseases with risky factors. The genetic algorithm and new hybrid model of neural network was used to optimize the connection weight of ANN to improve the performance of ANN model.

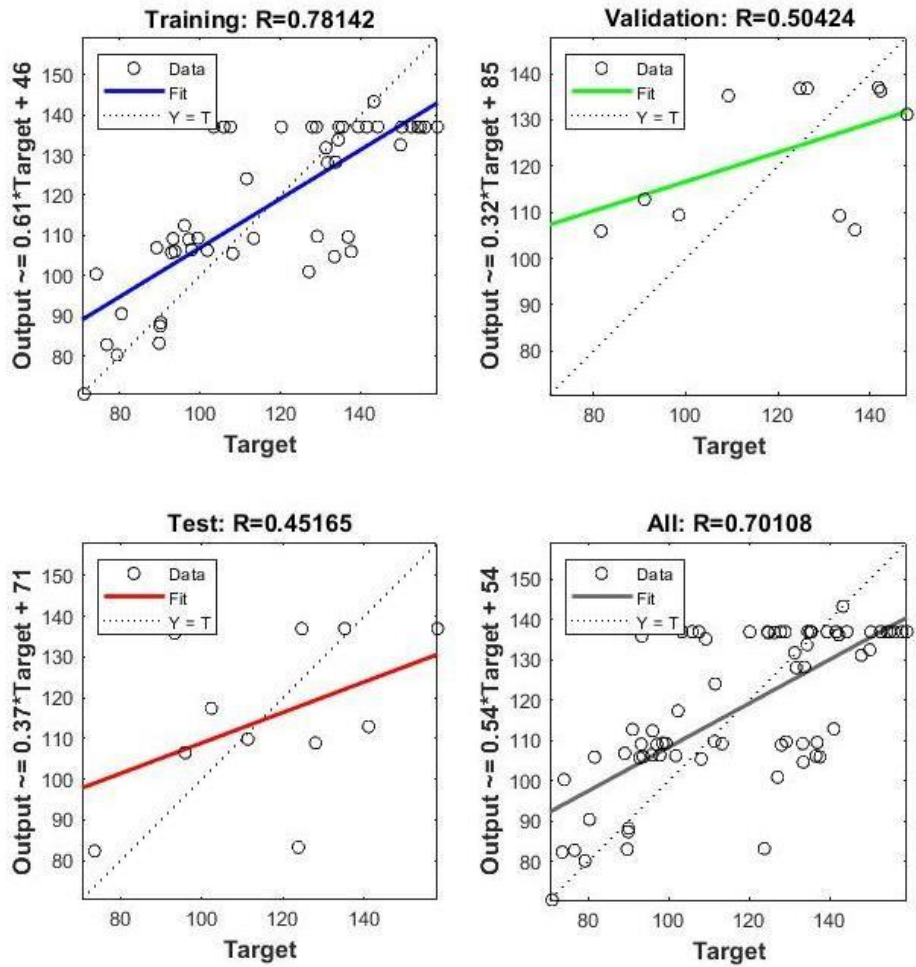


Fig 29. Regression plot of uninfested maida sample using LM-FNN algorithm

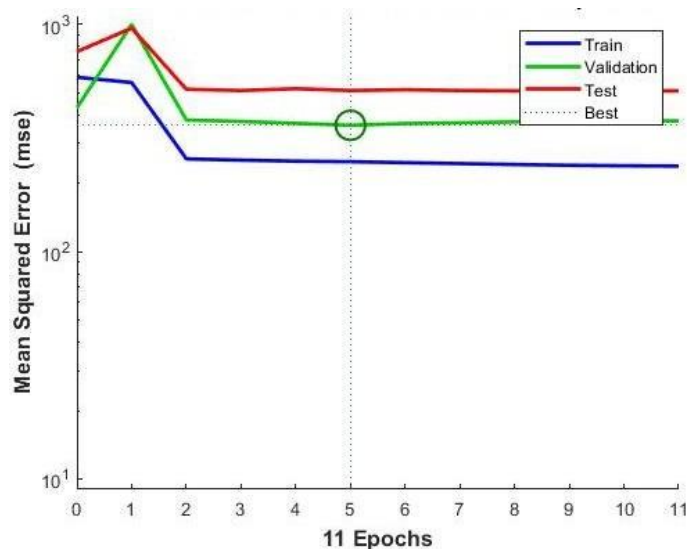


Fig 30. Performance plot of uninfested maida sample using LM-FNN algorithm

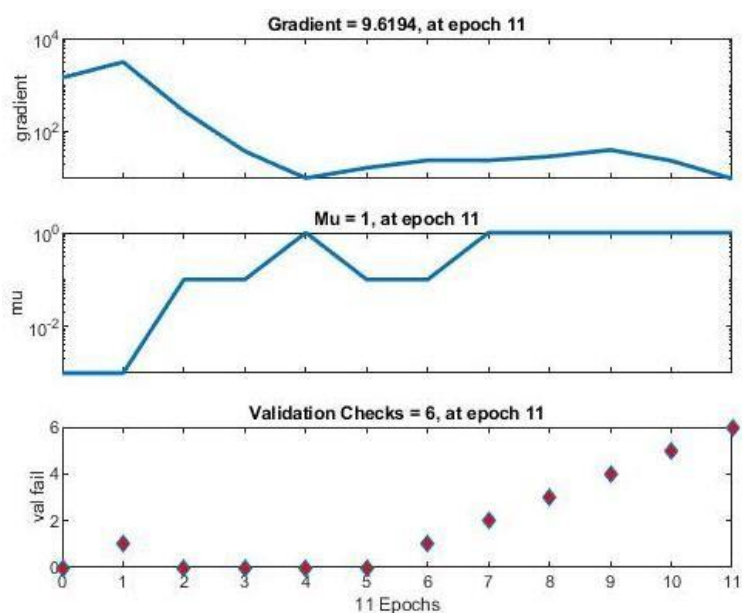


Fig 31. Training state of uninfested maida sample using LM-FNN algorithm

In infested maida samples, the overall R^2 of 0.9863 and the MSE of 11.041 were observed at 21st iteration among 24th iterations and the gradient value increased at 24th iteration with $4.972 \cdot 10^{-11}$ value and mu value also increased at 24th iteration with value of $1 \cdot 10^{-5}$. The other three algorithms showed less accuracy than LM-FNN (Fig 32-34). In this work, the estimation of clavulanic acid (CLV) and amoxicillin (AMX) present in tablets, blood serum and binary

mixtures using spectrophotometric method with combination of AI that include radial basis function neural network (RBF-NN) and FFBP-NN. The RBF-NN showed better prediction compared with FFBP-NN model (Salehian, Sohrabi, and Davallo 2021).

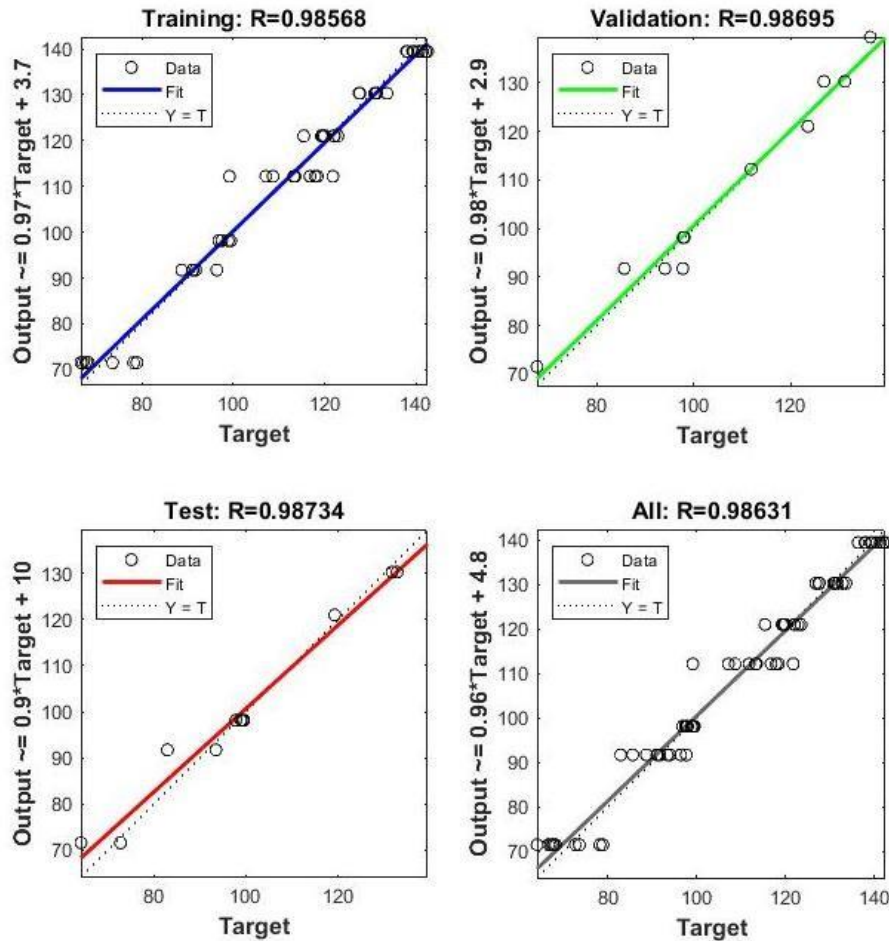


Fig 32. Regression plot of infested maida sample using LM-FNN algorithm

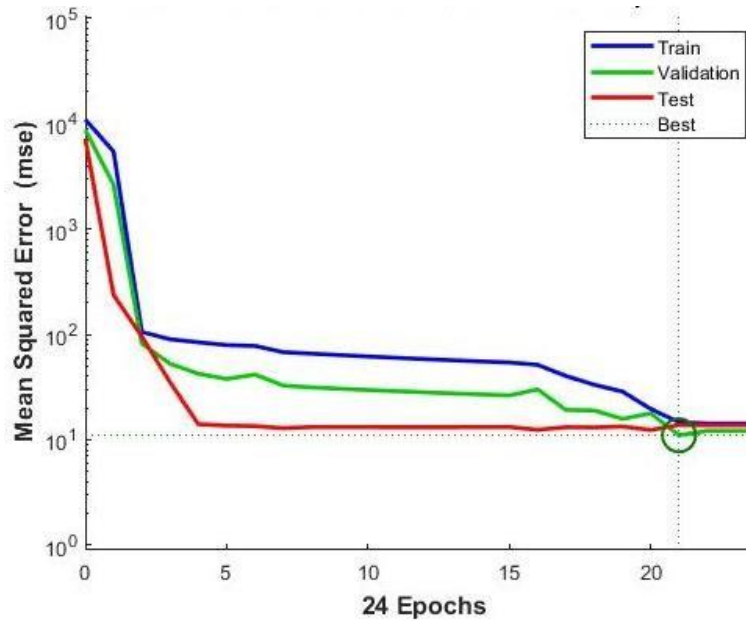


Fig 33. Performance plot of infested maida sample using LM-FNN algorithm

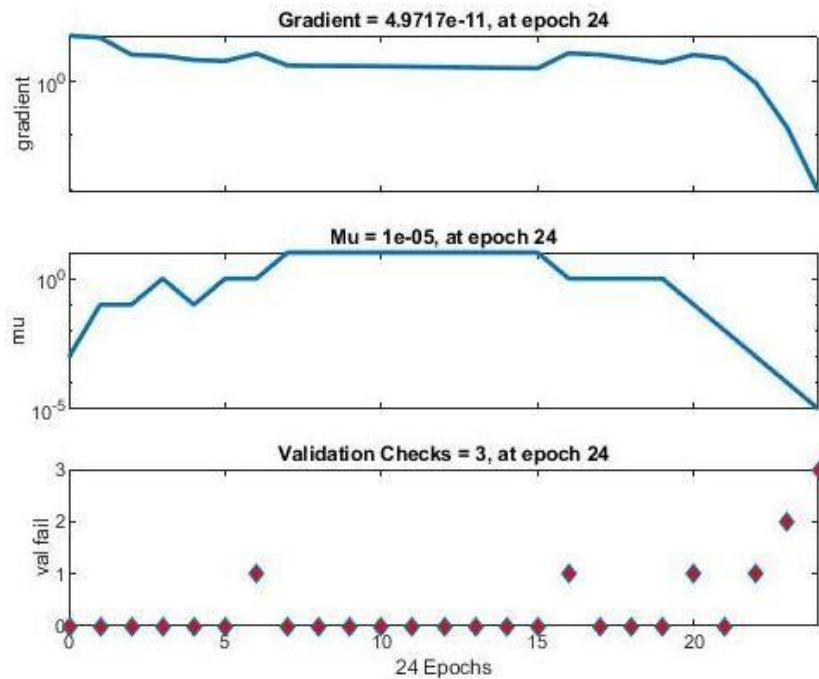


Fig 34. Training state of infested maida sample using LM-FNN algorithm

In uninfested rava sample, the overall R^2 of 0.2026 and the MSE of 235.406 were observed at 13th iteration among 19th iterations and the gradient value increased at 19th iteration with 30.112 value and mu value also increased at 19th iteration with value of 0.01. The LM algorithm showed better accuracy than other algorithm models (Fig 35-37).

The determination of fluticasone (FLU) and salmeterol (SMT) present in anti-asthma spray and synthetic mixtures was done using spectrophotometric method with combination of ANN (FFNN-LM and FFNN-GDA) and support vector regression (SVR) models (Valizadeh *et.al.*, 2021). The GDA algorithm showed less ability compared with LM algorithm in case of MSE. The LM algorithm of training, validation and test datasets showed RMSE of 0.168, 0.238 and 0.192 for SMT whereas 0.275, 0.360 and 0.331 for FLU. The LM algorithm showed best prediction and accuracy than GDA.

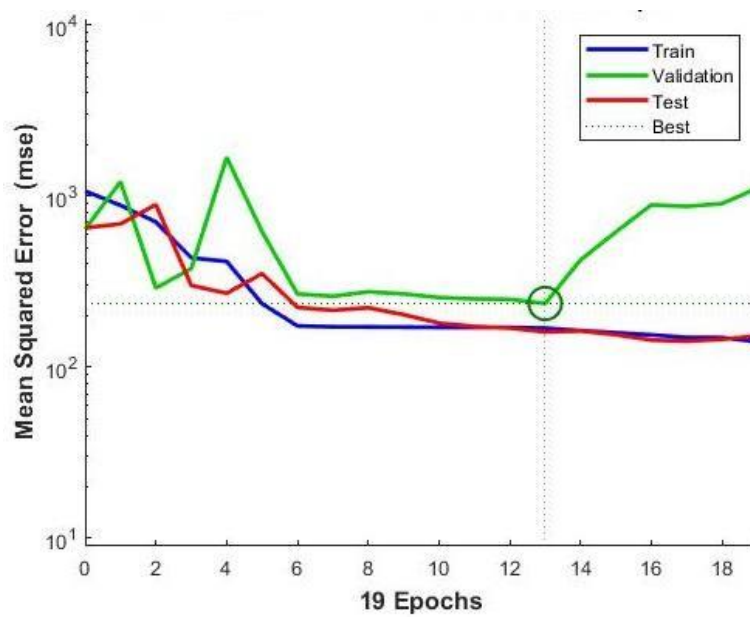


Fig 35. Performance plot of uninfested rava using LM-FNN algorithm

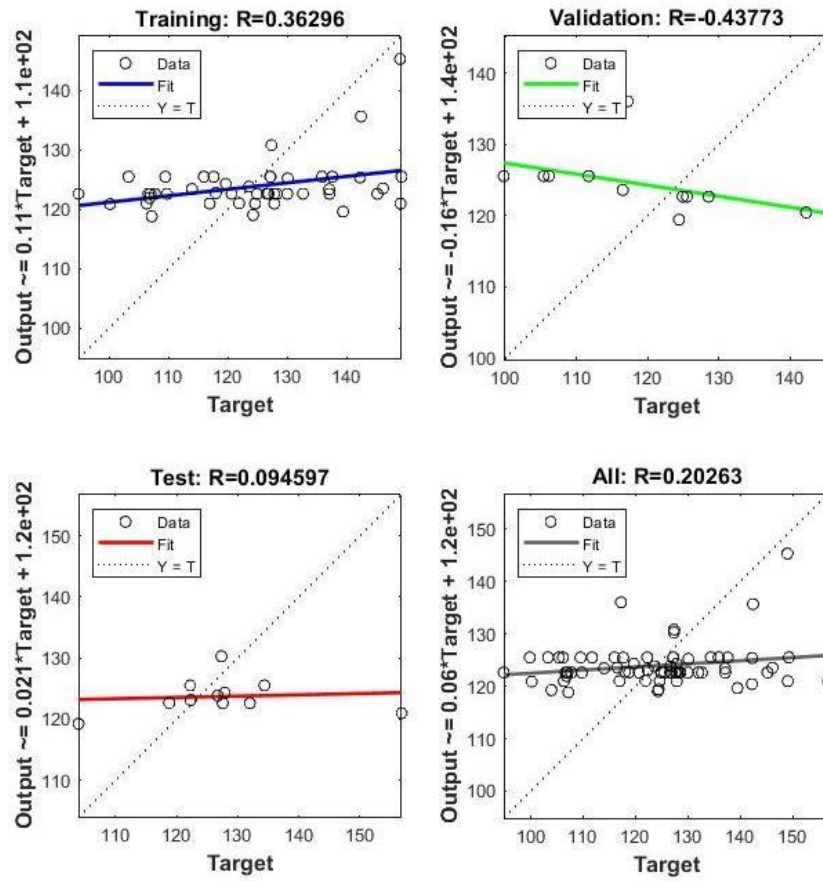


Fig 36. Regression plot of uninfested rava using LM-FNN algorithm

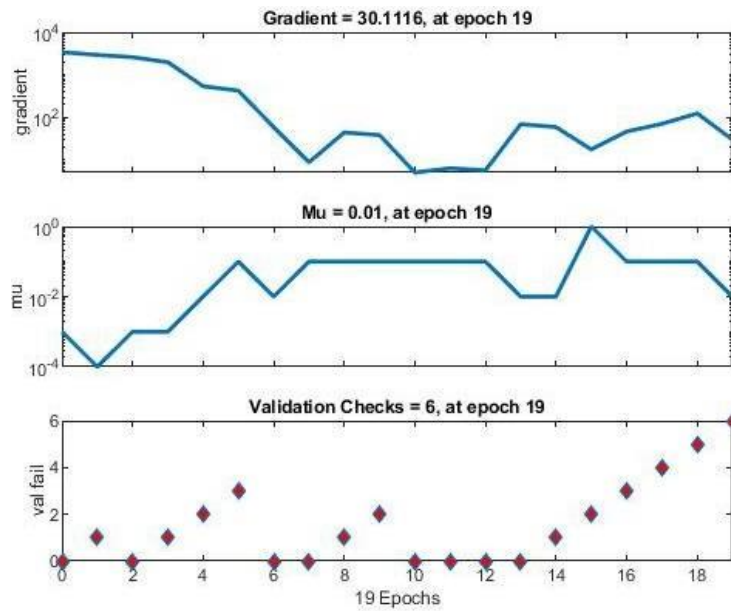


Fig 37. Training state of uninfested rava using LM-FNN algorithm

In infested rava sample, the overall R^2 of 0.7363 and the MSE of 166.045 were obtained at 10th iteration among 16th iterations and the gradient value increased at 16th iteration with 3.285 value and mu value also increased at 16th iteration with value of 0.001. The BFG-FNN and RP-FNN showed less accuracy compared to LM-FNN and SCG-FNN. When compared with control rava sample, the infested rava sample was more accurate (Fig 38-40).

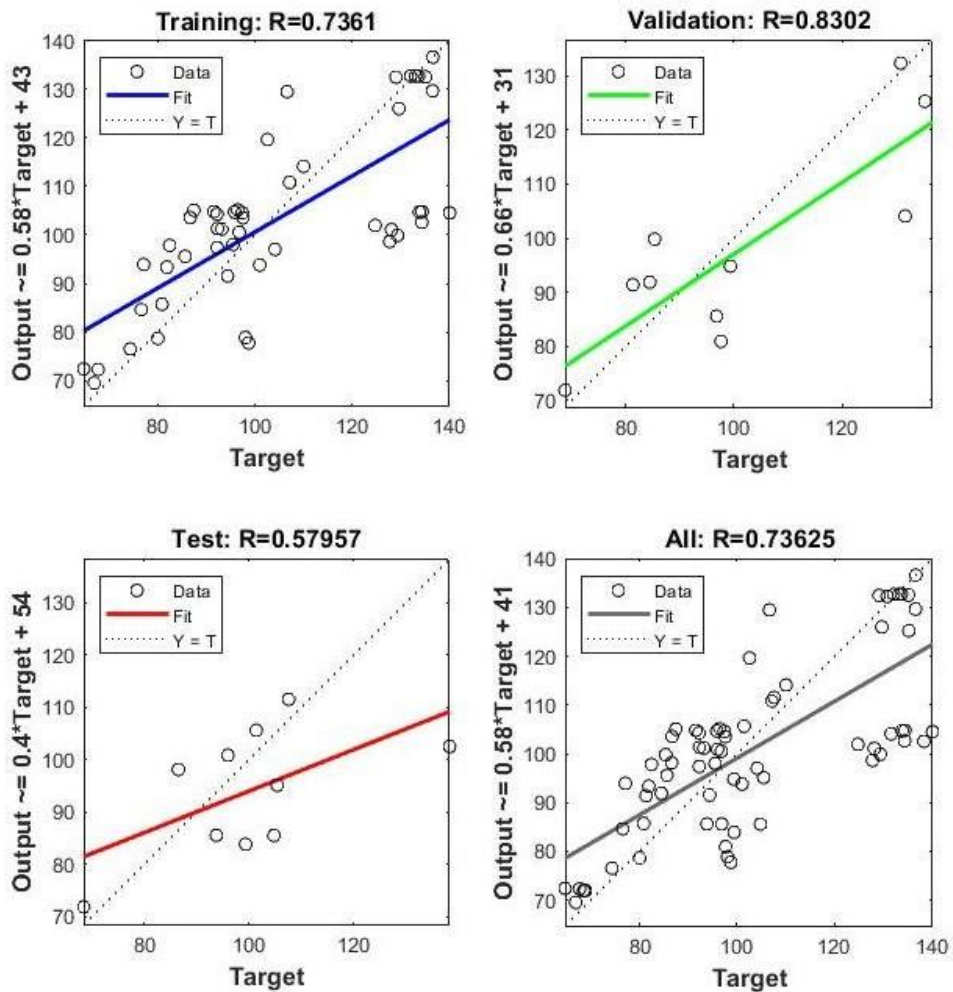


Fig 38. Regression plot of infested rava sample using LM-FNN algorithm

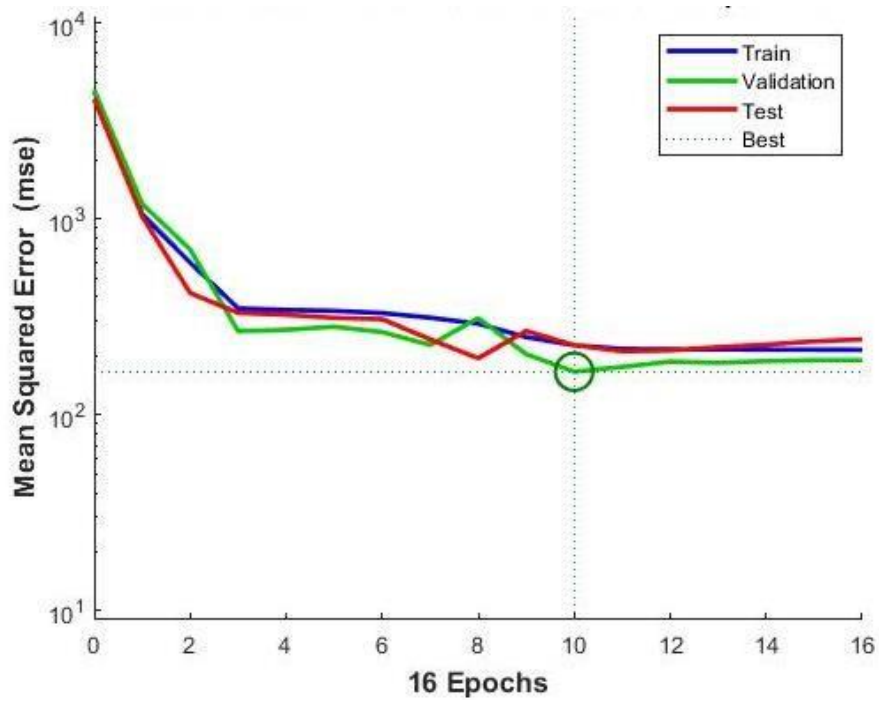


Fig 39. Performance plot of infested rava sample using LM-FNN algorithm

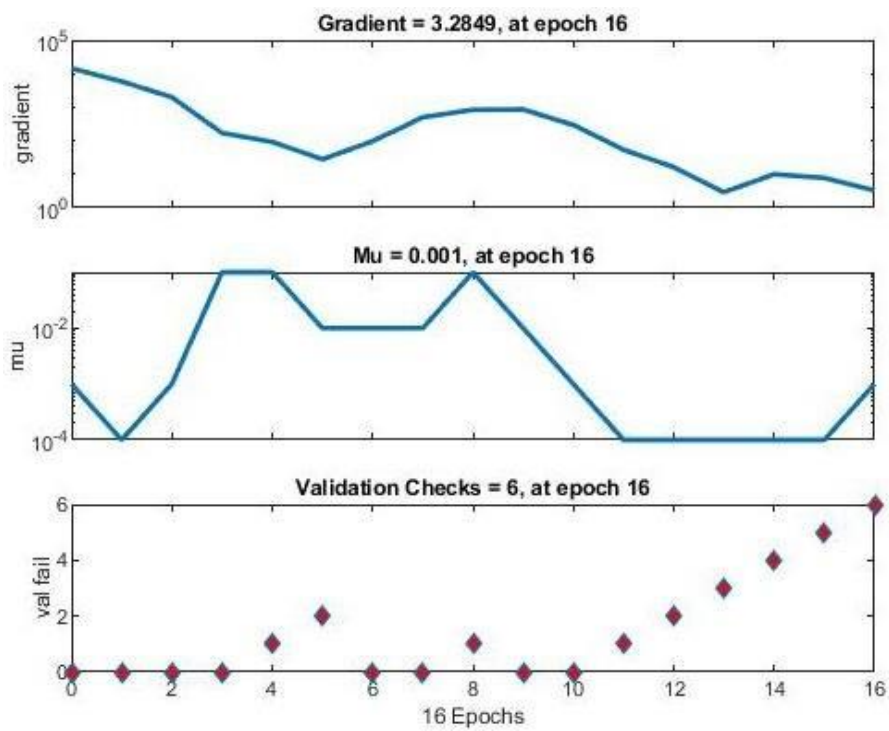


Fig 40. Training state of infested rava sample using LM-FNN algorithm

The overall R^2 of uninfested wheat flour showed 0.5232 and the MSE of 351.093 at 683rd iteration among 689th iterations and the gradient value increased at 689th iteration with

12.677 value and validation fail due to validation check at 689th iteration with value of 6 in BFG-FNN algorithm which is similar to SCG-FNN (Fig 41-43).

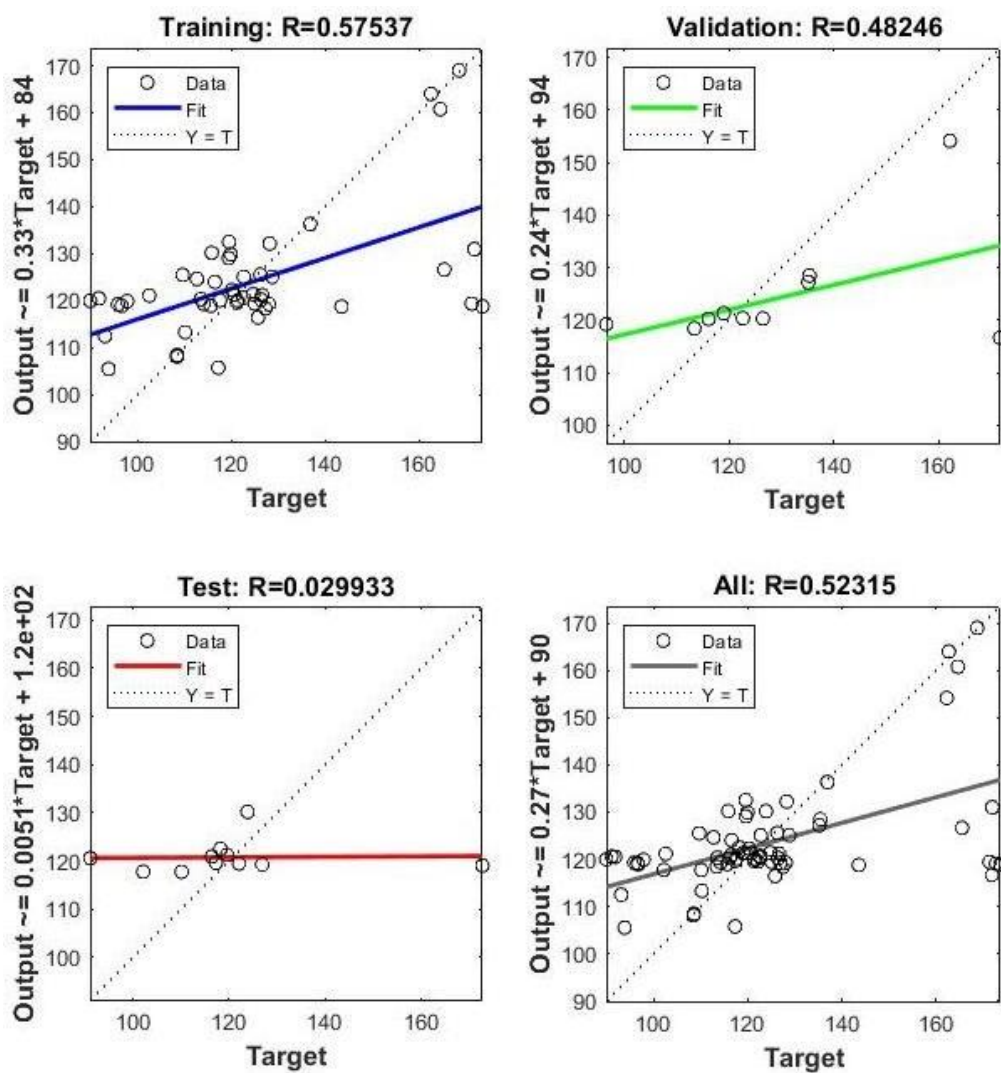


Fig 41. Regression plot of uninfested wheat flour sample using BFG-FNN algorithm

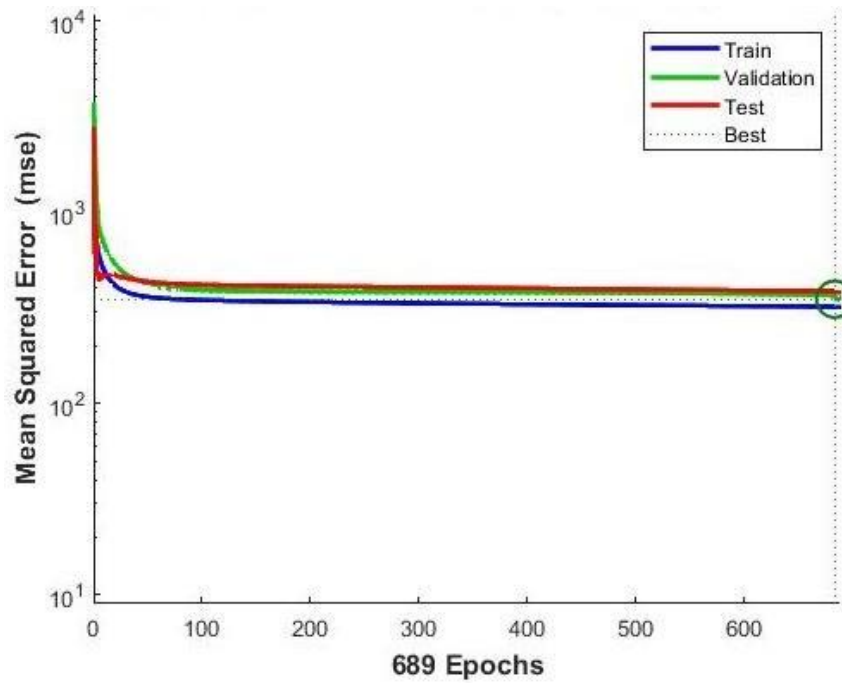


Fig 42. Performance plot of uninfested wheat flour using BFG-FNN algorithm

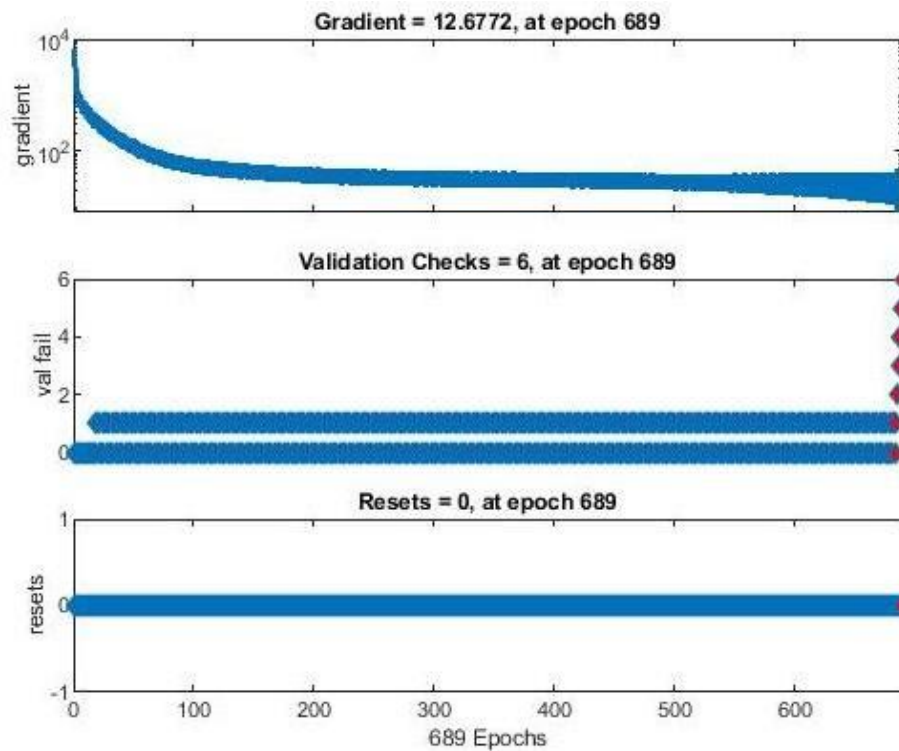


Fig 43. Training state of uninfested wheat flour sample using BFG-FNN algorithm

In infested wheat flour sample, the overall R^2 of 0.9611 and the MSE of 10.276 were showed at 39th iteration among 45th iterations and the gradient value increases at 45th iteration

with 15.737 value and validation fail due to validation check at 45th iteration with value of 6 in RP-FNN algorithm (Fig 44-46).

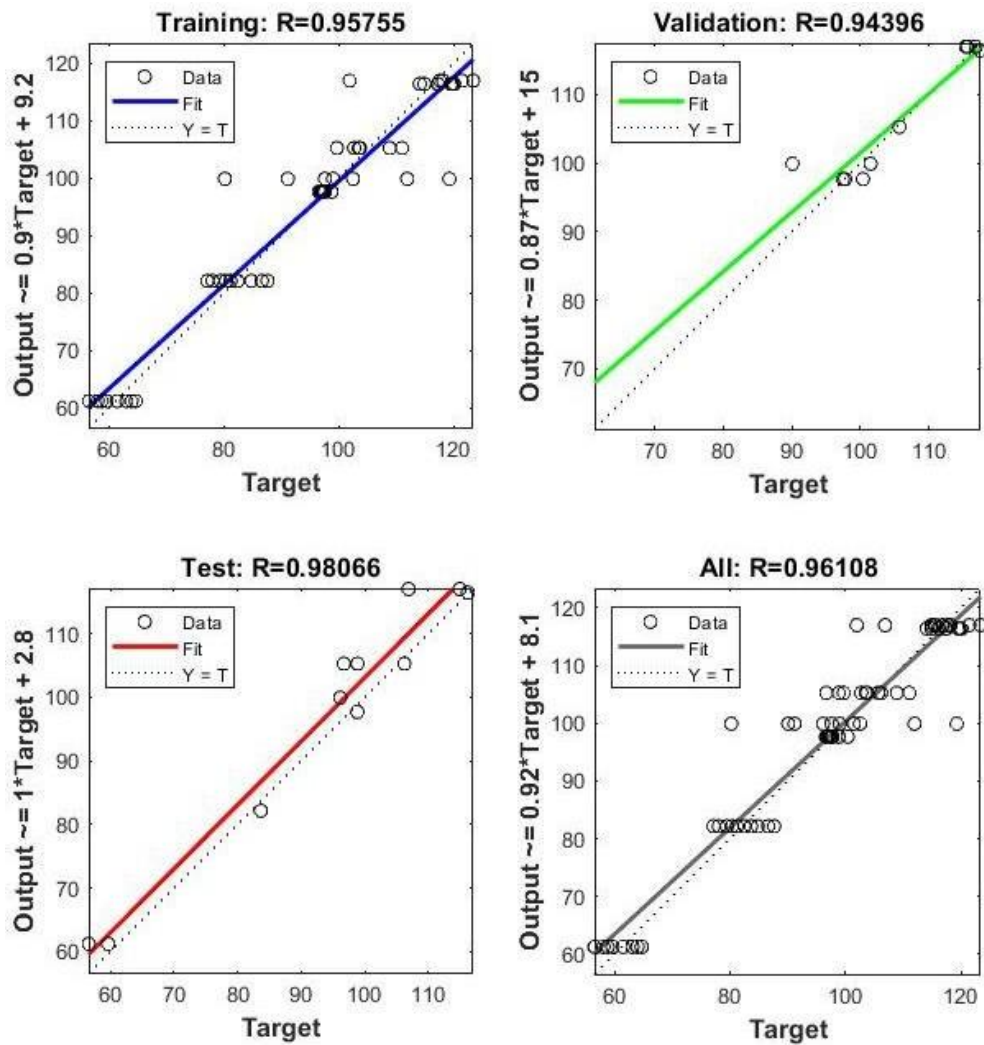


Fig 44. Regression plot of infested wheat flour sample using RP-FNN algorithm

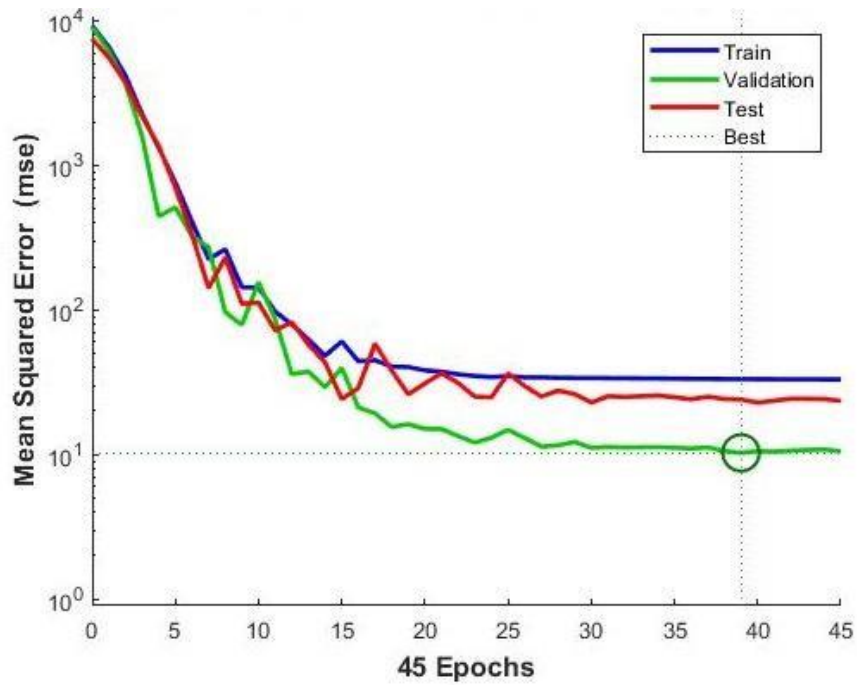


Fig 45. Performance plot of infested wheat flour sample using RP-FNN algorithm

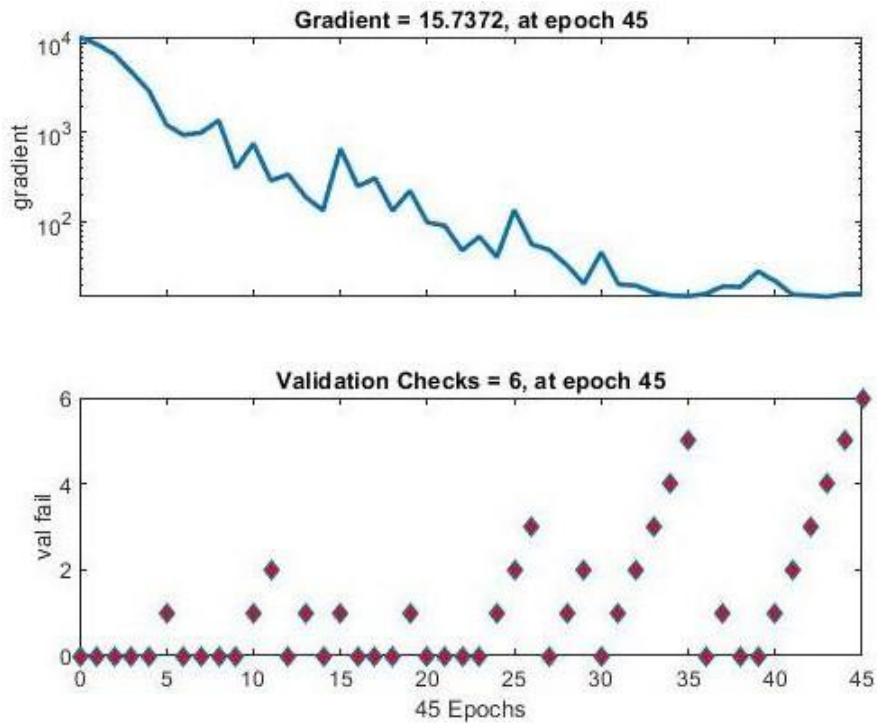


Fig 46. Training state of infested wheat flour sample using RP-FNN algorithm

The convolutional neural network (CNN) showed the coefficient of determination of correction (R^2) of 0.8843 and RMSE of correction of 0.1182. The CNN model showed higher accuracy than SVR with OAPC to predict behenic acid in edible oils (Weng *et al.*, 2022)..

The quality of tablets was evaluated using the tensile strength (TS) and disintegration time (DT) as important indexes. The properties of herbal medicine plant extract were affected by TS and DT of tablets. The three predictive models were used to check the quality of tablets viz., Principal component analysis (PCA) and RBF-ANN), PCA- multiple regression analysis (MRA) and PCA-BP-ANN. The PCA-RBF-ANN model was used to predict the quality of tablets and provide reference for quality control of tablets (You *et al.* 2020).

In our study, the four algorithm was used in FNN model. The LM-FNN model showed good result for standard UA. The LM-FNN and BFG-FNN model showed better accuracy for the control and infested samples (wheat flour, maida and rava).

4.3.3 Recovery study

The known different concentrations (8-96 mg/100g) of uric acid has been added to the uninfested wheat products (wheat flour, rava and maida). Among these, the maida showed more recovery of 96-99.99 per cent when compared to rava (88-99.66%) and wheat flour (96-99.66%) and the relative standard deviation were in ranged below 5% in all the cases (Table 9).

Table 9. Recovery study of known UA added in wheat flour, maida and rava samples

Concentration added (mg/100g)	Recovery (%) of wheat flour	Recovery (%) of maida	Recovery (%) of rava
0.8	96.1187	96.45875	88.37875
1.6	98.0106	99.39938	95.78375
2.4	98.3025	99.39292	96.67833
3.2	99.9413	97.20563	91.70188
4.0	97.8445	99.0645	95.78025
4.8	99.1315	99.36208	99.02543
5.6	99.2934	99.63339	99.70411
6.4	98.6475	98.66859	97.13813
7.2	98.764	99.75597	99.87417
8.0	98.75	99.06913	98.96713
8.8	99.6659	99.61409	99.66602
9.6	98.94	99.99190	97.89771

The spiking with known amount of UA in different food samples to find the recovery percentage. The mean recovery of UA was 103% (Roy R. B. 1981). The author has studied about the determination of UA with dried poultry waste present in animal feeding stuffs. The UA (2-6 mg) was added to three types of feed (1g) was treated. The recovery percentage of three different types of feed ranged from 101.4% was found (Cox *et al.* 1976).

4.4 FTIR

The IR spectrum of standard UA and spiked wheat flour samples was shown in Fig 47 and 48. The spectra of standard UA showed high absorbance from 1633-1622 cm^{-1} due to the presence of amine group that corresponds to N-H bending. The band of absorbance at 1541-

1537 cm^{-1} was due to Nitroso group stretching whereas the band at 1425-1418 cm^{-1} was due to the hydroxyl group (O-H) stretch.

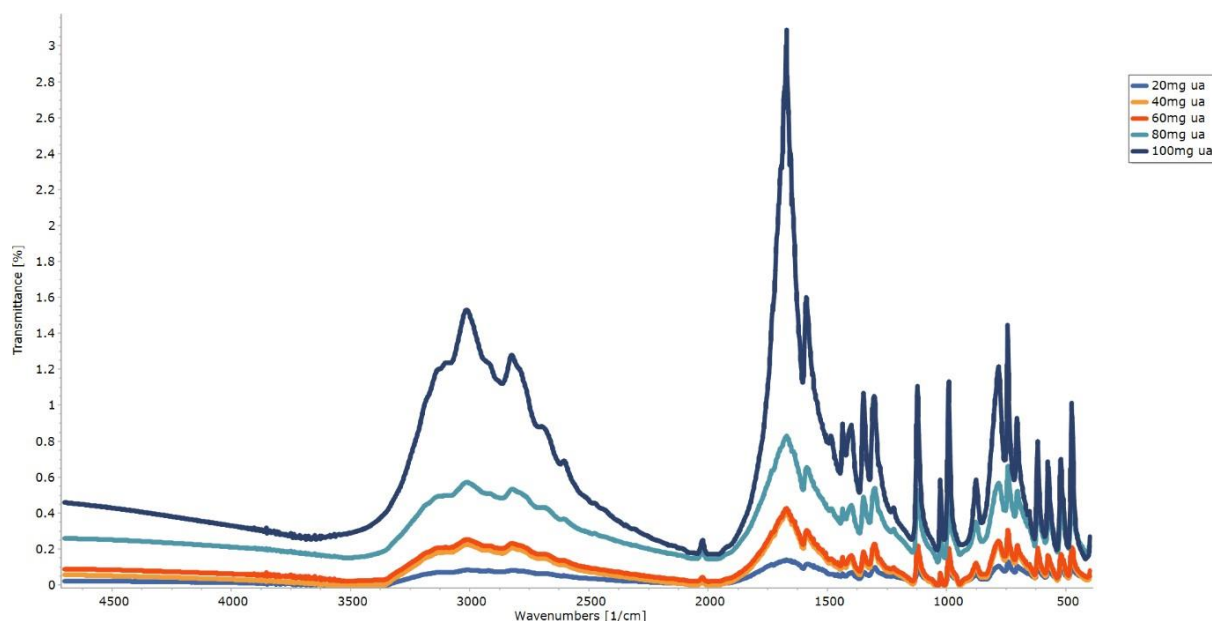


Fig 47. FTIR spectra of standard UA

The absorption band at 1135-1120 cm^{-1} was due to presence of carboxyl group that leads to C-O stretch. The frequency region of 1026-1000 cm^{-1} , 1388-1380 cm^{-1} and 1580-1576 cm^{-1} was due to the presence of nitrile group stretch. The band at 877-800 cm^{-1} was due to C-N bending (Asyana *et al.* 2016).

In spiked samples, the vibrational bands at 756.09 cm^{-1} showed the presence of isolated carbohydrate (C-OH, C-CH, O-CH bending), the presence of polysaccharides (cellulose) was observed at 929.69 cm^{-1} due to C-CH, O-CH and C-OH bending. The frequency region of 999.12 cm^{-1} was observed that the polysaccharides (C-OH bending) and starch, oligosaccharides like mannose and galactose (C-O stretching) are present. The band at 1076.28 cm^{-1} are assigned due to the presence of polysaccharides (C-O and C-C stretching), whereas the peak frequency at 1149.57 cm^{-1} occur due to coupled C-O and C-C stretching that leads to the presence of starch.

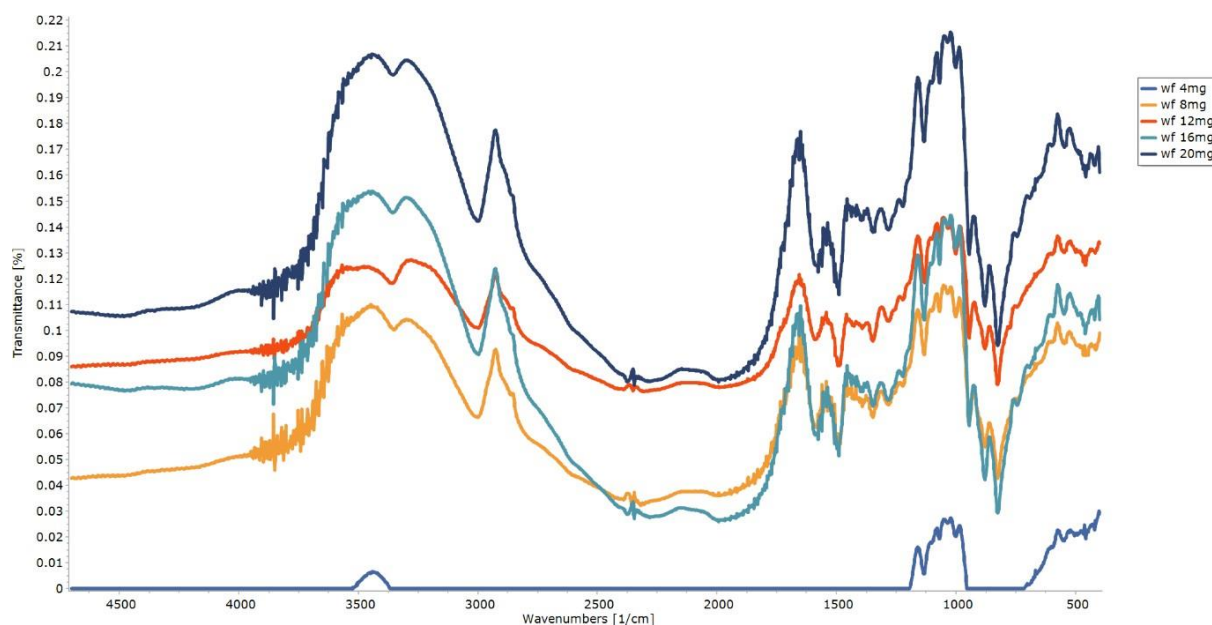


Fig 48. FTIR spectra of spiked wheat flour sample

The vibration of band at region of $1350\text{-}1100\text{ cm}^{-1}$ showed the presence of amide groups (N-H bending coupled with C-N stretching) in wheat flour spiked with known UA concentrations. The band at range of $1600\text{-}1400\text{ cm}^{-1}$ leads to the presence of phospholipids that attribute due to C-H and N-H bending coupled with C-H stretching (Indumathi *et al.* 2021).

4.5 Detection of uric acid in food samples using DNA based biosensor

4.5.1 Development of modified SPE

The interaction of UA with the modified SPE (DNA immobilized electrode) can be investigated by the Tris-Cl buffer (10mM) containing different concentration of UA ranged from 0-100 ppm. The UA reduction was determined using this biosensor. The cyclic voltammogram of bare electrode and Chitosan-AgNPs-DNA-glutaraldehyde immobilized electrode with Tris-Cl buffer containing UA (Fig.49). The bare electrode showed the current value of 0.48 at 0.0899V but the immobilized electrode current values increased to 1.39 at 0.0899V. The different concentrations of UA (0-100 ppm) with Tris-Cl buffer gets decreased due to the presence of ABC gene in DNA (Annexure 2) which was immobilized in the working

electrode (Fig 50). The current values for 25 (2.00), 50 (1.89), 75 (1.43) and 100 ppm (1.13) at 0.089 V (potential) due to reduction of ATP to ADP and phosphate.

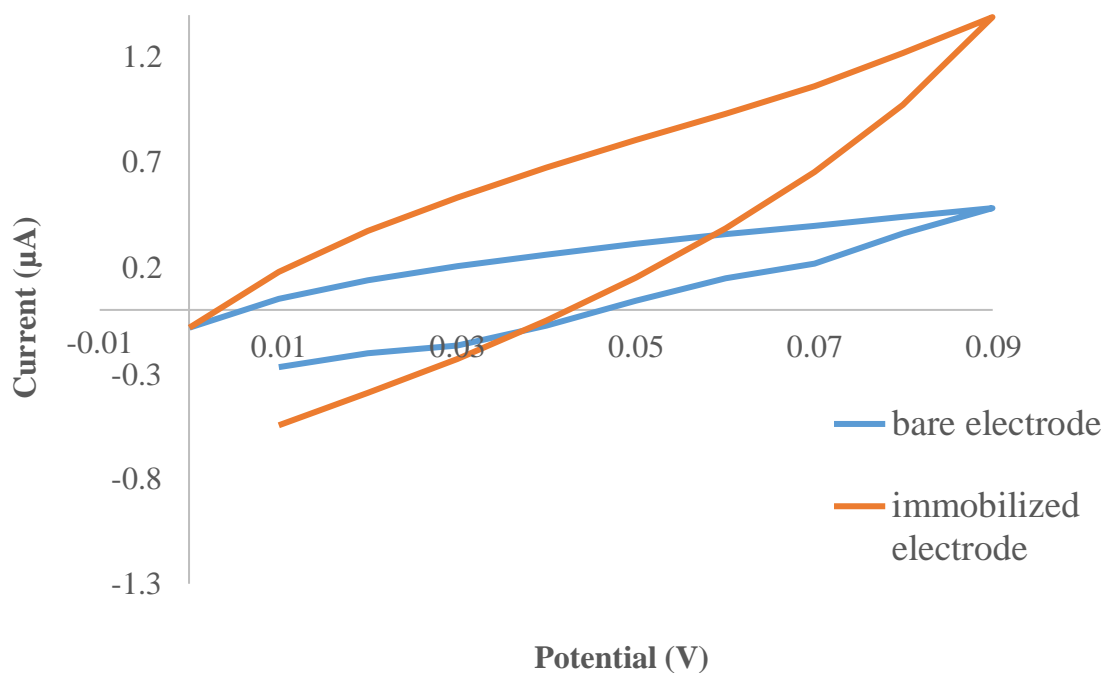


Fig 49. Cyclic voltammogram of bare and immobilized electrode

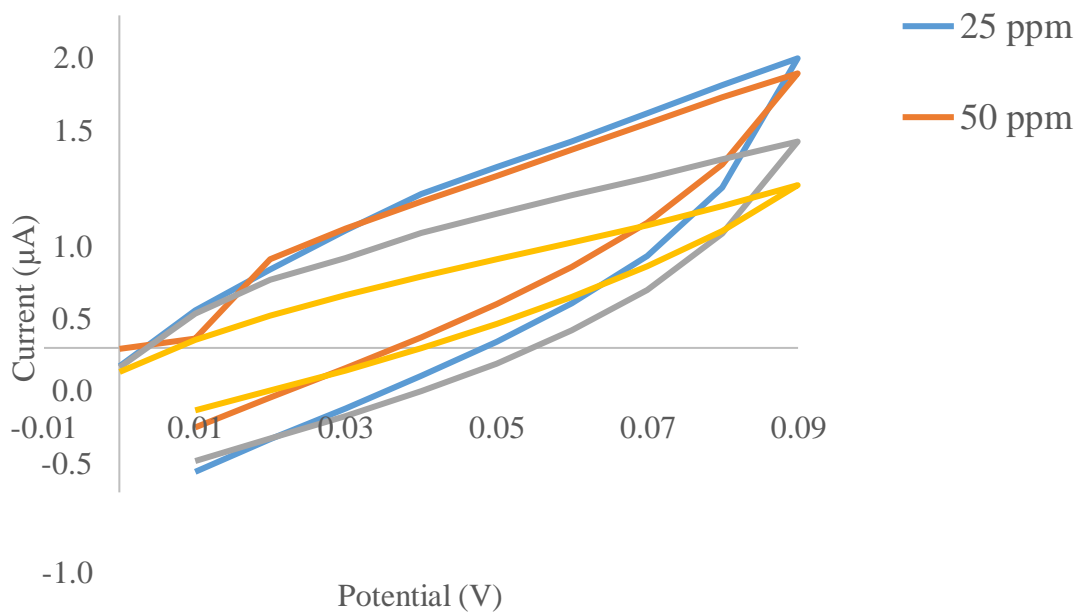


Fig 50. Cyclic voltammogram of different concentration of UA

The anodic peak represents the oxidation reaction and the cathodic peak represents the reduction reaction against the square root of scan rate. The anodic peak showed the regression

coefficient (R^2) of 0.96143 with equation $y=0.02325x-0.0082$ whereas the cathodic peak

showed the R^2 of 0.97288 with the equation $y = -0.03896x - 0.05799$ (Fig 51). In the cathodic peak, the equation denotes the slope value in negative sign which occurs due to the decrease in current value when the concentrations of UA increased as explained by Rezaei *et al.* (2018).

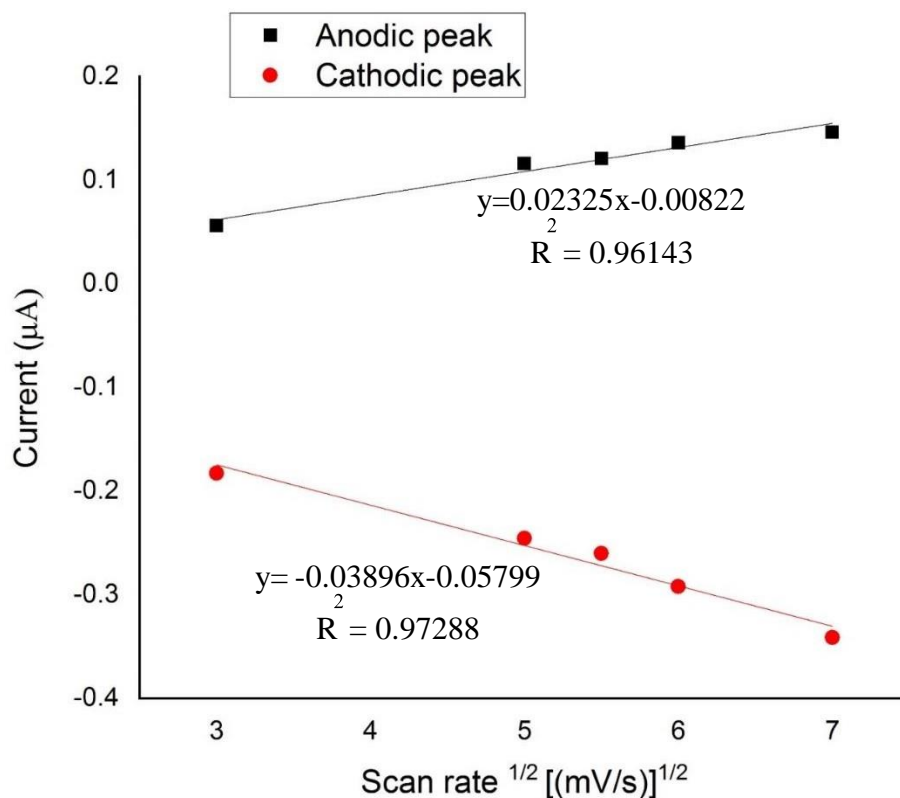


Fig 51. Linear relationship of peak current and scan rate

4.5.2 Optimization and performance evaluation of DNA based biosensor

4.5.2.1 Optimization of DNA based biosensor

4.5.2.1.1 Effect of DNA immobilization

The UA response was observed using the fabricated SPE (Chitosan mediated AgNPs-DNA-Glutaraldehyde immobilized SPE) with different immobilization time. It was found that the optimized time with optimal current signal for DNA immobilization was 1 hour whereas at 2 and 3 hour of DNA immobilization leads to decrease in the current value which was observed

using the CV (Cyclic voltammetry) (Fig 52). The optimized DNA immobilization time was used for the rest of the optimization, performance evaluation and for real-time sample analysis.

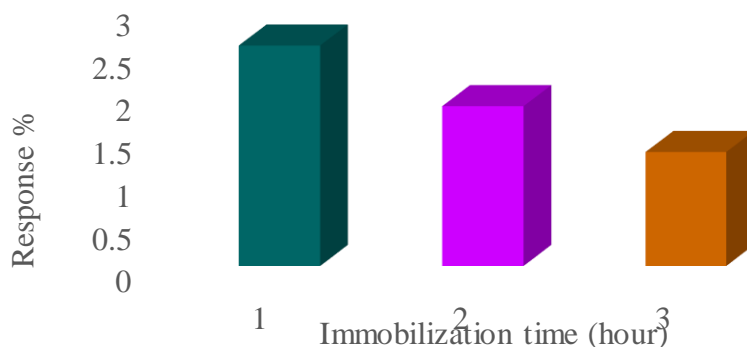


Fig 52. Effect of DNA immobilization

4.5.2.2 Effect of DNA hybridization

The DNA hybridization time of modified SPE was optimized and investigated from 20 to 40 minutes. The DNA hybridization was optimized at 40 mins where the DNA hybridization time increased trend along with increased current value (Fig 53). The DNA hybridization on graphene nanospheres – Pyrene butyric acid (GNS-PBA SPE) was investigated from 30 min to 3 hrs. The DNA hybridization (70%) was achieved within 1 hour time duration. The trend of the UA response was found that the increase in electrochemical signal with increasing DNA hybridization time as reported by Karadeniz *et al.* (2008).

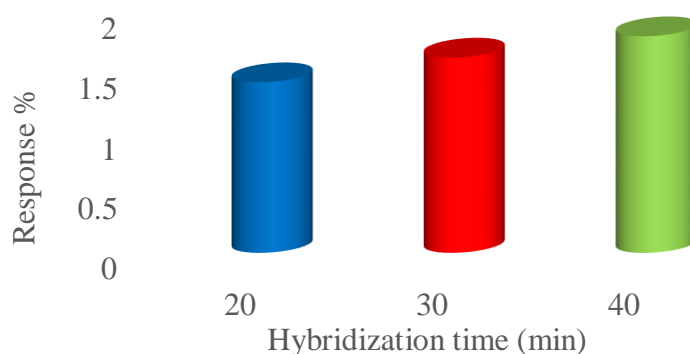


Fig 53. Effect of DNA hybridization

4.5.2.2 Performance evaluation of DNA based biosensor

4.5.2.2.1 Linearity

The DNA based biosensor response increased with the increasing concentration of UA (0-100 ppm). The UA concentration was found to be linear with the regression coefficient (R^2) of 0.9952 with the equation of $y = -0.0119x + 2.3238$ (Fig 54). The cDNA concentration (2.0×10^{-15} to 2.0×10^{-9} M) has increased with the biosensor response. The range of cDNA concentration was found to be linear with the R^2 of 0.982 as reported by Hassan *et al.* (2019).

Similar study was done by Ulianas *et al.* (2014) who reported that the concentration of *P. aeruginosa* increased with the increase of peak current signal. The intensity of current signal showed good linear relationship with the concentration of *P. aeruginosa* that ranges from 10-106 CFU/ml. The linear regression equation $I (\mu A) = 4.40 \log c + 10.05$ with the R^2 of 0.99 that quantify the detection of *P. aeruginosa*

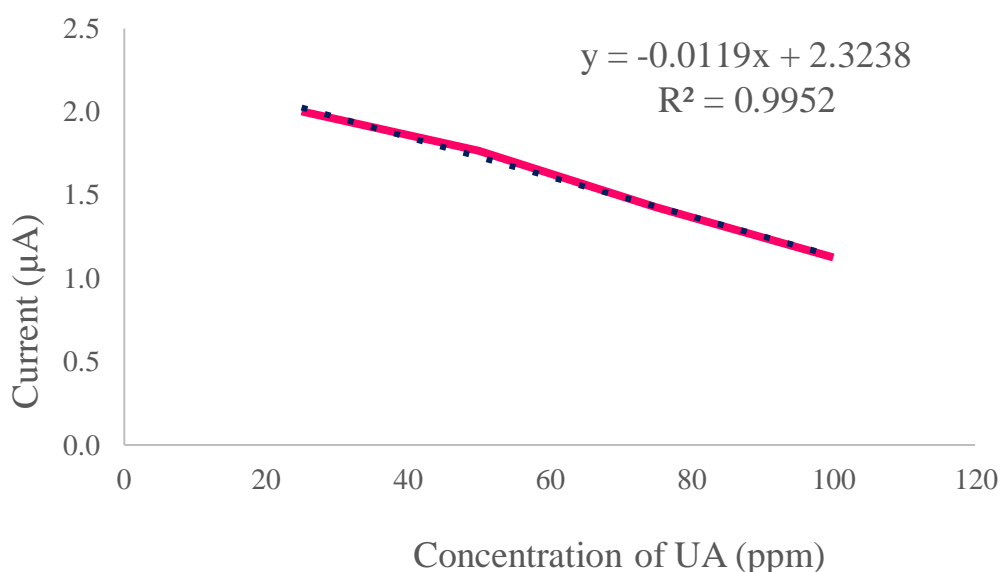


Fig 54. Calibration curve of standard UA that shows the linearity of DNA based biosensor

4.5.2.2.2 LOD

The LOD (Limit of detection) of DNA based biosensor was estimated as 97 ppm of UA where the LOD was calculated using the equation: $LOD = 3 SD/k$, where SD was represented as the standard deviation and k was denoted as slope of linear regression equation.

The LOD of cDNA was predicted as $7.79 \times 10^{-16} M$ which was calculated based on the equation mentioned above (Raja Jamaluddin *et al.* 2020).

Zhang *et al.* (2019) used the similar method and the LOD was estimated as 2 CFU/ml for the detection of *P. aeruginosa*. The electrochemical biosensor showed good performance based on linearity range and LOD for the detection of *P. aeruginosa*.

4.5.2.2.3 Operational stability

The operational stability of DNA based biosensor was obtained by running 5 times per day (Fig 55). The operational stability of DNA based biosensor was evaluated using the relative standard deviation (RSD %) by measuring the biosensor response with 100 ppm concentration of UA. The RSD (%) of the DNA based biosensor was 0.41% which was less than 10% that showed the reliable and response of sensitive of developed biosensor.

Imran *et al.* (2020) used poly (acrylic acid) (PAA) and poly (1-vinyl imidazole) (PVI) based biosensor to detect activity of invertase enzyme. The operational stability of this matrix based biosensor was achieved by running 30 times in the same day. After the fifth use of biosensor, the activity loss was reduced to 20 % and was maintained constantly for other 25 measurements. But the present study obtained the operational stability of DNA based biosensor by running 5 times per day which showed the good operational stability.

The polypyrrole (PPy) and PPy-containing chitosan-coated Fe₃O₄ was polymerized on pencil graphite electrodes (PGEs). The fabricated biosensor was used to detect the glucose-6-phosphate in blood serum samples. The operational stability of BS-1 (PPy/G6PD (Glucose-6-phosphate dehydrogenase)) and BS-2 (CS/Fe₃O₄-PPy/G6PD) was evaluated using the RSD. The RSD value of BS-1 and BS-2 biosensor was 3.80 and 4.60% which was below the 10% showed that the both biosensors was sensitive and reliable (Ebrahimi *et al.* 2011).

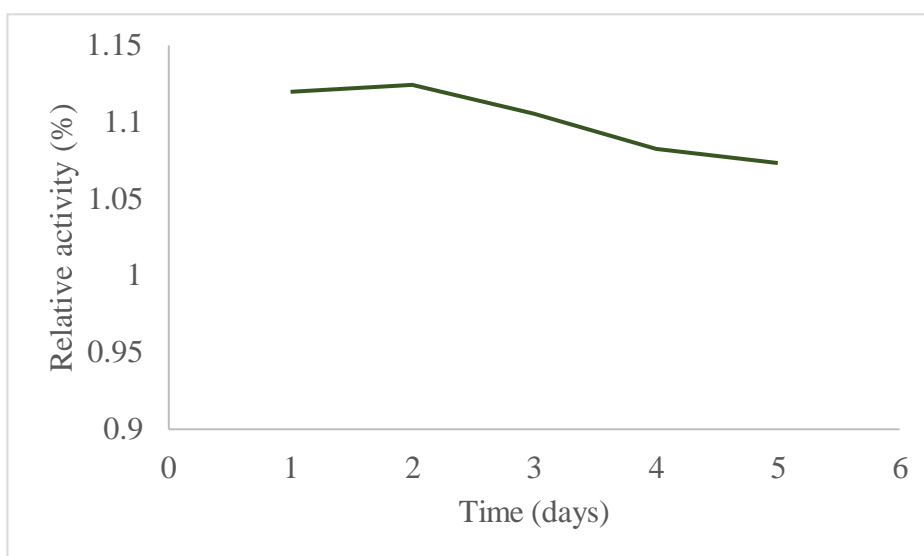


Fig 55. Operational stability of DNA based biosensor

4.5.2.2.4 Regeneration

The regeneration of DNA hybridization was studied using the 0.1M NaOH as a regeneration solution to break the hydrogen bond in basepairs of DNA. The percentage of regeneration in biosensor before addition of NaOH solution (I_b) and after addition of NaOH solution (10 μ l) (I_a) was calculated as regeneration per cent of DNA based biosensor = (I_b/I_a)*100. The regeneration per cent from 0th to 4th cycle was 99.96, 92.84, 88.94, 86.27 and 78.56 (Fig. 56).

The acrylic microspheres and AuNPs (gold nanoparticles) and dsDNA was coated on SPE to determine the presence of 35 S promoter from cauliflower mosaic virus (CaMV 35 S)

gene in soybean. The regeneration of DNA biosensor was declined after soaking with 0.1M NaOH. After immersion of 0.1M NaOH solution on DNA biosensor was noticed from 5 to 180 s dipping time was 34.5, 30.3, 22.4, 4.7 and 4.6% to initial biosensor response. The response of biosensor get dropped due to the increase in dipping time that indicates the breakdown of hydrogen bonds between the basepairs of dsDNA using the NaOH regeneration solution (Ulianas *et al.* 2014).

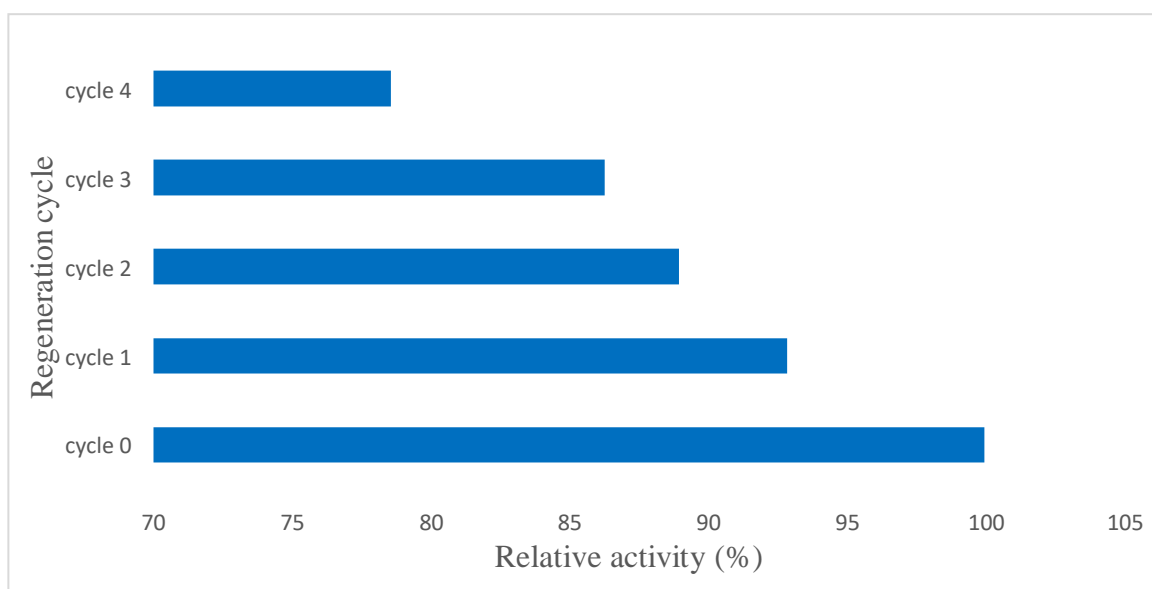


Fig 56. Regeneration cycle of DNA based biosensor

4.5.2.2.5 Reproducibility

The reproducibility of DNA based biosensor was tested using 100 ppm of UA concentration. The DNA based biosensor showed good reproducibility with 0.006-1.05% RSD with five number of electrode (Fig 57). In a similar study, the reproducibility of DNA biosensor for the detection of CaMV 35 S gene in soy bean was performed with two cDNA concentration with 2.0×10^{-4} and 2.0×10^{-2} μM and gave satisfactory reproducibility with 2.7 - 4.7% RSD (Karadeniz *et al.* 2008).

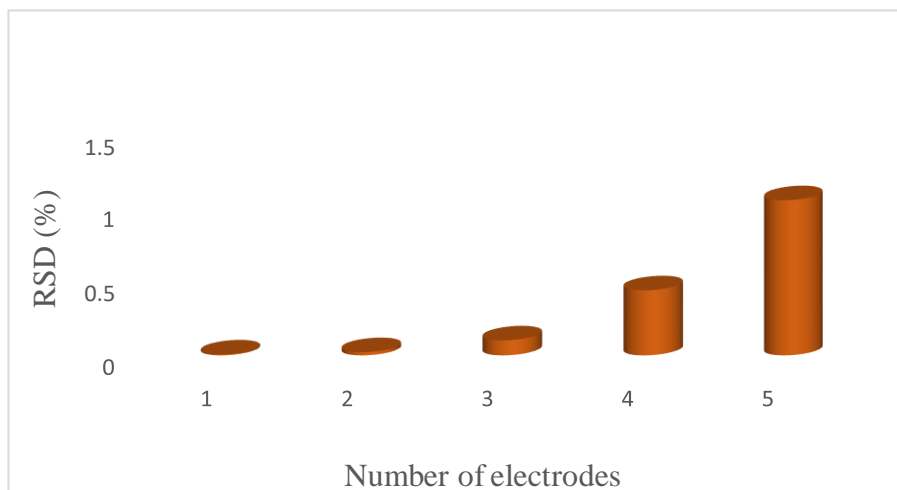


Fig 57. Reproducibility of DNA based biosensor

Manoj *et al.* (2020) found that the reproducibility of triglyceride content (0.5mM) evaluated based on the terms of variation of coefficient, average value, standard deviation (SD) which was found to be 1.97%, 0.515 mM and 0.043×10^{-3} mM.

4.5.3 Characterization of DNA based biosensor

4.5.3.1 FTIR

The functional groups which responds for IR absorption in bare, AgNPs, DNA immobilized and substrate (UA) immobilized electrode was shown in Fig 58. The absorption peak at 1314 cm^{-1} (Amide III), 1544 cm^{-1} (Amide II) and 1647 cm^{-1} (Amide I) showed the presence of amide groups. The presence of lipids was characterized by peaks at 2850 cm^{-1} that shows the bending of CH_2 groups (methylene group), 2922 cm^{-1} and 2963 cm^{-1} shows the presence of CH_3 (Methyl group) and CH_2 groups (stretch).

The hexaferrocenium tri [hexa (isothiocyanato) iron (III)] trihydroxonium (HexaFc) complex can be detected using the DNA probe immobilized on Glutaraldehyde/ silica nanospheres- (3-aminopropyl) triethoxysilane/ Gold nanoparticles/SPE (GA/SiNS-APTES/AuNP/SPE). The absorption peak at 3400 cm^{-1} and 1543 cm^{-1} showed the presence of

amine group due to N-H stretching and N-H bending. The peak at 1715 cm^{-1} showed the presence of carbonyl group due to the C=O stretching and 1630 cm^{-1} showed the presence of cyano groups (C=N stretching) as observed in SPE by Ramesh *et al.* (2015).

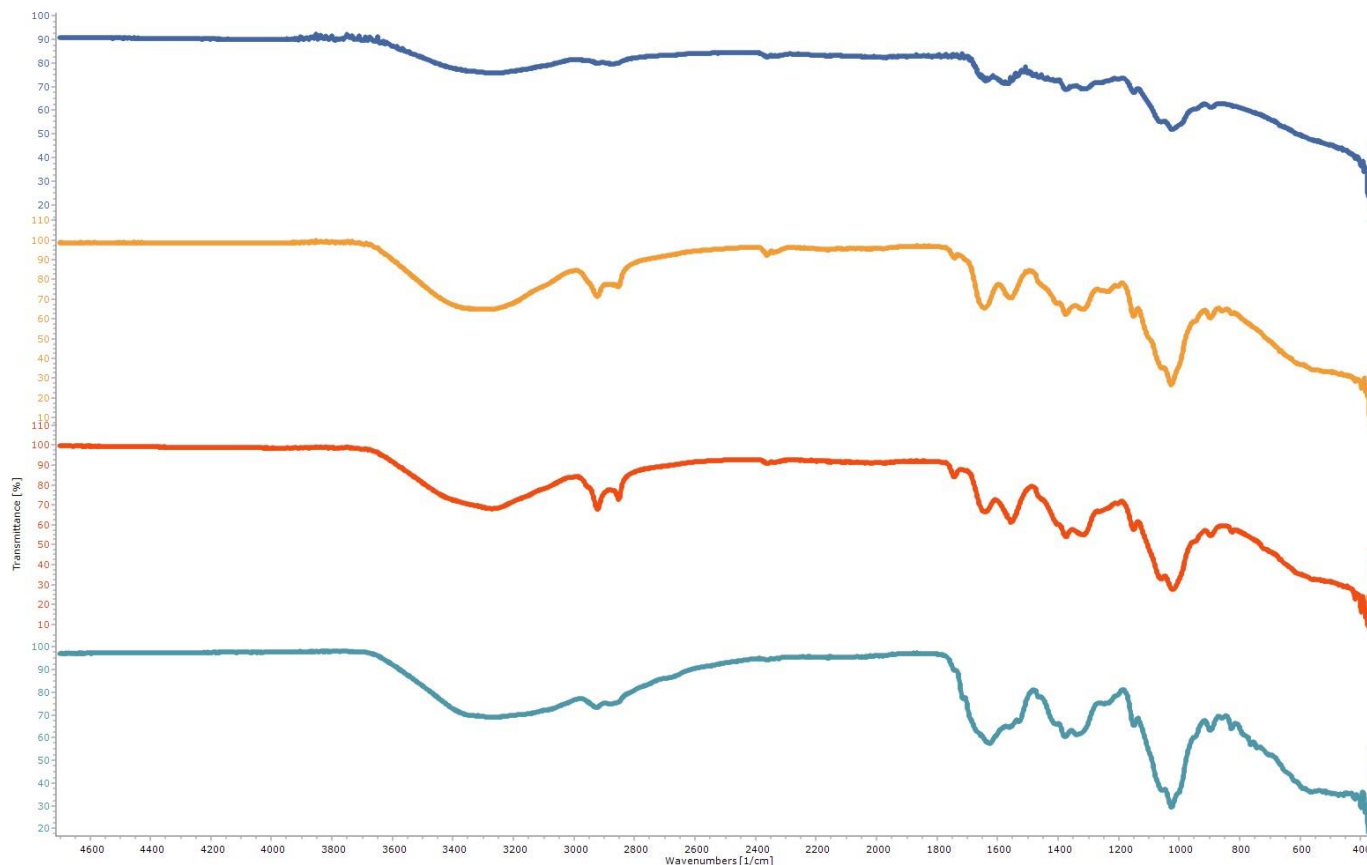


Fig 58. FTIR analysis of DNA based biosensor, bare electrode (dark blue), AgNPs coated electrode (orange), DNA immobilized electrode (red) and substrate immobilized electrode (light blue)

4.5.3.2 SEM analysis

The SEM images of bare, AgNPs, DNA and substrate immobilized electrode (Fig 59 A) showed rough surface area (Fig 59 A) whereas AgNPs immobilized electrode showed smooth surface with the size distribution varies from 56.61 to 122.2nm in diameter (Fig 59 B). The DNA immobilized electrode showed the smooth surface with various particle size that ranges from 162.6 to 235.0 nm in diameter that shows the particle size has become large, after

the addition of DNA and glutaraldehyde (Fig 59 C). The substrate (UA) crystals that reduce the presence of particles due to the reduction of ATP to ADP and phosphate (Fig 59 D).

The genetically modified (GM) DNA biosensor with acrylic microspheres was developed to determine the presence of CaMV 35 S gene by Ulianas *et al.* (2014) and found that the homogenous distribution of acrylic microspheres that will be useful for the development of GM DNA biosensor.

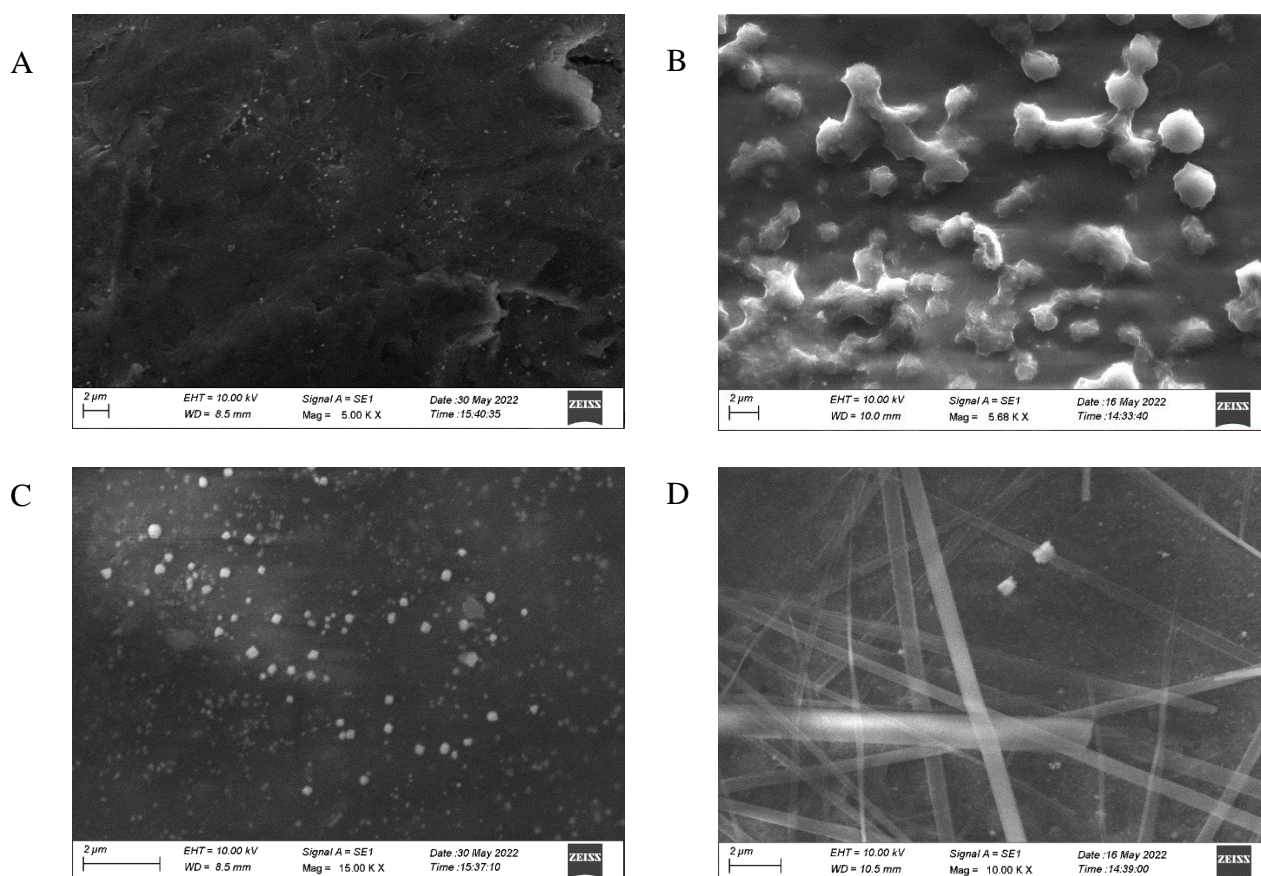


Fig 59. SEM analysis of SPE, bare (A), AgNPs (B), DNA (C) and UA immobilized electrode (D)

4.5.4 Validation of DNA based biosensor using real time samples

The wheat flour sample was spiked with the known concentrations of UA (25, 50, 75 and 100 ppm/ 50g of samples). The DNA based biosensor showed RSD values ranges from 6.90 to 9.09 % and the recovery (%) ranged from 92.6 to 113.34 % and the UA concentration calculated was close to HPLC method (Table 10). The correlation between the DNA based

biosensor and HPLC method showed the regression coefficient (R^2) of 0.993 (Fig 60). The HPLC chromatogram of UA in uninfested and spiked samples was shown in Annexure 3.

Table 10. The correlation of DNA based biosensor and HPLC method to detect UA

S.No	Uric acid concentration (ppm)		RSD %	Recovery %
	DNA based Biosensor	HPLC		
1	0.002	0.001	-	-
2	23.15	24.39	6.94	92.6
3	52.42	52.69	6.90	104.84
4	81.84	82.06	7.27	109.12
5	113.34	120.00	9.09	113.34

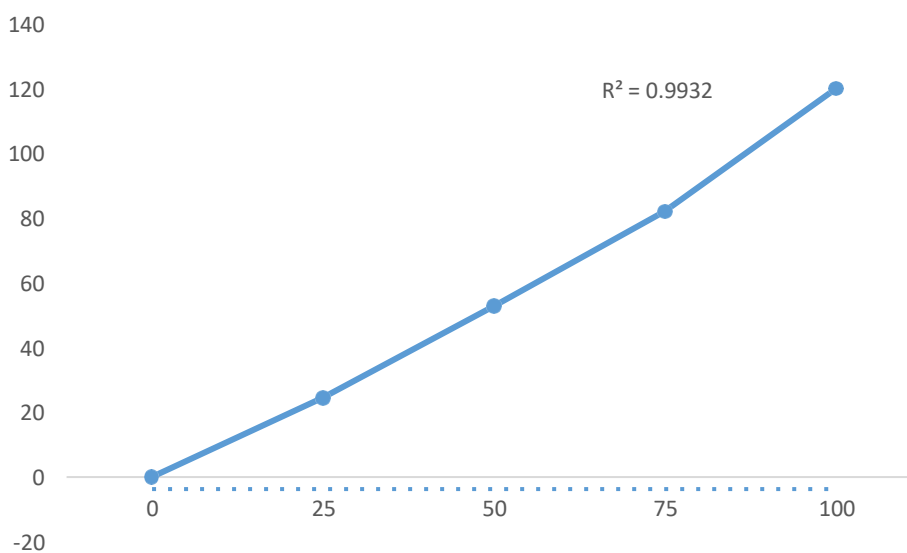


Fig 60. The correlation of DNA based biosensor with HPLC method

4.6 Isolation and identification of microorganisms from contaminated food samples and its preventive measures

4.6.1 Isolation of microorganisms in infested food samples

The bacterial (one) and fungal (three) strains was isolated and utilized by the growth media (NA-UA for bacteria and RBA-UA for fungi) (Fig 61). The strains was named as TM1 for bacteria and FS1, FS2 and FS3 for fungi. The zone of clearance was formed due to the utilization of uric acid by bacterial and fungal strains. The uric acid crystals were observed by microscope at 10x magnification (Fig 62).

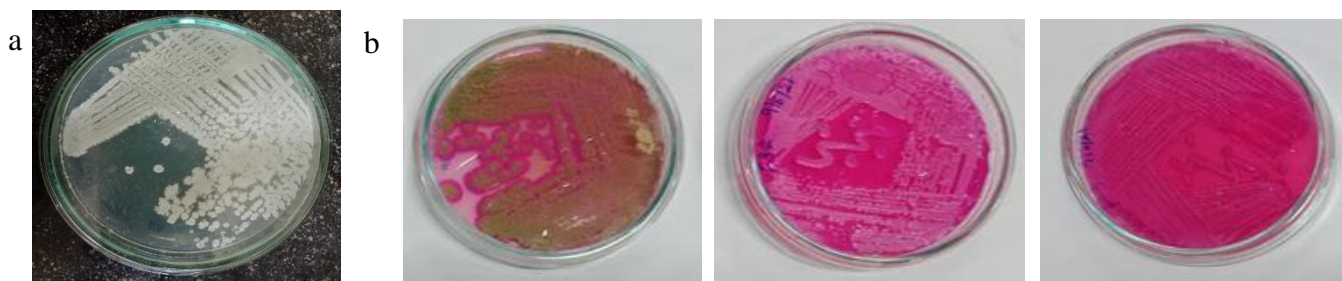


Fig 61. Pure isolates of bacteria (TM1) (a) and fungal strains (FS1, FS2 and FS3) (b)

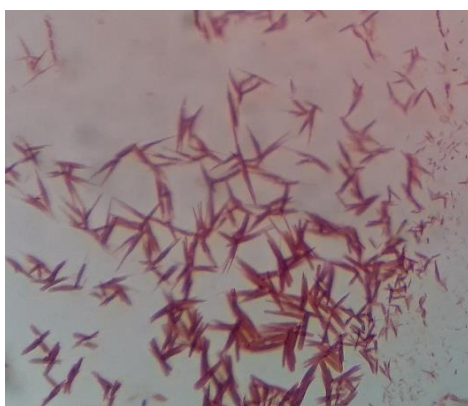


Fig 62. Observation of uric acid crystals

The primary characteristics of bacterial strain was done on the basis of cellular, colony morphology and gram staining characteristics. The colony morphology of bacterial strain was white in colour, small in size, appearance was wrinkle, dull and dry in nature, lobated ends and

flat elevation. The bacterial strain (TM1) was Gram positive, rod (bacilli) shaped bacteria (Fig 63).

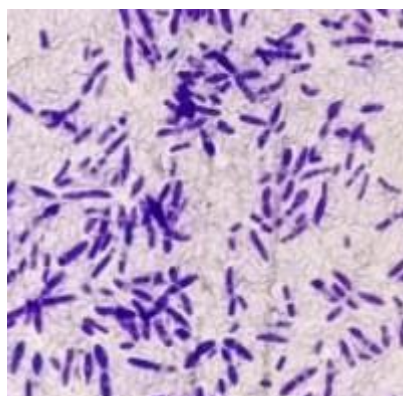


Fig 63. Gram staining of bacterial strain (TM1)

The biochemical characteristics of the bacterial strain was performed in terms of motility, endospore, starch hydrolysis, oxidase, catalase, indole, methyl red, voges-proskauer, citrate utilization, urea, nitrate reduction, gelatin liquefaction and carbohydrate fermentation tests (Table 11). The morphology of fungal strains (FS1, FS2 and FS3) was identified using Lacto phenol cotton blue staining (Fig 64). The aerobic batch culture and uric acid consumption was shown in Annexure 5 and the uricase enzyme assay was shown in Annexure 6. Earlier, Femi Kariy Atty *et.al* (2016) have isolated and identified 9 cultures of aerobic bacteria that have ability to grow on a media that contain UA has source of carbon nitrogen and energy.

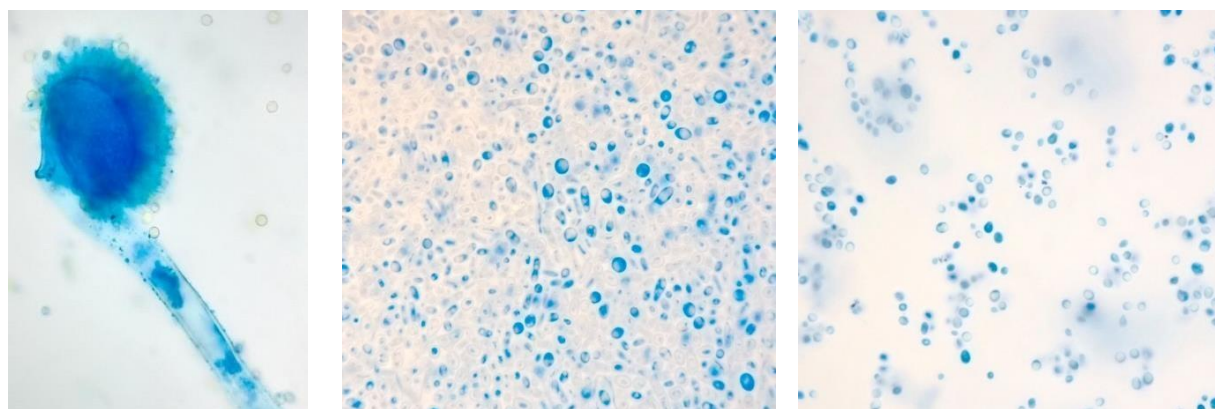


Fig 64. Lacto phenol cotton blue staining for fungal strain (FS1, FS2 and FS3)

Table 11. Morphological and biochemical tests for bacterial strain identification

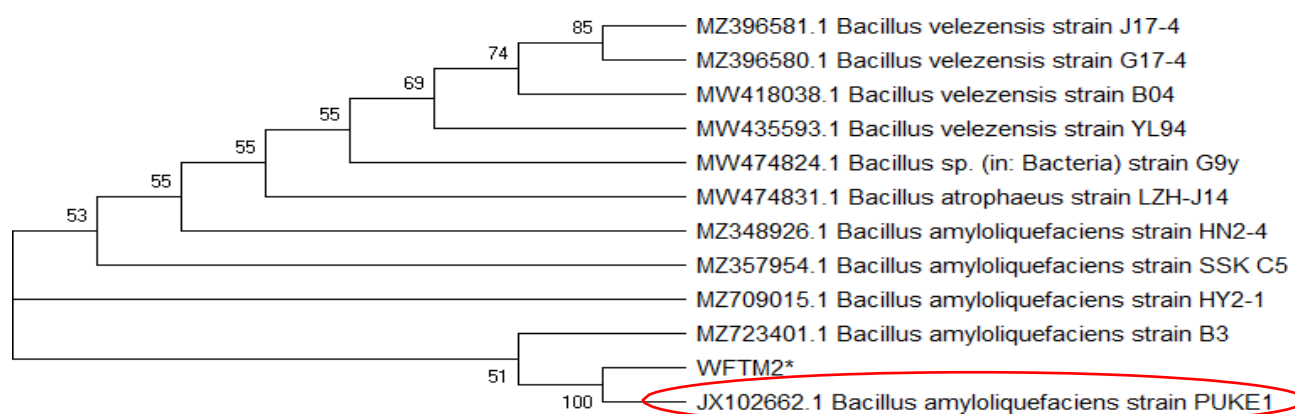
Morphological and biochemical tests	Results
Motility	+
Endospore	+
Starch Hydrolysis	+
Oxidase	-
Catalase	+
Indole production	+
Methyl Red	-
Voges Proskauer	+
Citrate utilization	+
Urea	-
Nitrate reduction	+
Gelatin liquefaction	+
Glucose	+
Sucrose	+
Maltose	+
Mannitol	+
Xylose	+
Tryptone	+

The yeast *Cryptococcus neoformans* was isolated from pigeon guano showed the UA catabolism. The UA can be utilized by the yeast and leads to urease and cryptococcal virulence factor production (Ghosh *et.al*, 2014). The bacteria that degrades the UA from soil was isolated

and it was studied for strain identification using 16S rRNA sequencing. The *Comamonas* sp BT UA strain was identified which was the uricase producing bacteria and purified enzyme was used to measure UA by spectrophotometric and electrochemical method (Rouf *et.al*, 1968).

4.6.2 Identification of microorganisms using molecular techniques

The PCR product of bacterial and fungal strains were assessed by 2% agarose gel in Annexure 4. The 16S rRNA nucleotide and ITS sequences of one bacterial and three fungal strains were subjected to BLASTN and the strains were classified based on the sequences similarity in GenBank database. All the bacterial and fungal strains gene sequences were submitted to Genbank (NCBI) and accession numbers were assigned to bacterial and fungal strains. The strains were identified as *Bacillus amyloliquefaciens* (TM1); *Aspergillus flavus* (FS1); *Candida parapsilosis* (FS2) and *Trichosporon asahii* (FS3). Nucleotide sequences was aligned by ClustalW (both pairwise and multiple alignment) with Gap opening penalty of 15 and Gap extension penalty of 6.66. The branching pattern was generated by neighbour-joining method using MEGA11, software version 11.0.11 based on 1,000 replications with bootstrap percentages above 50% (Tamura *et al.* 2007). The bootstrap test of phylogeny was chosen depending upon the sequence similarity. The neighbour-joining method was used for bacterial and fungal strains (Fig 65).



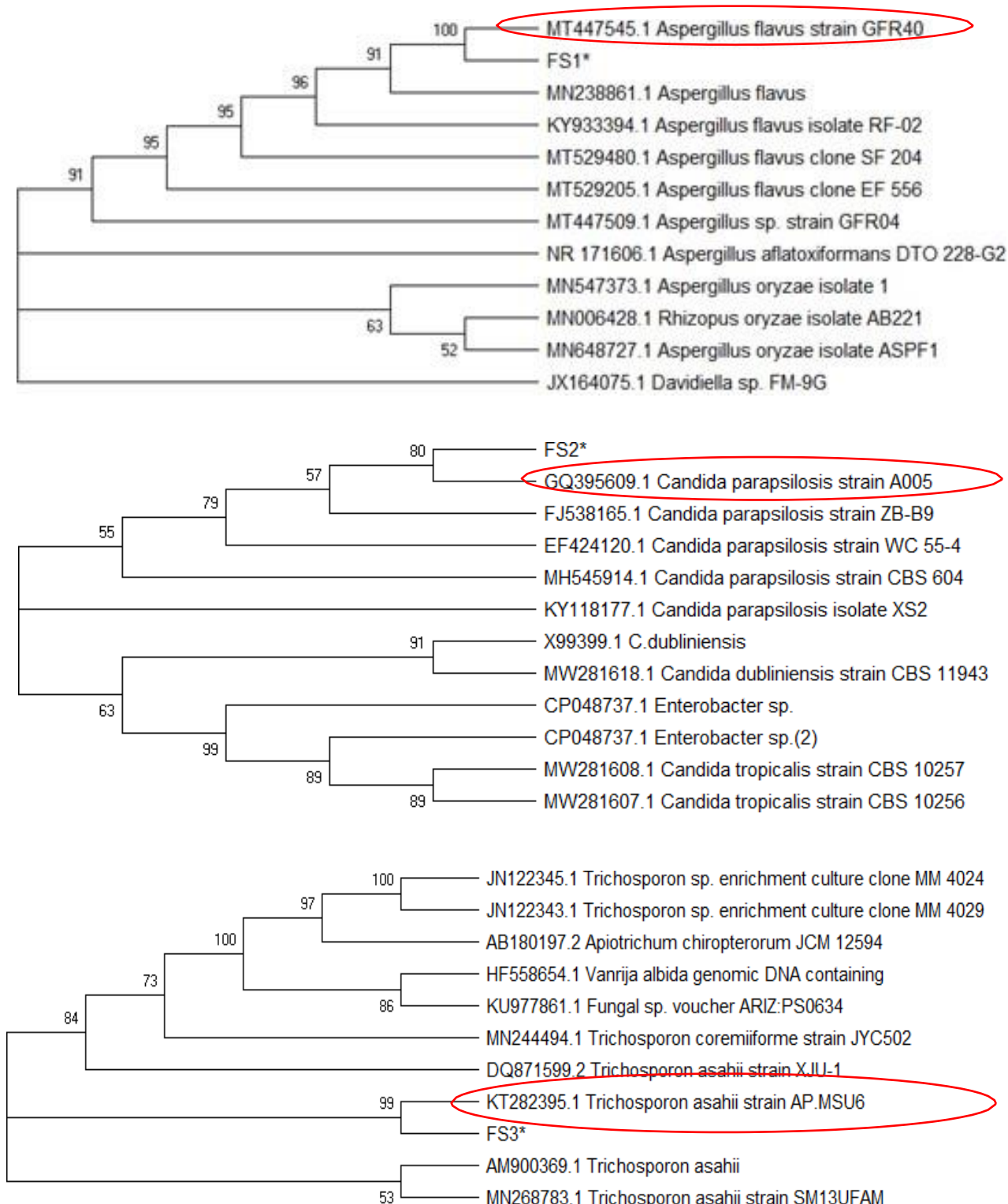


Fig 65. Phylogenetic tree of bacterial and fungal strains

Femi Kariy Atty *et.al* (2016) isolated the cultures and identified as *Aerobacter aerogenes*, *Klebsiella pneumonia* (two), *B. subtilis*, *P. aeruginosa* using 16 S rRNA

sequencing. Similarly, Pascal *et.al* (2005) the UA degrading bacteria was isolated from various environment in and around the Kerala (Ernakulum district). The bacterial strains was identified by biochemical, cultural and morphological analysis. The strain was identified and confirmed by PCR reaction of 16S rDNA primers, sequenced and BLAST analysis was carried. The *Ochrobacterium anthropic* showed 99% homology.

4.6.3 Extraction of essential oil using hydrodistillation method (Clevenger apparatus)

The yield of essential oils obtained from selected plant parts (Table 12). The per cent yield of essential oil was observed more in orange peel, lemon, lemongrass, cinnamon, clove, black pepper, Mosambi and orange peel and fruit.

The essential oil obtained from *Phyllanthus emblica* based on the weight of samples, the yield of EO was 0.11% (Amir *et.al*, 2014). The EO yield obtained from *Physalia angulate* using hydrodistillation was 0.12% (v/w) calculated based on dry weight. The percentage yield of extract and EO was 17.03 and 0.05% was obtained (Anwar *et.al*, 2009).

Table 12. Yield percentage of essential oils obtained from selected plants

Raw materials	Weight (g)	Yield (%) within 5 hrs
Orange peel	100	2.0
Lemon	100	1.5
Lemongrass	100	1.25
Rosemary	100	1.0
Cinnamon	100	1.5
Clove	100	1.5
Star anise	100	1.0
Cumin seed	100	0.8
Caradamon	100	1.0
Ginger	100	1.0
Fennel seed	100	0.9
Java plum	100	0.6
Juniper seed	100	0.5
Black pepper	100	1.5
Nutmeg	100	1.0
Mint	100	0.7
Guava leaf	100	0.5
Black cumin seed	100	1.0
Curry leaf	100	0.5
Tumeric	100	0.6
Thyme	100	1.0
sweet marjorum	100	0.5
Basil	100	0.5
Sage	100	0.7
Mosambi	100	1.0
Eucalyptus	100	1.5
Mace	100	1.0
Citron	100	1.0
Orange peel and fruit	100	1.5
Coriander	100	0.9
Betel leaf	100	0.5

4.6.4 Antioxidant assay

The antioxidant assay for essential oils was estimated by DPPH method using ascorbic acid as a standard. The violet colour DPPH solution was reduced to yellow colour due to the essential oil which contains antioxidant compounds. The ascorbic acid solution (10-50mg/ml) (Fig 66) at 515nm showed the regression coefficient of 0.9823 and the equation was $y=0.003x$

+ 0.78. The antioxidant content of essential oils obtained from selected plants was shown in Fig 67.

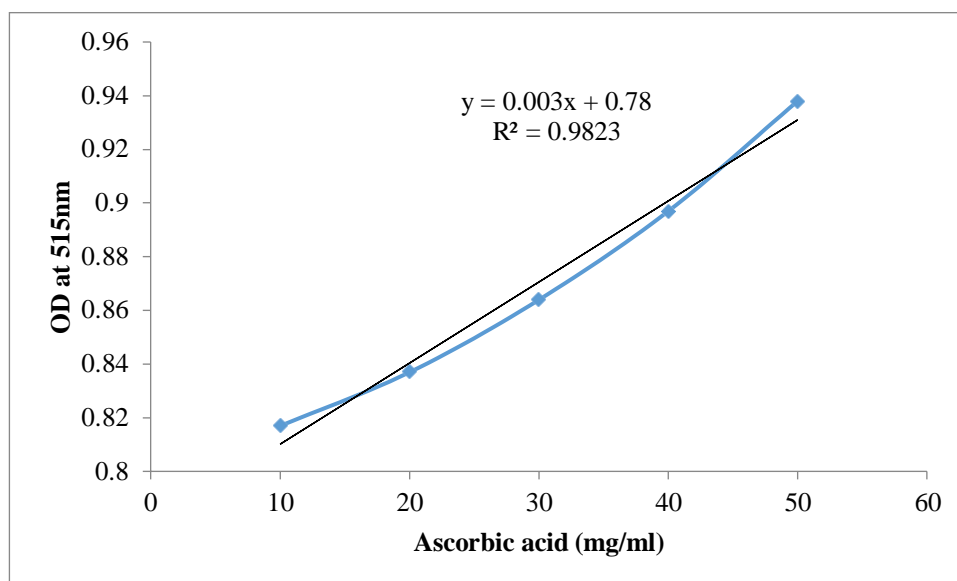


Fig 66. Calibration curve of ascorbic acid

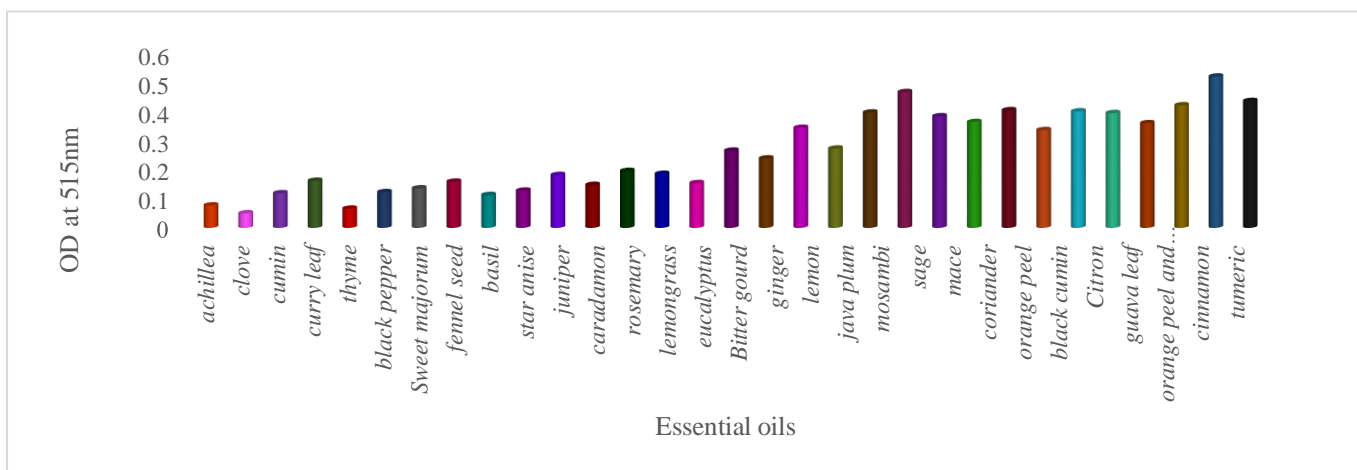


Fig 67. Antioxidant content of essential oils

The ascorbic acid (AA) and methanolic extract of *Zingiber officinale* (MEZO) showed an increase in an inhibition of DPPH with concentrations. The inhibition (%) of DPPH of methanolic extract was less than AA. The IC_{50} was recorded as $36.44 \pm 1.78 \mu\text{g/ml}$ and $47.05 \pm 2.03 \mu\text{g/ml}$ for AA and MEZO (Yusuf *et.al*, 2018).

4.6.5 Total phenolic content

The total phenolic content (TPA) for essential oils obtained from various plant sources was estimated using Folin-ciocalteu's method by using Gallic acid as a standard. The reagent was formed from the mixture of phosphomolybdic acid and phosphotungstic acid. The blue colour was produced at maximum absorption of 765nm and was proportional to total quantity of phenolic compounds present in essential oils. The Gallic acid solution (50-250µg/ml) (Fig 68) at 765nm showed the regression coefficient of 0.9913 and the equation was $y=0.007x + 0.009$. The antioxidant content of essential oils obtained from selected plants (Fig 69).

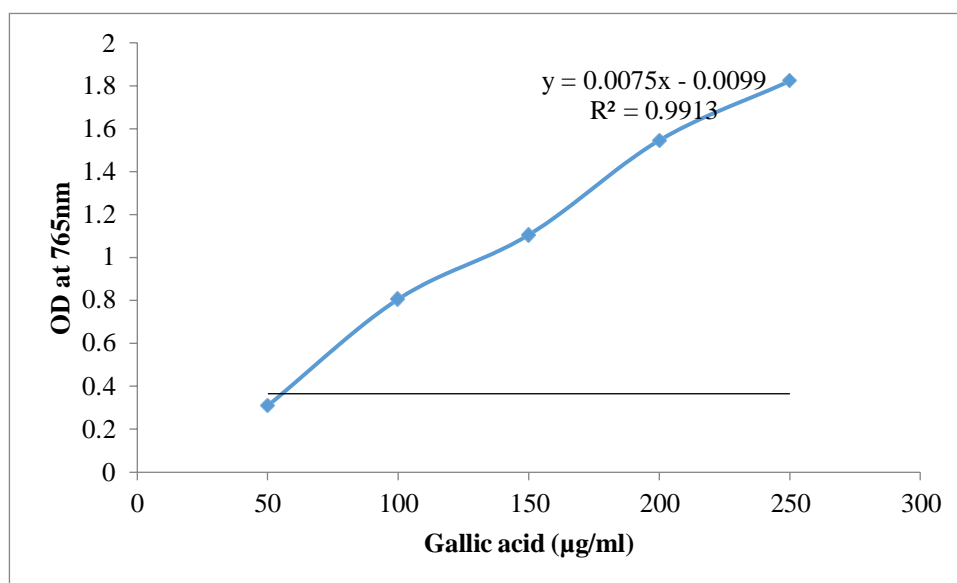


Fig 68. Standard curve of Gallic acid

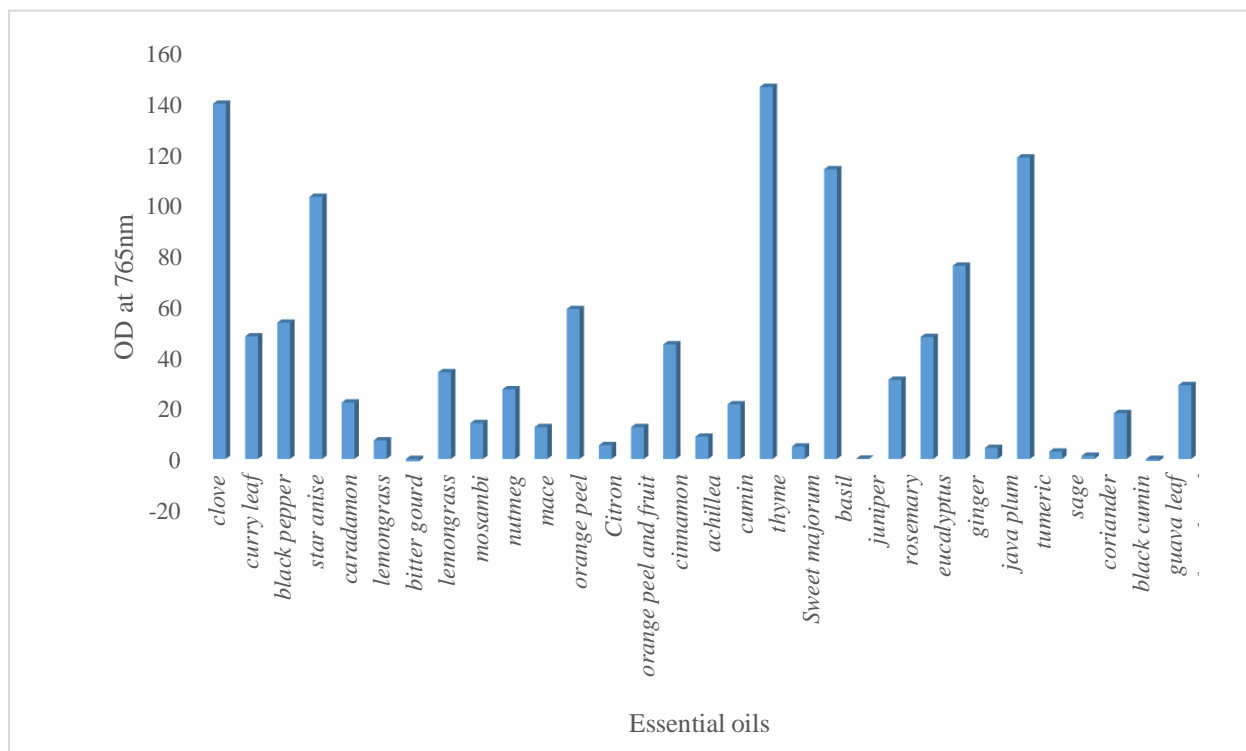


Fig 69. TPA content of essential oils

In a similar study, the presence of tannins, alkaloids, phenols, saponins, terpenoids, anthraquinone and glycoside was identified using the qualitative analysis of phytochemicals. The TPC of MEZO was found to be 15.24 ± 0.02 mg GAE/g sample (Gedikoğlu *et.al*, 2019).

4.6.7 Antimicrobial activity

The various essential oils (31) were examined for the inhibition of bacterial and fungal growth by well diffusion method. The essential oils shown the zone of inhibition against *Bacillus amyloliquefaciens* was thyme (22mm), cinnamon (17 mm), cumin seed (13mm), clove (12mm), rosemary (11mm), orange peel and fruit (10mm), mace (8mm), black cumin seed (8mm), eucalyptus (8mm), ginger (7mm), lemon (7mm) and some other essential oils also showed the zone of inhibition against *Bacillus amyloliquefaciens* (Table 13). The zone of inhibition against *Aspergillus flavus* showed by Cinnamon (29mm), thyme (21mm) and ginger (15mm) (Table 14). The EOs such as thyme (16mm) and cinnamon (13mm) shows zone of

inhibition against *Candida parapsilosis*. The EOs like ginger (8mm) and star anise (7mm) shows good antimicrobial activity against the *Trichosporon asahii*.

Table 13. Antimicrobial activity of TM1 strain (*Bacillus amyloliquefaciens*)

Essential oils	Zone of inhibition (mm)
Rosemary	11mm
Mace	8mm
Thyme	22mm
Guava leaf	6mm
Orange peel and fruit	10mm
Clove	12mm
Black cumin seed	8mm
Mint	6mm
Mosambi	5mm
Ginger	7mm
Lemon	7mm
Caradamon	6mm
Curry leaf	5mm
Cinnamon	17mm
Cumin seed	13mm
Eucalyptus	8mm
Betel leaf	5mm
Nutmeg	6mm

The methanolic extract of cumin seed was observed for the growth of inhibition of bacteria by using the well diffusion method. The zone of inhibition by methanolic extract of cumin seed was examined for *E.coli* (10.7mm), *P.aeruginosa* (13.1mm), *B. pumilus* (12.8mm) and *S.aureus* (14mm) (Benlafya *et al.* 2014).

Table 14. Antimicrobial activity of *Aspergillus flavus* (FS1)

Essential oils	Zone of inhibition (mm)
Rosemary	10mm
Nutmeg	10mm
Eucalyptus	10mm
Ginger	15mm
Basil	10mm
Sweet majorum	13mm
Thyme	21mm
Curry leaf	8mm
Black cumin seed	8mm
Cinnamon	29mm
Star anise	10mm
Caradamon	11mm
Fennel seed	10mm

The antimicrobial activity against pathogenic microbes was evaluated using aqueous and methanolic extract of *Aegle marmelos*. The aqueous extract of *Aegle marmelos* showed best antimicrobial activity against *S. epidermidis* (14.3 mm), *S. aureus* (13mm) and *K. pneumonia* (10.6mm). The maximum zone of inhibition was achieved at the concentration of

40 mg/ml. The methanolic extract of *Aegle marmelos* against the *S.aureus* was potent and evaluated with maximum concentration of 40 mg/ml (Karmase *et al.* 2014).

Table 15. Antimicrobial activity of *Candida parapsilosis* (FS2)

Essential oils	Zone of clearance (mm)
Cinnamon	13mm
Black cumin seed	8mm
Nutmeg	9mm
Ginger	8mm
Star anise	6mm
Cumin seed	6mm
Curry leaf	8mm
Mace	9mm
Lemon	9mm
Clove	7mm
Thyme	16mm

Anh *et al.* (2019) reported that the antimicrobial activity was carried out against the Gram positive bacteria and fungi using the disc diffusion method that indicates the *B. subtilis* (29mm) and *A. niger* (28mm) showed largest zone of inhibition and shows the low minimum inhibitory concentration (MIC) values for *B. subtilis* (62.6 µg/ml) and *A. niger* (80.6 µg/ml).

Table 16. Antimicrobial activity of *Trichosporon asahii* (FS3)

Essential oils	Zone of clearance (mm)
Cumin seed	5mm
Curry leaf	7mm
Star anise	7mm
Fennel seed	6.8mm
Ginger	8mm

The antimicrobial activity of thyme essential oil and plant extract was extracted and tested against the Gram negative and gram positive bacteria. The plant extract of thyme does not showed any antimicrobial activity against *Staphylococcus aureus* and *Salmonella typhimurium*. The essential oil extracted from the thyme showed good antimicrobial activity against both organisms. The *S.aureus* (35mm) and *S. typhimurium* (14.5mm) showed zone of inhibition by thyme essential oil (Lagouri, Guldaz, and Gurbuz 2011).

The antibacterial activity of MEZO was assessed by the zone of inhibition with different concentration of 25-100µg/ml, where the zone of inhibition increases. The *K. pneumoniae*, *E.coli*, *P. aeruginosa* and *S. typhi* showed susceptibility of 29.39, 22.87, 26.44 and 18.26mm respectively (Gedikoğlu *et.al*, 2019).

4.6.8 GC-MS analysis

The results revealed that some essential oils like thyme, cinnamon, cumin seed, star anise and ginger showed good antimicrobial activity against both bacteria and fungi. The major volatile compounds present in the ginger EO (Fig 70) and the chemical constituent of EO was cis-alpha-Bergamotene (22.65%), alpha-Terpineol (1.06%), Neral (4.40%), 2, 6-Octadienal, 3, 7-dimethyl, (E) – (8.90%), benzene, alpha-Farnesene (10.22%), beta-bisabolene (9.01%) and cedrene (11.55%) (Table 17) which showed the antimicrobial activity against *A. flavus* and *T. asahii*.

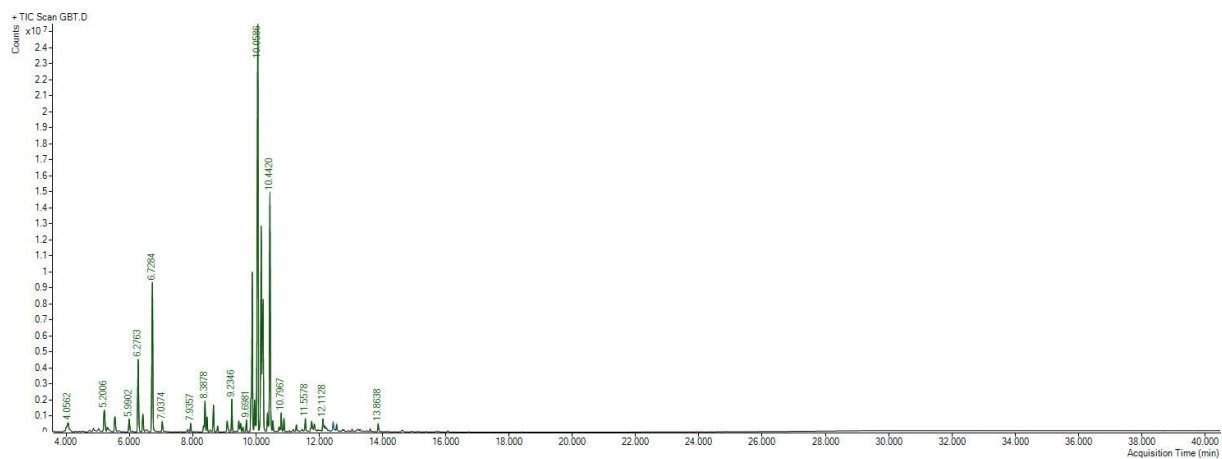


Fig 70. Chromatogram of essential oil extracted from ginger

Table 17. Phytochemical compounds present in ginger essential oil

Peaks	Area (%)	Compound Name
5.2006	1.65	endo-Borneol
5.5382	1.06	alpha.-Terpineol
6.2763	4.40	Neral
6.7284	8.90	2,6-Octadienal, 3,7-dimethyl-, (E)-
9.8812	8.74	Benzene, 1-(1,5-dimethyl-4-hexenyl)-4-methyl-
10.0586	22.65	cis-.alpha.-Bergamotene
10.1616	10.22	alpha.-Farnesene
10.2245	9.01	.beta.-Bisabolene
10.4420	11.55	Cedrene

The Anethole (100%) was the major chemical compound present in star anise EO which (Fig 71 and Table 18) and it showed antimicrobial activity against *T. asahii*. In cumin seed

EO, the important bioactive compounds (Fig 72) was γ -Terpinene (9.47%), Cuminal (28.98%), 1, 4 - p - Menthadien-7-al (20.25%), 2, 4- Di-tert-butylphenol (2.72%), 1, 2- Benzenedicarboxylic acid, and Dibutyl phthalate (6.95%) (Table 19). These compounds showed good antimicrobial activity against *B. amyloliquefaciens*.

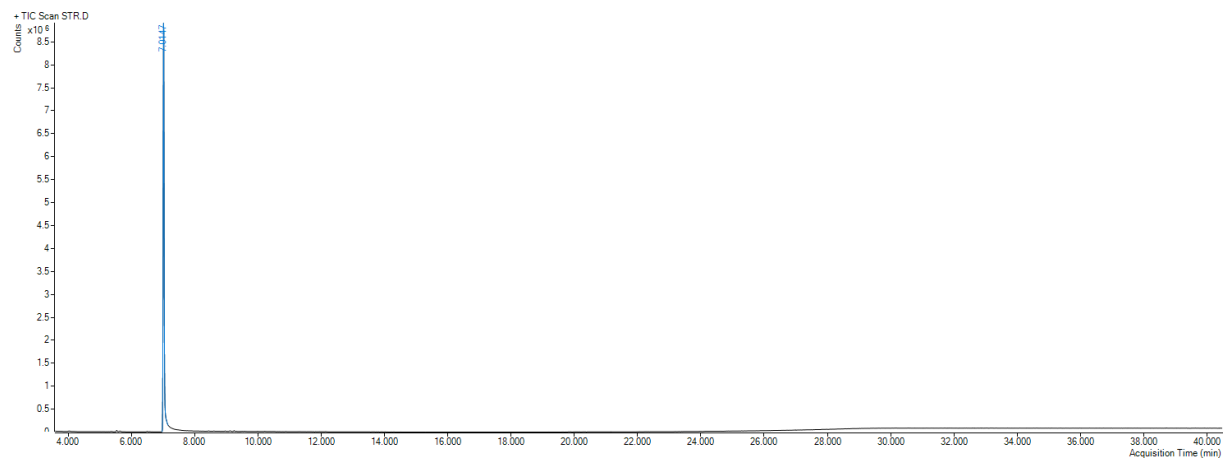


Fig 71. Chromatogram of star anise essential oil

Table 18. Phytochemical compounds present in star anise essential oil

Peaks	Area (%)	Compound Name
7.0147	100	Anethole

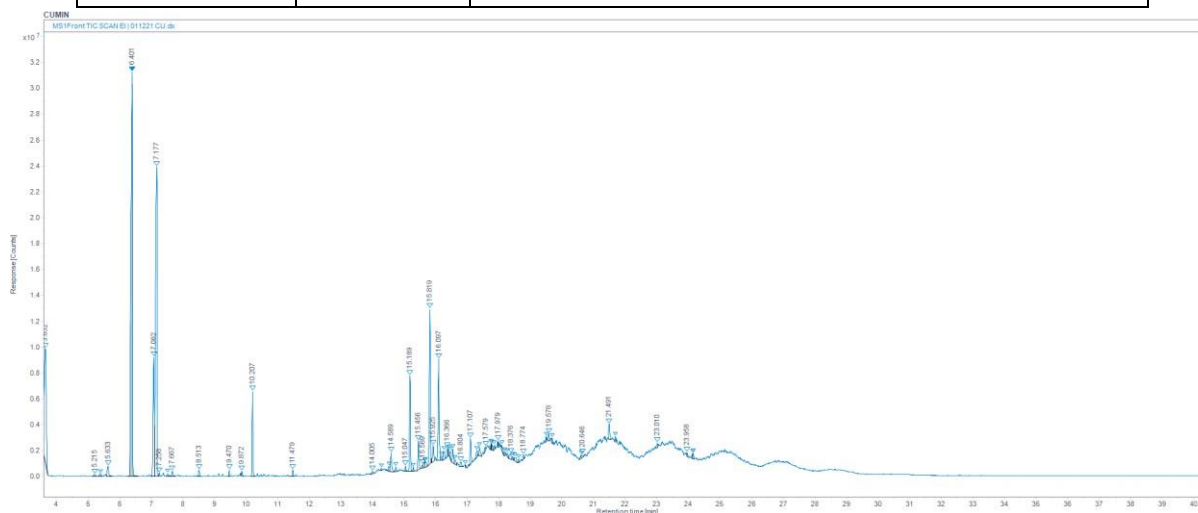


Fig 72. Chromatogram of Cumin seed EO.

Table 19. Bioactive compounds in Cumin seed EO

Peaks	Area (%)	Compound Name
3.652	9.47	γ -Terpinene
6.401	28.98	Cuminal
7.082	6.20	4-Isopropylcyclohexa-1,3-dienecarbaldehyde
7.177	20.25	1,4-p-Menthadien-7-al
10.207	2.72	2,4-Di-tert-butylphenol
15.189	3.66	1,2-Benzenedicarboxylic acid, butyl 2-ethylhexyl Ester
15.819	6.95	Dibutyl phthalate

The major volatile compound in cinnamon EO (Fig 73) was Cinnamaldehyde, (E) – (27.55%), (Z) – 3 – Phenylacrylaldehyde (13.83%) and 2 – Propenal, 3 – phenyl – (6.54%) (Table 20) that showed the antimicrobial activity against the *B. amyloliquefaciens*, *A. flavus* and *C. parapsilosis*. In thyme EO, the chromatogram of the volatile compounds (Fig 74) and the compounds was tabulated (Table 21). The major chemical compounds were Phenol, 2-methyl-5-(1- methylethyl) – (44.34%), Monobutyl phthalate (8.17%), thymol (6.34%) and γ – Terpinene (5.50%). These compounds have the ability to reduce the growth of *C. parapsilosis*, *A. flavus* and *B. amyloliquefaciens*.

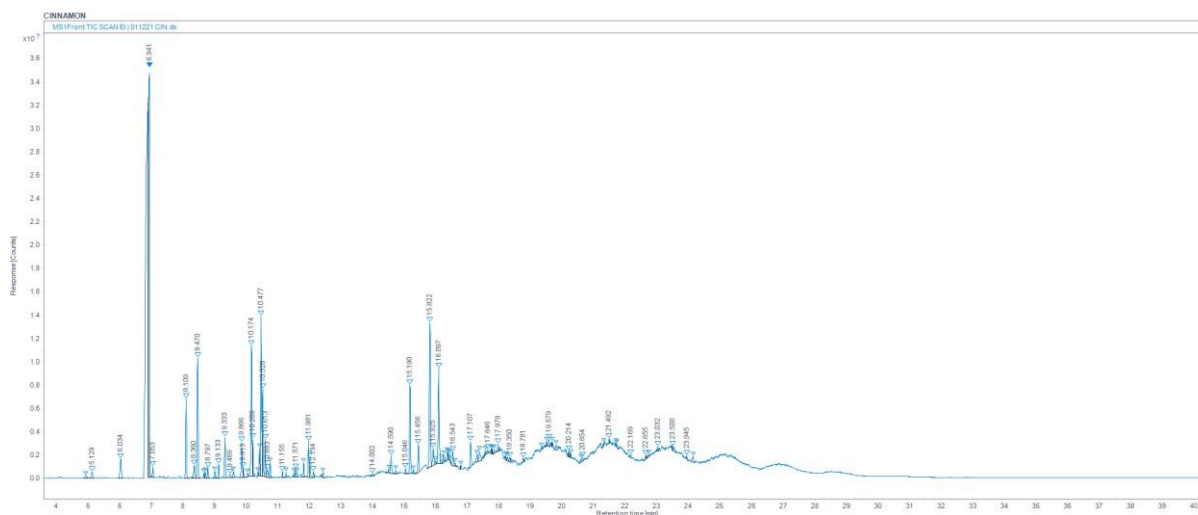


Fig 73. Chromatogram of Cinnamon EO

Table 20. Phytochemical compounds in Cinnamon EO

Peaks	Area (%)	Compound Name
6.890	27.55	Cinnamaldehyde, (E)-
6.910	6.54	2-Propenal, 3-phenyl-
6.941	13.83	(Z)-3- Phenylacrylaldehyde
8.109	2.21	Eugenol
8.470	3.49	Copaene
9.333	1.43	Acetic acid, cinnamyl ester
9.866	1.12	γ -Muurolene
10.174	4.28	α -Muurolene
10.477	4.95	Naphthalene, 1,2,3,5,6,8a-hexahydro- 4,7-dimethyl-1-(1-methy
10.528	2.47	(Z)-2- Methoxycinnamaldehyde
11.981	1.05	.tau.-Muurolol
15.190	2.77	1,2-Benzenedicarboxylic acid, butyl 2-ethylhexyl Ester
15.822	5.29	Dibutyl phthalate

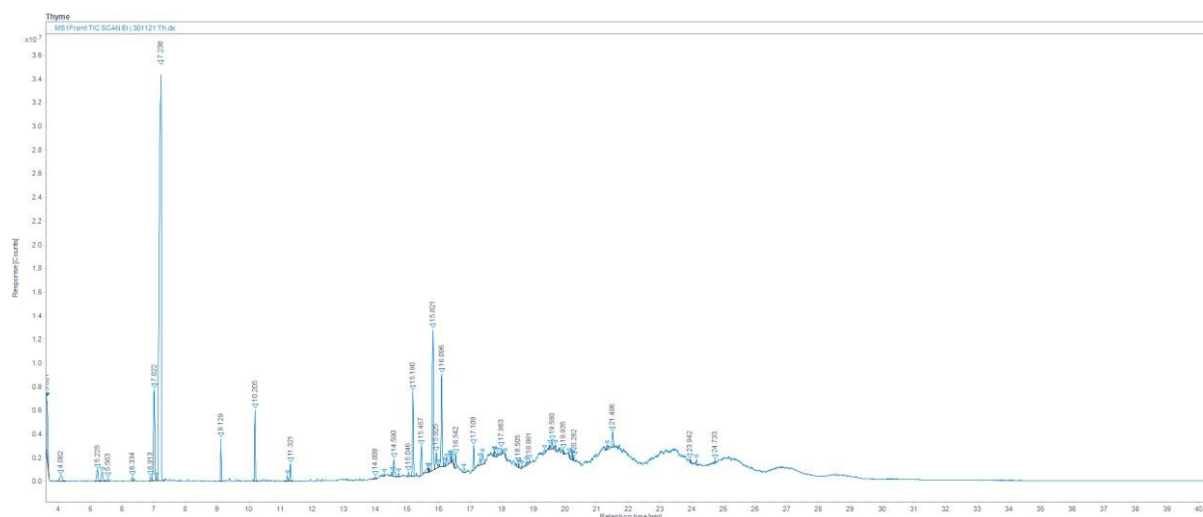


Fig 74. Chromatogram of thyme EO

Table 21. Bioactive compounds in thyme EO

Peaks	Area (%)	Compound Name
7.238	44.34	2-methyl-5-(1- methylethyl)- phenol
7.022	6.34	Thymol
3.621	5.50	γ -Terpinene
9.129	1.85	Caryophyllene
10.205	2.85	2,4-Di-tert-butylphenol
14.590	1.06	1,2-Benzenedicarboxylic acid, butyl decyl ester
15.457	1.49	2-Amino-4H- [1,3,5]triazino[2,1-b][1,3]benzoxazole-4- thione
15.821	8.17	Monobutyl phthalate

The antimicrobial and antioxidant activity of fennel EO was performed and the chemical composition of fennel EO was identified using GC-MS. The major bioactive

compounds of EO were trans-Anethole (69.87%), estragole (5.45%), fenchone (10.23%) and limonene (5.10%). The fenchone, estragole and Trans – anethole were the major monoterpene whereas the limonene was the major monoterpene (Martati and Akmalina 2018).

CHAPTER 5

SUMMARY AND CONCLUSION

The determination of uric acid was carried out using rapid and preceding UV-Visible spectrophotometric method. The validation of both rapid and preceding method was done by linear regression, CART and cluster analysis. The linear regression model revealed that the R^2 of preceding and rapid method was 0.991 and 0.994 which illustrate that the rapid method was more accurate than the preceding method. The time required to analyse a sample with extraction process using preceding and rapid method was 40 and 20 minutes/sample.

In CART[®] regression model, the result shown that the absorbance increases with the uric acid concentration showed optimal R^2 value for preceding and rapid method was 0.8803 and 0.9363. The optimum R^2 value told that the rapid method was more accurate than the preceding method. The scatter plot indicated that the actual and predicted values were scattered away in the preceding method whereas in rapid method the predicted and actual values were identical and the prediction was accurate. In hierarchical cluster analysis, the similarity level was 40% and 50% for preceding and rapid method. The cluster analysis showed the similarity among the observations in preceding and rapid method.

The paper strip was developed using Whatman filter paper No 40 with dimension of 20mm (width) and 60mm (height). The paper was treated with ferric chloride and different concentration of uric acid and sample filtrate was treated with potassium ferricyanide. The potassium ferricyanide react with uric acid and forms potassium ferrocyanide. This mixture was added to the treated paper strip and it leads to form Prussian blue colour that indicates the presence of uric acid in infested food samples. The colour development was captured using the image processing camera. The captured images were used to develop the MATLAB coding to

find out the concentration of unknown samples. The validation of paper strip method was done by using linear regression and CART[®] model.

In linear regression model, the R^2 of paper strip method was 0.993 and adjusted R^2 was 0.992 whereas the MSE, RMSE, MAPE, DW test value was less than 7 which showed that the paper strip method was accurate. In CART[®] regression, the optimal R^2 (0.9615) was obtained when the colour intensity decreases where the concentration of uric acid increases at the terminal node 11. In same way, the standard UA and real time samples were validated using ANN with feed forward model. The standard UA showed best accuracy by BFG-FNN algorithm with R^2 of 0.9833 and MSE was less compared with other three algorithms. The uninfested and infested samples shown that LM-FNN model had best accuracy for maida and rava samples whereas RP-FNN model shown best result for wheat flour.

The results revealed that the UV-Visible spectroscopy and paper strip method gave best accuracy. The determination of uric acid can be done previously using enzyme based colorimetric method, HPLC, GC-MS which are highly equipped instruments, costly and take too much time period for analysis of a sample. The UV-Visible and paper strip method are fast and time consuming method.

The DNA based biosensor was developed to detect the UA in wheat flour samples. The DNA based biosensor was optimized with the DNA immobilization showed that within 1 hour, and the biosensor was stable. The DNA immobilization for 2 and 3 hours showed that the biosensor response decreases while the DNA immobilization time increases. The DNA hybridization was carried on from 20 – 40 minutes. After incubation of 40 mins, the DNA hybridization increases with 0.089 V. The different concentrations of UA (25, 50, 75 and 100 ppm) showed the biosensor response decreases with concentration. The performance

evaluation of DNA based biosensor was evaluated based on the linearity, LOD, regeneration, operational stability and reproducibility.

The linearity of DNA based biosensor shown the R^2 of 0.9952 and LOD of DNA based biosensor was obtained as 97 ppm. The regeneration of DNA based biosensor was performed using the 0.1 M NaOH that breakdown the hydrogen bonds between the basepairs of DNA. The regeneration cycle shows the biosensor response was decreased to 78.56%. The operational stability was evaluated by running 5 times in same day with 100 ppm concentration of UA. The RSD (0.41%) was obtained by the operational stability of DNA based biosensor. The DNA based biosensor showed the good reproducibility with 0.006-1.05 % of RSD with the five number of electrodes.

The FTIR analysis of DNA based biosensor was characterized and the peaks observed the presence of amide, methylene and methyl groups. The SEM analysis of bare electrode shows the rough surface and after the addition of AgNPs and DNA, the surface of SPE appears smooth and the particle size get increases. The UA immobilized SPE reduce the ATP to ADP and phosphate (Pi).

The DNA based biosensor was compared with the HPLC method. The regression coefficient (R^2) of 0.993 showed the good correlation between the DNA based biosensor and HPLC method.

The UA concentration decreases due to the presence of UA degrading microbes like bacteria and fungi was isolated using the NA-UA and RBA-UA. The isolated bacterial and fungal strains were identified using the 16 S and ITS sequencing. The bacteria waere identified as the *B. amyloliquefaciens* and fungal strains as *A. flavus*, *C. parapsilosis* and *T. asahii*. The EOs was extracted using the hydrodistillation and DPPH assay was performed to found the antioxidant content in EOs. The TPA was also performed. The antimicrobial activity of EOs

such as thyme, cinnamon, cumin seed, ginger and star anise against the *B. amyloliquefaciens*, *A. flavus*, *C. parapsilosis* and *T. asahii*. The GC-MS analysis was performed to found the phytochemical compounds present in the EOs.

Future aspects

- To develop a device to determine UA using the MATLAB with incorporation of Arduino
- Sandwich type of biosensor can be developed to detect the UA
- A mobile based application device can be developed
- A chitin based packaging material can be developed with incorporation of EOs that can control the growth of microbes and also reduce the contaminations in stored food samples.

REFERENCES

- Abalone, R., A. Gastón, R. Bartosik, L. Cardoso, and J. Rodríguez. 2011. "Gas Concentration in the Interstitial Atmosphere of a Wheat Silo-Bag. Part II: Model Sensitivity and Effect of Grain Storage Conditions." *Journal of Stored Products Research* 47(4):276–83. doi: 10.1016/j.jspr.2011.05.003.
- Abasi, Negar, Mahmoud Reza Sohrabi, Fereshteh Motiee, and Mehran Davallo. 2021. "The Application of Artificial Neural Network and Least Square Support Vector Machine Methods Based on Spectrophotometry Method for the Rapid Simultaneous Estimation of Triamcinolone, Neomycin, and Nystatin in Skin Ointment Formulation." *Optik* 241(April):167-210. doi: 10.1016/j.ijleo.2021.167210.
- Achmad, Adji, and Rinaldo Fernandes. 2021. "Comparison of Cluster and Linkage Validity Indices in Integrated Cluster Analysis with Structural Equation Modeling War-PLS Approach. War-PLS." (April).
- Alshannaq, Ahmad, and Jae Hyuk Yu. 2017. "Occurrence, Toxicity, and Analysis of Major Mycotoxins in Food." *International Journal of Environmental Research and Public Health* 14(6). doi: 10.3390/ijerph14060632.
- Amin, Syed Umar, Kavita Agarwal, and Rizwan Beg. 2013. "Genetic Neural Network Based Data Mining in Prediction of Heart Disease Using Risk Factors." *2013 IEEE Conference on Information and Communication Technologies, ICT 2013 (Ict)*:1227–31. doi: 10.1109/CICT.2013.6558288.
- Amir, Dalia El, Sameh F. Abouzid, Mona H. Hetta, Abdelaaty A. Shahat, and Mohamed A. El. 2014. "Composition of the Essential Oil of the Fruits of *Phyllanthus Emblica* Cultivated

- in Egypt.” *Journal of Pharmaceutical, Chemical and Biological Sciences* 2(November):202–7.
- Anh, Trieu Tuan, Lam Thi Thu Ngan, and Tri Duc Lam. 2019. “Essential Oil from Fresh and Dried Rosemary Cultivated in Lam Dong Province, Vietnam.” *IOP Conference Series: Materials Science and Engineering* 544(1). doi: 10.1088/1757-899X/544/1/012025.
- Anwar, Farooq, Muhammad Ali, Abdullah Ijaz Hussain, and Muhammad Shahid. 2009. “Antioxidant and Antimicrobial Activities of Essential Oil and Extracts of Fennel (*Foeniculum Vulgare* Mill.) Seeds from Pakistan.” *Flavour and Fragrance Journal* 24(4):170–76. doi: 10.1002/ffj.1929.
- Asyana, V., F. Haryanto, L. A. Fitri, T. Ridwan, F. Anwary, and H. Soekersi. 2016. “Analysis of Urinary Stone Based on a Spectrum Absorption FTIR-ATR.” *Journal of Physics: Conference Series* 694(1). doi: 10.1088/1742-6596/694/1/012051.
- Atty, FemiKariy, and Jini JosepH. 2016. “Isolation and Identification of Uric Acid Degrading Bacteria, Optimization of Uricase Production and Purification of Uricase Enzyme.” *International Journal of Advanced Research* 4(12):2732–42. doi: 10.21474/ijar01/2702.
- Badawy, Mohamed E. I., Tesby M. R. Lotfy, and Samar M. S. Shawir. 2019. “Preparation and Antibacterial Activity of Chitosan-Silver Nanoparticles for Application in Preservation of Minced Meat.” *Bulletin of the National Research Centre*. 43(1). doi: 10.1186/s42269-019-0124-8.
- Banga, Km Sheetal, Nachiket Kotwaliwale, Debabandya Mohapatra, and Saroj Kumar Giri. 2018. “Techniques for Insect Detection in Stored Food Grains: An Overview.” *Food Control*. 94: 167-196. doi: 10.1016/j.foodcont.2018.07.008.
- Benlafya, Kamal, Khalid Karrouchi, Yassine Charkaoui, Miloud El Karbane, and Youssef

- Ramli. 2014. "Antimicrobial Activity of Aqueous, Ethanolic, Methanolic, Cyclohexanic Extracts and Essential Oil of Nigella Sativa Seeds." *Journal of Chemical and Pharmaceutical Research* 6(8):9–11.
- Binimeliz, Marina Fernandes, Mariana Leonel Martins, Julio Cesar Campos Ferreira Filho, Lucio Mendes Cabral, Adriano Gomes da Cruz, Lucianne Cople Maia, and Andréa Fonseca-Gonçalves. 2020. "Antimicrobial Effect of a Cardamom Ethanolic Extract on Oral Biofilm: An Ex Vivo Study." *Natural Oral Care in Dental Therapy* 121–31. doi: 10.1002/9781119618973.ch8.
- Chtita, Samir, Mounir Ghamali, Majdouline Larif, Azeddine Adad, Hmamouchi Rachid, Mohammed Bouachrine, and Tahar Lakhli. 2007. "Prediction of Biological Activity of Imidazo[1,2- a]Pyrazine Derivatives by Combining DFT and QSAR Results." *International Journal of Innovative Research in Science, Engineering and Technology (An ISO Certified Organization)*. 3297(12):7951–62.
- Cleophas, M. C., L. A. Joosten, L. K. Stamp, N. Dalbeth, O. M. Woodward, and Tony R. Merriman. 2017. "ABCG2 Polymorphisms in Gout: Insights into Disease Susceptibility and Treatment Approaches." *Pharmacogenomics and Personalized Medicine* 10:129–42. doi: 10.2147/PGPM.S105854.
- Cooper, Nancy, Reza Khosravan, Carol Erdmann, John Fiene, and Jean W. Lee. 2006. "Quantification of Uric Acid, Xanthine and Hypoxanthine in Human Serum by HPLC for Pharmacodynamic Studies." *Journal of Chromatography B: Analytical Technologies in the Biomedical and Life Sciences*.837(1-2):1-10 doi: 10.1016/j.jchromb.2006.02.060.
- Cox, G. B., C. R. Loscombe, and J. A. Upfield. 1976. "The Determination of Uric Acid in Animal Feeding Stuffs Using High-Performance Liquid Chromatography." *The Analyst* 101:381–85. doi: 10.1039/an9760100381.

- Dayakar., T., K. Venkateswara Rao., K. Bikshalu., V. Rajendar., and Si Hyun Park. 2017. “Novel Synthesis and Structural Analysis of Zinc Oxide Nanoparticles for the Non Enzymatic Glucose Biosensor.” *Materials Science and Engineering C* 75:1472–79. doi: 10.1016/j.msec.2017.02.032.
- Dev, N., A. K. Das, M. A. Hossain, and S. M. M. Rahman. 2010. “Chemical Compositions of Different Extracts of *Ocimum Basilicum* Leaves.” *Journal of Scientific Research* 3(1):197. doi: 10.3329/jsr.v3i1.5409.
- Dhakal, Chuda Prasad. 2019. “Interpreting the Basic Outputs (SPSS) of Multiple Linear Regression.” (January 2018) 8(6): 1448-52. doi: 10.21275/4061901.
- Dowell, F. E., J. E. Throne, D. Wang, and J. E. (Baker. 1999. “Identifying Stored-Grain Insects Using near-Infrared Spectroscopy.” *Journal of Economic Entomology*.92(1):165-69. doi: 10.1093/jee/92.1.165.
- Dowell, Floyd E., James E. Throne, and James E. Baker. 1998. “Automated Nondestructive Detection of Internal Insect Infestation of Wheat Kernels by Using Near-Infrared Reflectance Spectroscopy.” *Journal of Economic Entomology*. 91(4): 899-904. doi: 10.1093/jee/91.4.899.
- Ebrahimi, Bahman, Seyed Abbas Shojaosadati, Parandis Daneshgar, Parviz Norouzi, and Seyyed Mohammad Mousavi. 2011. “Performance Evaluation of Fast Fourier-Transform Continuous Cyclic-Voltammetry Pesticide Biosensor.” *Analytica Chimica Acta* 687(2):168–76. doi: 10.1016/j.aca.2010.12.005.
- El-Desouky, Tarek A., Samy S. Elbadawy, Hassan B. H. Hussain, and Nilly A. Hassan. 2018. “Impact of Insect Densities *Tribolium Castaneum* on the Benzoquinone Secretions and Aflatoxins Levels in Wheat Flour During Storage Periods.” *The Open Biotechnology Journal* 12(1):104–11. doi: 10.2174/1874070701812010104.

- El-Hameed, Ahmed Abd, and Juyoul Kim. 2021. "Machine Learning-Based Classification and Regression Approach for Sustainable Disaster Management: The Case Study of APR1400 in Korea." *Sustainability (Switzerland)* 13(17): 1-14. doi: 10.3390/su13179712.
- Elizabeth B. Maghirang, Floyd E. Dowell, James E. Baker, and James E. Throne. 2013. "Detecting Single Wheat Kernels Containing Live or Dead Insects Using Near-Infrared Reflectance Spectroscopy." *American society of Agricultural engineers*.46(4): 1277-82.
- Fatih, Abdul, Senol Celik, Ecevit Eyduran, Cem Tirink, Mohammad Masood Tariq, Irfan Shahzad Sheikh, Asim Faraz, and Abdul Waheed. 2021. "Use of MARS Algorithm for Predicting Mature Weight of Different Camel (*Camelus Dromedarius*) Breeds Reared in Pakistan and Morphological Characterization via Cluster Analysis." *Tropical Animal Health and Production* 53(1):191. doi: 10.1007/s11250-021-02633-2.
- Fike, Alice, Julia Hartman, Christopher Redmond, Sandra G. Williams, Yanira Ruiz-Perdomo, Jun Chu, Sarfaraz Hasni, Michael M. Ward, James D. Katz, and Pravitt Gourh. 2021. "Risk Factors for COVID-19 and Rheumatic Disease Flare in a US Cohort of Latino Patients." *Arthritis and Rheumatology* 73(7):1129–34. doi: 10.1002/art.41656.
- Franke, Stanley R. Benedict & Elizabeth. 1922. "A Method for the Direct Determination of Uric Acid in Urine." *J.Biol.Chem* 52(2):387-91.
- Gedikoğlu, Ayça, Münevver Sökmen, and Ayşe Çivit. 2019. "Evaluation of Thymus Vulgaris and Thymbra Spicata Essential Oils and Plant Extracts for Chemical Composition, Antioxidant, and Antimicrobial Properties." *Food Science and Nutrition* 7(5):1704–14. doi: 10.1002/fsn3.1007.
- Ghadimloozadeh, Shaghayegh, Mahmoud Reza Sohrabi, and Hassan Kabiri Fard. 2021. "Development of Rapid and Simple Spectrophotometric Method for the Simultaneous

- Determination of Anti-Parkinson Drugs in Combined Dosage Form Using Continuous Wavelet Transform and Radial Basis Function Neural Network.” *Optik* 242(April):1670-88. doi: 10.1016/j.ijleo.2021.167088.
- Ghaedian, Ahmad R., and Randy L. Wehling. 1997. “Discrimination of Sound and Granary-Weevil-Larva-Infested Wheat Kernels by Near-Infrared Diffuse Reflectance Spectroscopy.” *Journal of AOAC International*. 80(5): 997-1005. doi: 10.1093/jaoac/80.5.997.
- Ghanta, Susanta, Chanchal Bhaumik, and Mriganka Sekhar Manna. 2022. “Process Development for Isolation of Dietary Eugenol from Leaves of Basil (*Ocimum Sanctum*) in Combination of Optimization of Process Variables and Modeling by Artificial Neural Network.” *Journal of the Indian Chemical Society* 99(1):100-280. doi: 10.1016/j.jics.2021.100280.
- Gharagheizi, Farhad, and Gholam Reza Salehi. 2011. “Prediction of Enthalpy of Fusion of Pure Compounds Using an Artificial Neural Network-Group Contribution Method.” *Thermochimica Acta* 521(1–2):37–40. doi: 10.1016/j.tca.2011.04.001.
- Ghosh, Tanushree, and Priyabrata Sarkar. 2014. “Isolation of a Novel Uric-Acid-Degrading Microbe *Comamonas* Sp. BT UA and Rapid Biosensing of Uric Acid from Extracted Uricase Enzyme.” *Journal of Biosciences* 39(5):805–19. doi: 10.1007/s12038-014-9476-2.
- Gin Farn, D. Morison Smith. 1963. “Rate of Excretion of Uric Acid by the Rust-Red Flour Beetle.” *Journal of AOAC INTERNATIONAL*. 46(3): 517-21doi: 10.1093/jaoac/46.3.517.
- Hafez, Rehab M., Tahany M. Abdel-Rahman, and Rasha M. Naguib. 2017. “Uric Acid in Plants and Microorganisms: Biological Applications and Genetics - A Review.” *Journal of Advanced Research* 8(5):475–86. doi: 10.1016/j.jare.2017.05.003.

- Haliloglu, Yesim, Temel Ozek, Mehmet Tekin, Fatih Goger, Kemal Husnu Can Baser, and Gulmira Ozek. 2017. "Phytochemicals, Antioxidant, and Antityrosinase Activities of Achillea Sivasica Çelik and Akpulat." *International Journal of Food Properties* 20(1):S693–706. doi: 10.1080/10942912.2017.1308954.
- Hassan, Riyadh Abdulmalek, Lee Yook Heng, and Ling Ling Tan. 2019. "Novel DNA Biosensor for Direct Determination of Carrageenan." *Scientific Reports* 9(1):1–9. doi: 10.1038/s41598-019-42757-y.
- Hubert, Jan, Vaclav Stejskal, Christos G. Athanassiou, and James E. Throne. 2018. "Health Hazards Associated with Arthropod Infestation of Stored Products." *Annual Review of Entomology* 63:553–73. doi: 10.1146/annurev-ento-020117-043218.
- Ibupoto, Zafar Hussain, Syed Muhammad Usman Ali, Kimleang Khun, Chan Oeurn Chey, Omer Nur, and Magnus Willander. 2011. "Zno Nanorods Based Enzymatic Biosensor for Selective Determination of Penicillin." *Biosensors* 1(4):153–63. doi: 10.3390/bios1040153.
- Imran, Muhammad, Christopher J. Ehrhardt, Massimo F. Bertino, Muhammad R. Shah, and Vamsi K. Yadavalli. 2020. "Chitosan Stabilized Silver Nanoparticles for the Electrochemical Detection of Lipopolysaccharide: A Facile Biosensing Approach for Gram-Negative Bacteria." *Micromachines* 11(4): 413. doi: 10.3390/MI11040413.
- Induja C, Loganathan M, Shanmugasundaram S. 2022. "Development of A Simple Rapid Method for Determination of Uric Acid Using UV-Visible Spectroscopy." *International Journal of Life Science and Pharma Research* 12(1):200–205.
- Induja C, and Loganathan M. 2021. "Influence of Host and Duration of Storage on Uric Acid Contamination in Wheat Products Infested with Confused Flour Beetle , Tribolium Confusum." *International Journal of Entomology Research*. 6(6):84–86.

- Indumathi, C., D. Manoj, M. Loganathan, and S. Shanmugasundaram. 2021. "Impact of Radiofrequency Disinfestation on *Tribolium Castaneum* (Herbst) in Wheat Flour and Its Influence on the Functional Characteristics of Wheat Flour." *Journal of Food Processing and Preservation* 45(10):1–14. doi: 10.1111/jfpp.15770.
- Islam, Md Nazibul, Isteaque Ahmed, Muzahidul Islam Anik, Md Sakib Ferdous, and Mohidus Samad Khan. 2018. "Developing Paper Based Diagnostic Technique to Detect Uric Acid in Urine." *Frontiers in Chemistry*. 6: 496. doi: 10.3389/fchem.2018.00496.
- Jayas, Digvir S. 2012. "Storing Grains for Food Security and Sustainability." *Agricultural Research* 1(1):21–24. doi: 10.1007/s40003-011-0004-4.
- Jen, Jen Fon, Shih Liang Hsiao, and Kang Hsiung Liu. 2002. "Simultaneous Determination of Uric Acid and Creatinine in Urine by an Eco-Friendly Solvent-Free High Performance Liquid Chromatographic Method." *Talanta*. 58(4):711-17. doi: 10.1016/S0039-9140(02)00377-6.
- Jirakunakorn, Ratchaneekorn, Suntisak Khumngern, Jittima Choosang, Panote Thavarungkul, Proespichaya Kanatharana, and Apon Numnuam. 2020. "Uric Acid Enzyme Biosensor Based on a Screen-Printed Electrode Coated with Prussian Blue and Modified with Chitosan-Graphene Composite Cryogel." *Microchemical Journal* 154(September 2019):104-24. doi: 10.1016/j.microc.2020.104624.
- Karadeniz, Hakan, Arzum Erdem, and Ayfer Caliskan. 2008. "Electrochemical Monitoring of DNA Hybridization by Multiwalled Carbon Nanotube Based Screen Printed Electrodes." *Electroanalysis* 20(17):1932–38. doi: 10.1002/elan.200804270.
- Karmase, Aniket, K. Prasanna, Sruti Rasabattula, and Kamlesh K. Bhutani. 2014. "Quantification and Comparison of Extraction Methods for Alkaloids in *Aegle Marmelos* Leaves by HPLC." *Natural Product Communications* 9(7):981–83. doi:

10.1177/1934578x1400900725.

Kartini, K., W. A. Wulandari, N. I. E. Jayani, and F. Setiawan. 2021. "TLC-Based Fingerprinting for *Phyllanthus Niruri* from Diverse Geographical Origins in East and Central Java Indonesia." *IOP Conference Series: Earth and Environmental Science* 948(1). doi: 10.1088/1755-1315/948/1/012003.

Karunakaran, Chithra, Digvir S. Jayas, and Noel D. G. White. 2003. "Soft X-Ray Inspection of Wheat Kernels Infested by *Sitophilus Oryzae*." *Transactions of the American Society of Agricultural Engineers*. 46(3): 739-45. doi: 10.13031/2013.13576.

Khan, Mohidus Samad, and Gil Garnier. 2014. "Novel Image Analysis Technique to Measure Enzymatic Activity and Stability on Paper Surfaces." in *Advances in Image Analysis Research*. C10: 217-38.

Kim, Sang Sook, Mee Ra Rhyu, Jae Min Kim, and Sang Hyo Lee. 2003. "Authentication of Rice Using Near-Infrared Reflectance Spectroscopy." *Cereal Chemistry*. 80(3): 346-49. doi: 10.1094/CCHEM.2003.80.3.346.

Kogularasu, Sakthivel, Muthumariappan Akilarasan, Shen Ming Chen, Tse Wei Chen, and Bih Show Lou. 2019. "Urea-Based Morphological Engineering of ZnO; for the Biosensing Enhancement towards Dopamine and Uric Acid in Food and Biological Samples." *Materials Chemistry and Physics*. 227(1): 5-11. doi: 10.1016/j.matchemphys.2019.01.041.

Kumari, Khushbu, and Suniti Yadav. 2018. "Linear Regression Analysis Study." *Journal of the Practice of Cardiovascular Sciences* 4(1):33. doi: 10.4103/jpcs.jpcs_8_18.

Lagouri, Vasiliki, Metin Guldaz, and Ozan Gurbuz. 2011. "In Vitro Antioxidant/Free Radical Scavenging and Antibacterial Properties of Endemic Oregano and Thyme Extracts from

- Greece.” *Food Science and Biotechnology* 20(6):1487–93. doi: 10.1007/s10068-011-0206-3.
- Mahato, Dipendra K., Kyung Eun Lee, Madhu Kamle, Sheetal Devi, Krishna N. Dewangan, Pradeep Kumar, and Sang G. Kang. 2019. “Aflatoxins in Food and Feed: An Overview on Prevalence, Detection and Control Strategies.” *Frontiers in Microbiology* 10(October):1–10. doi: 10.3389/fmicb.2019.02266.
- Mak, Yin Wei, Li Oon Chuah, Rosma Ahmad, and Rajeev Bhat. 2013. “Antioxidant and Antibacterial Activities of Hibiscus (*Hibiscus Rosa-Sinensis* L.) and Cassia (*Senna Bicapsularis* L.) Flower Extracts.” *Journal of King Saud University - Science* 25(4):275–82. doi: 10.1016/j.jksus.2012.12.003.
- Manoj, D., I. Auddy, S. Nimbkar, S. Chittibabu, and S. Shanmugasundaram. 2020. “Development of Co-Immobilised Enzymes Amperometric Biosensor for the Determination of Triglycerides in Coconut Milk.” *International Food Research Journal* 27(5):875–82.
- Martati, E., and M. A. Akmalina. 2018. “Antioxidant Activity and Estragole Content of Ethanolic and Methanolic Extract of Fennel (*Foeniculum Vulgare* Mill.) and Its Risk Assessment Using Margin of Exposure (MOE).” *International Food Research Journal* 25(December):S43–49.
- Martinez, Andres W., Scott T. Phillips, Emanuel Carrilho, Samuel W. Thomas, Hayat Sindi, and George M. Whitesides. 2008. “Simple Telemedicine for Developing Regions: Camera Phones and Paper-Based Microfluidic Devices for Real-Time, off-Site Diagnosis.” *Analytical Chemistry*. 80(10): 3699-3707. doi: 10.1021/ac800112r.
- Mehmood, Khalid, Mureed Husain, Muhammad Aslam, Muhammad Shoaib Ahmedani, Azhar Mehmood Aulakh, and Farid Asif Shaheen. 2018. “Changes in the Nutritional

- Composition of Maize Flour Due to *Tribolium Castaneum* Infestation and Application of Carbon Dioxide to Manage This Pest.” *Environmental Science and Pollution Research* 25(19):18540–47. doi: 10.1007/s11356-018-2063-6.
- Milner, M., Lee, M. R., & Katz, R. 1952. “Radiography Applied to Grain and Seeds.” *Food Technology* 6:44–45.
- Neethirajan, S., C. Karunakaran, D. S. Jayas, and N. D. G. White. 2007. “Detection Techniques for Stored-Product Insects in Grain.” *Food Control* 18(2):157–62. doi: 10.1016/j.foodcont.2005.09.008.
- Negi, Aditi, Arunkumar Anandharaj, Sureshkumar Kalakandan, and Meenatchi Rajamani. 2021. “A Molecular Approach for the Detection and Quantification of *Tribolium Castaneum* (Herbst) Infestation in Stored Wheat Flour.” *Food Technology and Biotechnology* 59(1):112–21. doi: 10.17113/ftb.59.01.21.6902.
- Olsson, J., T. Börjesson, T. Lundstedt, and J. Schnürer. 2002. “Detection and Quantification of Ochratoxin A and Deoxynivalenol in Barley Grains by GC-MS and Electronic Nose.” *International Journal of Food Microbiology* 72(3):203–14. doi: 10.1016/S0168-1605(01)00685-7.
- Oppert, Brenda, Samantha Stoss, Alaysha Monk, and Timothy Smith. 2019. “Optimized Extraction of Insect Genomic Dna for Long-Read Sequencing.” *Methods and Protocols* 2(4):1–7. doi: 10.3390/mps2040089.
- Oswald, Frederick L. 2012. “Interpreting Multiple Linear Regression : A Guidebook of Variable Interpreting Multiple Linear Regression : A Guidebook of Variable Importance.” 17(9): 1-19.
- Palacios, Sara M., Alberto Bertoni, Yanina Rossi, Rocío Santander, and Alejandro Urzúa.

2009. "Efficacy of Essential Oils from Edible Plants as Insecticides against the House Fly, *Musca Domestica* L." *Molecules* 14(5):1938–47. doi: 10.3390/molecules14051938.
- Paolesse, Roberto, Adriano Alimelli, Eugenio Martinelli, Corrado Di Natale, Arnaldo D'Amico, Maria Grazia D'Egidio, Gabriella Aureli, Alessandra Ricelli, and Corrado Fanelli. 2006. "Detection of Fungal Contamination of Cereal Grain Samples by an Electronic Nose." *Sensors and Actuators, B: Chemical* 119(2):425–30. doi: 10.1016/j.snb.2005.12.047.
- Papa, E., P. Pilutti, and P. Gramatica. 2008. "Prediction of PAH Mutagenicity in Human Cells by QSAR Classification." *SAR and QSAR in Environmental Research* 19(1–2):115–27. doi: 10.1080/10629360701843482.
- Pappas, Peter W., and Sarah E. Morrison. 1995. "Benzoquinones of the Beetles, *Tribolium Castaneum* and *Tribolium Confusum*." *Preparative Biochemistry* 25(3):155–68. doi: 10.1080/10826069508010117.
- Pascal, Nathalie Colloc'h, Denis Vivarès, Françoise Bonneté, Bertrand Castro, Mohamed El Hajji, and Thierry Prangé. 2005. "Urate Oxidase from *Aspergillus Flavus*: New Crystal-Packing Contacts in Relation to the Content of the Active Site." *Acta Crystallographica Section D: Biological Crystallography* 61(3):218–29. doi: 10.1107/S0907444904031531.
- Pearson, Tom C., Daniel L. Brabec, and Carrie R. Schwartz. 2003. "Automated Detection of Internal Insect Infestations in Whole Wheat Kernels Using a Perten SKCS 4100." *Applied Engineering in Agriculture*. 19(6): 727-33.
- Perez-Mendoza, J., J. E. Throne, F. E. Dowell, and J. E. Baker. 2003. "Detection of Insect Fragments in Wheat Flour by Near-Infrared Spectroscopy." *Journal of Stored Products Research*. 39(3): 305-12. doi: 10.1016/S0022-474X(02)00021-8.

- Peter T Kissinger, Lawrence J Felice, Ralph M Riggan, Lawrence A Pachla, David C. Wenke. 1974. "Electrochemical Detection of Selected Organic Components in the Eluate from High Performance Liquid Chromatography." *Clinical Chemistry*. 20(8): 992-97.
- Pixton S.W. 1965. "Detection of Insect Infestations in Cereals by Measurement of Uric Acid." *Cereal Chem* 85(42):315–22.
- Raja Jamaluddin, Raja Zaidatul Akhmar, Ling Ling Tan, Kwok Feng Chong, and Lee Yook Heng. 2020. "An Electrochemical DNA Biosensor Fabricated from Graphene Decorated with Graphitic Nanospheres." *Nanotechnology* 31(48). doi: 10.1088/1361-6528/abab2e.
- Rajendran, S. 1999. "Detection of Insect Infestation in Stored Food Commodities." *Journal of Food Science and Technology* 36(4):283–300.
- Rajendran, Somiahnadar. 2005. "Detection of Insect Infestation in Stored Foods." *Advances in Food and Nutrition Research*. 49(4): 163-232. doi: 10.1016/S1043-4526(05)49005-1.
- Rajendran, Somiahnadar, and United Phosphorus Limited. 2015. "Grain Storage : Perspectives and Problems Grain Storage : And Problems Perspectives." (January 2003): 183-214.
- Ramadas, Sendhil, T. M. Kiran Kumar, and Gyanendra Pratap Singh. 2020. "Wheat Production in India: Trends and Prospects." *Recent Advances in Grain Crops Research* (July).156. doi: 10.5772/intechopen.86341.
- Ramesh, Rajendran, Puhazhselvan Puhazhendi, Jitendra Kumar, Marichetti Kuppaswami Gowthaman, Stanislaus Francis D'Souza, and Numbi Ramudu Kamini. 2015. "Potentiometric Biosensor for Determination of Urea in Milk Using Immobilized *Arthrobacter Creatinolyticus* Urease." *Materials Science and Engineering C* 49:786–92. doi: 10.1016/j.msec.2015.01.048.
- Randy L Wehling, David L Wetzel, John R. Pedersen. 1984. "Stored Wheat Insect Infestation

- Related to Uric Acid as Determined by Liquid Chromatography.” *Journal of the Association of Official Analytical Chemists*. 67(3):644-7. doi: 10.1093/jaoac/67.3.644-47.
- Rezaei, Rasoul, Mohammad Mehdi Foroughi, Hadi Beitollahi, and Reza Alizadeh. 2018. “Electrochemical Sensing of Uric Acid Using a ZnO/Graphene Nanocomposite Modified Graphite Screen Printed Electrode.” *Russian Journal of Electrochemistry* 54(11):860–66. doi: 10.1134/S1023193518130347.
- Ridgway, Christopher, and John Chambers. 1998. “Detection of Insects inside Wheat Kernels by NIR Imaging.” *Journal of Near Infrared Spectroscopy*. 6(1):115-19 doi: 10.1255/jnirs.128.
- Ron P Haff, and David C. Slaughter. 2013. “X-Ray Inspection of Wheat for Granary Weevils. Realtime Digital Imaging vs. Film.” *American society of Agricultural Engineers*.47(2):531-37.
- Rouf, M. A., and R. F. Lomphey. 1968. “Degradation of Uric Acid by Certain Aerobic Bacteria.” *Journal of Bacteriology*. 96(3):617–22. doi: 10.1128/jb.96.3.617-622.1968.
- ROY R. B., KVENBERG J. E. 1981. “Determination of Insect Infestation in Food: A Semiautomated Calorimetric Analysis for Uric Acid with Immobilized Uricase.” *Journal of Food Science*. 46(5): 1439-45. doi: 10.1111/j.1365-2621.1981.tb04193.x.
- S, Kamatchi Devi, and S. Shanmugasundaram. 2021. “Studies on Detection of Tetracycline in Honey Using Screen Printed Electrode with Buffer Electrolytes.” 10(11):2841–48.
- Said, Farhan M., Jye Yi Gan, and Junaida Sulaiman. 2020. “Correlation between Response Surface Methodology and Artificial Neural Network in the Prediction of Bioactive Compounds of Unripe *Musa Acuminata* Peel.” *Engineering Science and Technology, an International Journal* 23(4):781–87. doi: 10.1016/j.jestch.2019.12.005.

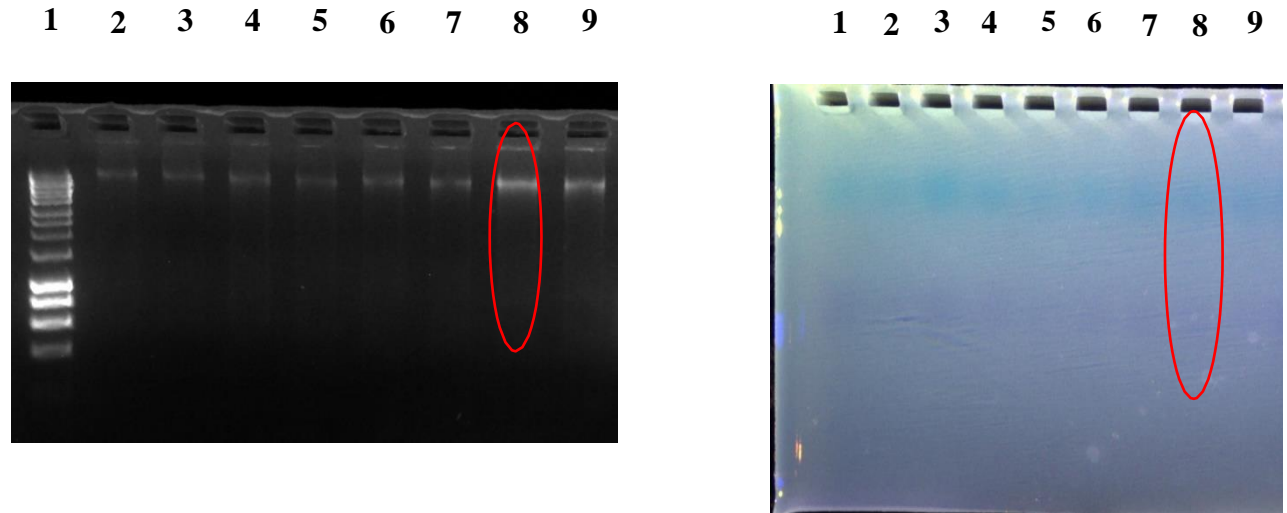
- Salehian, Samira, Mahmoud Reza Sohrabi, and Mehran Davallo. 2021. "Rapid and Simple Spectrophotometric Method Using Feedforward Backpropagation and Radial Basis Function Neural Networks for the Simultaneous Determination of Amoxicillin and Clavulanic Acid in Commercial Tablet and Human Blood Serum." *Optik* 247(September):167908. doi: 10.1016/j.ijleo.2021.167908.
- Singh, C. B., D. S. Jayas, J. Paliwal, and N. D. G. White. 2009. "Detection of Insect-Damaged Wheat Kernels Using near-Infrared Hyperspectral Imaging." *Journal of Stored Products Research* 45(3):151–58. doi: 10.1016/j.jspr.2008.12.002.
- Thanushree, M. P., Vimala, B. S. K., Moses, J. A., & Anandharamakrishnan, C. 2018. "Detection Techniques for Insect Infestation in Stored Grains." *Agriculture Engineering Today* 42(4):48–56.
- Toboc, Ani Alupului, and Vasile Lavric. 2012. "Artificial Neural Network Modelling of Ultrasound and Microwave Extraction of Bioactive Constituents from Medicinal Plants." *Revista de Chimie* 63(7):743–48.
- Ulianas, Alizar, Lee Yook Heng, Musa Ahmad, Han Yih Lau, Zamri Ishak, and Tan Ling Ling. 2014. "A Regenerable Screen-Printed DNA Biosensor Based on Acrylic Microsphere-Gold Nanoparticle Composite for Genetically Modified Soybean Determination." *Sensors and Actuators, B: Chemical* 190:694–701. doi: 10.1016/j.snb.2013.09.040.
- Valizadeh, Maryam, Mahmoud Reza Sohrabi, and Fereshte Motiee. 2021. "Simple Spectrophotometric Method for Simultaneous Determination of Salmeterol and Fluticasone as Anti-Asthma Drugs in Inhalation Spray Based on Artificial Neural Network and Support Vector Regression." *Optik* 240(April):166879. doi: 10.1016/j.ijleo.2021.166879.
- Vimala Bharathi, S. K., V. Vishnu Priya, Vishnu Eswaran, J. A. Moses, and Alice R. P.

- Sujeetha. 2017. "Insect Infestation and Losses in Stored Food Grains." *Ecology, Environment and Conservation* 23(1):286–91.
- Weng, Shizhuang, Zhaojie Chu, Manqin Wang, Kaixuan Han, Gongqin Zhu, Cunchuan Liu, Xinhua Li, and Linsheng Huang. 2022. "Reflectance Spectroscopy with Operator Difference for Determination of Behenic Acid in Edible Vegetable Oils by Using Convolutional Neural Network and Polynomial Correction." *Food Chemistry* 367(April 2021):130668. doi: 10.1016/j.foodchem.2021.130668.
- Yezerki, Ann, Timothy P. Gilmor, and Lori Stevens. 2004. "Genetic Analysis of Benzoquinone Production in *Tribolium Confusum*." *Journal of Chemical Ecology* 30(5):1035–44. doi: 10.1023/B:JOEC.0000028465.37658.ae.
- You, Guangjiao, Haining Zhao, Di Gao, Meng Wang, Xiaoliang Ren, and Yajing Wang. 2020. "Predictive Models of Tensile Strength and Disintegration Time for Simulated Chinese Herbal Medicine Extracts Compound Tablets Based on Artificial Neural Networks." *Journal of Drug Delivery Science and Technology* 60(July):102025. doi: 10.1016/j.jddst.2020.102025.
- Yusuf, Abubakar A., Bashir Lawal, Asmau N. Abubakar, Eustace B. Berinyuy, Yemisi O. Omonije, Sheriff I. Umar, Mohammed N. Shebe, and Yusuf M. Alhaji. 2018. "In-Vitro Antioxidants, Antimicrobial and Toxicological Evaluation of Nigerian Zingiber Officinale." *Clinical Phytoscience* 4(1):2–9. doi: 10.1186/s40816-018-0070-2.
- Zakladnoy, G. F., and A. V. Yaitskikh. 2020. "Dependence of Uric Acid Content in Stored Grain on the Population Density of the Rice Weevil *Sitophilus Oryzae* (L.) (Coleoptera, Dryophthoridae)." *Entomological Review* 100(2):170–72. doi: 10.1134/S0013873820020049.

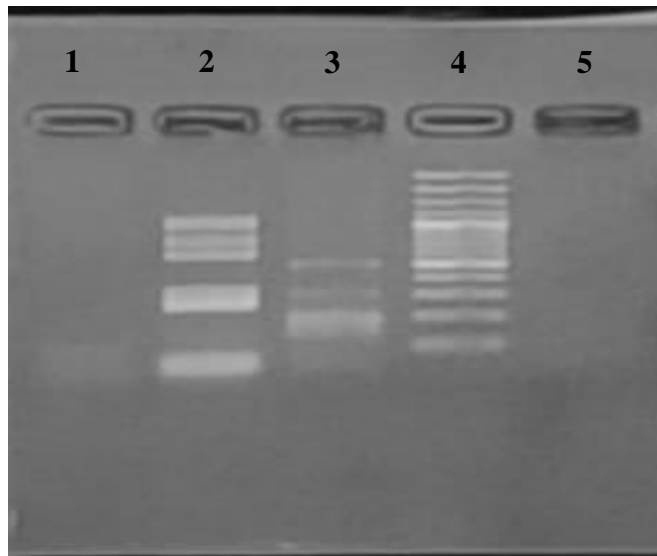
Zhang, Xin, Guoming Xie, Dan Gou, Peng Luo, Yuan Yao, and Hui Chen. 2019. "A Novel Enzyme-Free Electrochemical Biosensor for Rapid Detection of *Pseudomonas Aeruginosa* Based on High Catalytic Cu-ZrMOF and Conductive Super P." *Biosensors and Bioelectronics* 142(5):111486. doi: 10.1016/j.bios.2019.111486.

ANNEXURES

Annexure 1. Different duration of cell Lysis observed under UV exposure 1) 100 kb DNA ladder 2 and 3) two hours of incubation, 4 and 5) 1½ hours, 6 and 7) 1 hour and 8 and 9) 30 minutes shown in right side image and left side image shows the agarose gel bed.

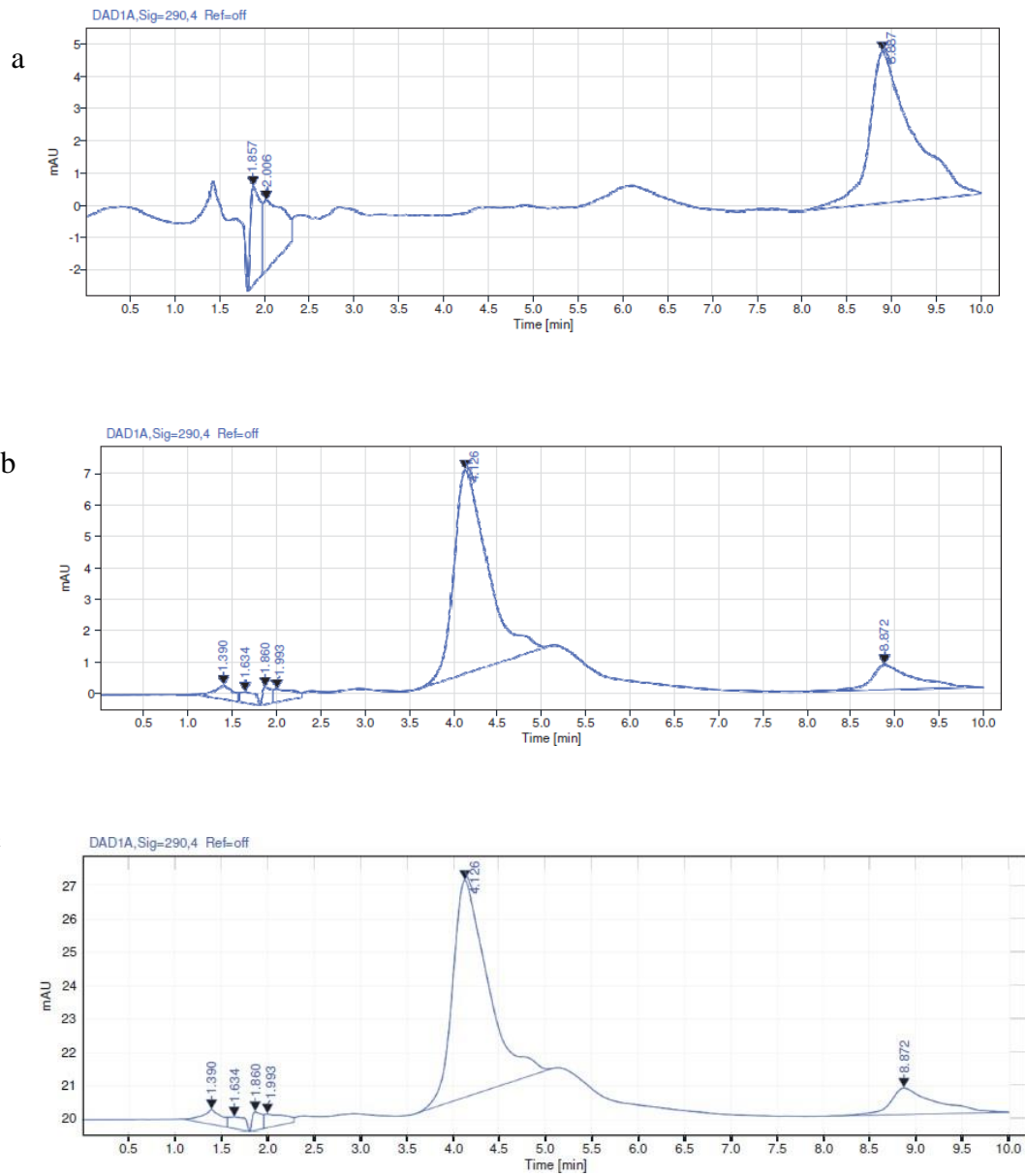


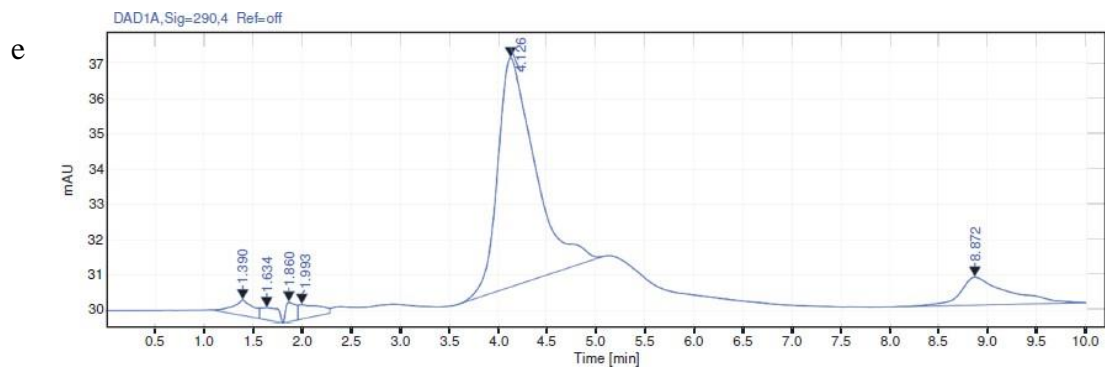
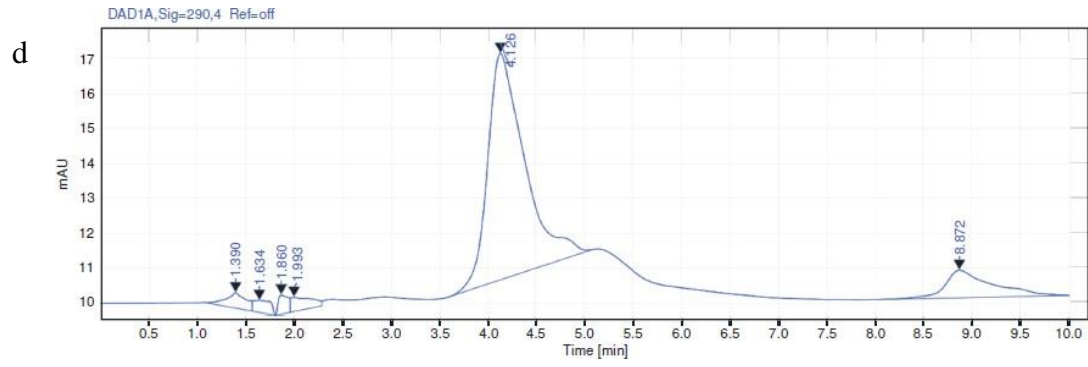
Annexure 2. Presence of ABC gene in isolated insect DNA



Lane 1: -ve control Abcg2
Lane 2: Sample (Abcg2)
Lane 3: sample (Oat3)
Lane 4: 100 bp ladder
Lane 5: -ve control of Oat3

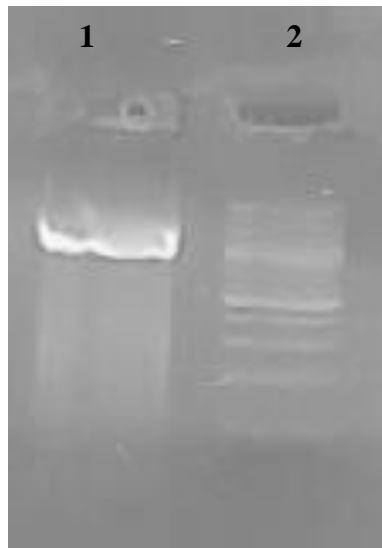
Annexure 3. HPLC analysis of spiked wheat flour samples a) control, b) 25ppm UA spiked in wheat flour, c) 50pp UA in wheat flour, d) 75ppm in wheat flour and e) 100ppm in wheat flour





Annexure 4. PCR product of bacteria (a) and fungi (b) in 2% agarose gel

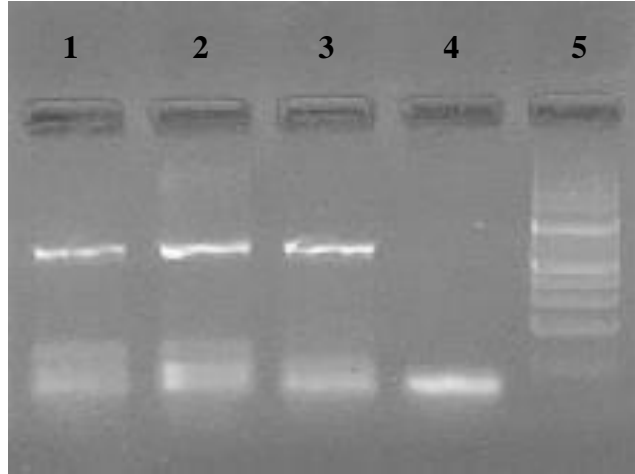
a



Lane 1: TM1
Lane 2: 100bp DNA ladder

b

Lane 1: FS1
Lane 2: FS2
Lane 3: FS3
Lane 4: -ve control
Lane 5: 100bp DNA ladder



Annexure 5. Aerobic batch culture and UA consumption

Observation (hrs)	TM1	
	600nm	720nm
3	-0.061	-0.064
6	0.018	0.031
9	0.013	0.022
12	0.005	0.008

Annexure 6. Uricase enzyme assay

Uricase enzyme assay (hrs)	TM1
24	0.034
48	0.075
72	0.021
96	0.118

PUBLICATIONS

List of published articles – Based on thesis

- Induja C, Loganathan M, Shanmugasundaram S. 2022. “Development of A Simple Rapid Method for Determination of Uric Acid Using UV-Visible Spectroscopy.” *International Journal of Life Science and Pharma Research* 12(1):200–205.
- Induja C, and Loganathan M. 2021. “Influence of Host and Duration of Storage on Uric Acid Contamination in Wheat Products Infested with Confused Flour Beetle, *Tribolium Confusum*.” 6(6):84–86.

Posters presented at National and International Conferences:

- Induja C, Durgalakshmi R and Loganathan M. 2018. “Studies on the preference and deterrence effect of food and botanicals with olfactometer” International Conference on Recent Advances in Food Processing Technology (iCRAFPT 2018) held at IIFPT, Thanjavur during August 17-19th, 2018, and Page. No: 140.
- Induja C, Durgalakshmi R and Loganathan M. 2018. “Application of silver nanoparticles as a colorimetric indicator for the detection of Chloropyrifos (Pesticide)” 8th International Food Convention held at CSIR-CFTRI, Mysuru during December 12-15th, 2018, Page.No:16
- Induja C and Loganathan M. 2019. “Spectrophotometric method to determine uric acid content in infested food commodities” National Conference on Doubling Farmers Income through Scientific Approaches held at Agricultural Engineering College and Research Institute, Kumalur, Trichy during December 20-21st, 2019, Page.No:281-282.

Proof for research articles published in journals approved by UGC

Paper 1

The screenshot shows the Web of Science Master Journal List interface. At the top, there is a navigation bar with the Web of Science Group logo, 'Master Journal List', and links for 'Search Journals', 'Match Manuscript', 'Downloads', and 'Help Center'. On the right, it says 'Welcome, Induja C' with 'Settings' and 'Log Out' options.

The main content area is titled 'INTERNATIONAL JOURNAL OF ENTOMOLOGY RESEARCH' with a 'Share This Journal' link. Below this, it lists the ISSN / eISSN as 2455-4758 and the publisher as GUPTA PUBLICATIONS, NO 169, C-11, SECTOR-3, ROHINI, DELHI, INDIA, 00000.

A 'General Information' section follows, containing a 'Return to Search Results' button on the left. The details include: 'Journal Website' with a 'Visit Site' link, 'Frequency' as 'Bi-monthly', and 'Country / Region' as 'INDIA'. The 'Issues Per Year' is listed as 6.

The 'Web of Science Coverage' section contains a table with the following data:

Collection	Index	Category	Similar Journals
Other	Biological Abstracts	Entomology	Find Similar Journals
Other	BIOSIS Previews	Entomology	Find Similar Journals
Other	Zoological Record	Entomology	Find Similar Journals



International Journal of Entomology Research

www.entomologyjournals.com

ISSN: 2455-4758

Received: 18-10-2021, Accepted: 04-11-2021, Published: 19-11-2021

Volume 6, Issue 6, 2021, Page No. 84-86

Influence of host and duration of storage on uric acid contamination in wheat products infested with confused flour beetle, *Tribolium confusum*

Induja C¹, Loganathan M²

¹ Research Scholar, National Institute of Food Technology, Entrepreneurship and Management (Formerly IIFPT), Thanjavur, Tamil Nadu, Affiliated by Bharathidasan University, Tiruchtrappalli, Tamil Nadu, India

² Professor (Entomology), Department of Academics & HRD National Institute of Food Technology, Entrepreneurship and Management (Formerly IIFPT), Thanjavur, Tamil Nadu, India

Abstract

The insect infestation in the food commodities affect the quality and reduce the quantity by direct feeding, excretion and contamination with uric acid and fragments. The insect infestation cause contamination such as uric acid and quinone that leads to unpleasant smell from the foods substances. There are different methods to detect internal and external insect infestation that occurs in food samples. A study was undertaken to find out the influence of host and duration storage on uric acid contamination in wheat products infested with confused flour beetle (*Tribolium confusum*) using a spectrophotometric method. The uric acid content in wheat flour was found to be 35.39, 49.63, 67.71 and 71.43 ppb on 7, 14, 21 and 28 days respectively. An increase in uric acid was due to increase in release by the larval stage. But the uric acid level is comparatively less in rava throughout the period when compared to maida and wheat flour which may be due to the variation in preference of food products by *T. confusum* beetle. The results revealed that the infestation in the stored food products leads to uric acid contamination and spoilage of food products in addition to weight loss.

Keywords: insect infestation, uric acid contamination and *Tribolium confusum*

Paper 2

Web of Science Group Master Journal List Search Journals Match Manuscript Downloads Help Center Welcome, Induja C [Settings](#) [Log Out](#)

General Information

Web of Science Coverage

Journal Citation Report

Peer Review Information

[Return to Search Results](#)

INTERNATIONAL JOURNAL OF LIFE SCIENCE AND PHARMA RESEARCH

[Share This Journal](#)

ISSN / eISSN 2250-0480
Publisher INT JOURNAL LIFESCIENCE & PHARMA RESEARCH, PLOT NO 10, 2 MAIN RD, RENGANAGAR NEAR TO OLD ALPHA SCH, SATHANOOR MAIN RD, TIRUCHIRAPALLI, TAMILNADU, India,

General Information

Journal Website	Visit Site	1st Year Published	2011
Frequency	Quarterly	Issues Per Year	4
Country / Region	INDIA	Primary Language	English

Web of Science Coverage

Collection	Index	Category	Similar Journals ¹
Core Collection	Emerging Sources Citation Index (ESCI)	Chemistry, Medicinal	Find Similar Journals



Development Of A Simple Rapid Method For Determination Of Uric Acid Using UV-Visible Spectroscopy

Induja C¹, Loganathan M² and Shanmugasundaram S¹

¹National Institute of Food Technology, Entrepreneurship and Management (Formerly IFFI), Thanjavur, Tamil Nadu, India
²Affiliated by Bharathidasan University, Tiruchtrappalli, Tamil Nadu, India

Abstract: Insect infestation is a major problem in the storage of food products and causes quality and quantity loss. The total weight loss of food products is about 10 per cent which occurs due to moisture loss, insect infestation, rodents, microorganism and birds during transportation and storage period. The insect infestation can be identified by detecting the presence of insect fragments, uric acid contamination, and quinone contamination. The uric acid can be determined by various instrumental methods but requires longer duration and high-tech equipment. The major objective of our study is to develop a simple rapid method to determine the uric acid content using UV-visible spectroscopy in the insect infested food materials. The rapid method is required for the food processing industries. A rapid method was developed to determine the uric acid with lesser time and accuracy. In the present study, a preceding method forms an unstable chromophore, whereas in case of a rapid method with UV-visible spectrophotometer, it was based on the formation of Prussian blue colour. The rapid method was validated with the preceding method. The R, R², standard error and Durbin-Watson test values of preceding method were 0.996, 0.991, 0.000572 and 1.103 respectively, whereas the values for rapid method were 0.997, 0.994, 0.024806 and 1.713 respectively. The results of the analysis showed that, the rapid spectrophotometric method required less time of 20 minutes for analysis, whereas the preceding method required 40 minutes. The results of the study concluded that, the new rapid method is a simple and easy method to determine the uric acid content in a lesser time. The outcome of the result will help the food processing industries to utilize this simple rapid method for testing the uric acid analysis in the food products in a lesser time.

Keywords: Uric acid, insect infestation, UV-visible spectrophotometer, rapid method, validation.



Influence of host and duration of storage on uric acid contamination in wheat products infested with confused flour beetle, *Tribolium confusum*

Induja C¹, Loganathan M^{2*}

¹ Research Scholar, National Institute of Food Technology, Entrepreneurship and Management (Formerly IIFPT), Thanjavur, Tamil Nadu, Affiliated by Bharathidasan University, Tiruchirappalli, Tamil Nadu, India

² Professor (Entomology), Department of Academics & HRD National Institute of Food Technology, Entrepreneurship and Management (Formerly IIFPT), Thanjavur, Tamil Nadu, India

Abstract

The insect infestation in the food commodities affect the quality and reduce the quantity by direct feeding, excretion and contamination with uric acid and fragments. The insect infestation cause contamination such as uric acid and quinone that leads to unpleasant smell from the foods substances. There are different methods to detect internal and external insect infestation that occurs in food samples. A study was undertaken to find out the influence of host and duration storage on uric acid contamination in wheat products infested with confused flour beetle (*Tribolium confusum*) using a spectrophotometric method. The uric acid content in wheat flour was found to be 35.39, 49.63, 67.71 and 71.43 ppb on 7, 14, 21 and 28 days respectively. An increase in uric acid was due to increase in release by the larval stage. But the uric acid level is comparatively less in rava throughout the period when compared to maida and wheat flour which may be due to the variation in preference of food products by *T. confusum* beetle. The results revealed that the infestation in the stored food products leads to uric acid contamination and spoilage of food products in addition to weight loss.

Keywords: insect infestation, uric acid contamination and *Tribolium confusum*

Introduction

The major food source for humans and domesticated animals over worldwide are cereals, oilseeds and legumes. The food commodities have to be stored for a shorter and longer period depends on the requirement and condition of the product. There are possibilities of quality and quantity deterioration of food material during storage by biotic and abiotic factors. The damage of food grains occurs due to the insects, mites, rodents, birds and microorganisms (Vimala Bharathi *et al.* 2017). The primary quality consideration of food products is insect infestation by various insect species. A severe loss may happen to processors by the contamination of food product with the presence of live insects, webbing, protective secretions, feces, cast skins (Indumathi *et al.* 2021) [4]. There are possibilities of reduction in profitable value of food products and returns of product occurs due to the presence of live insects that reduces the consumer confidence because of insect infestation (Johnson, 2013) [5]. The presence of insects has to be identified in the early stage to safeguard the food materials. There are physical and chemical methods to determine the insect infestation in stored food grains. The hidden infestation can be detected by X-ray imaging, specific gravity, insect fragment count, staining techniques, NMR and NIR techniques. The external infestation can be detected by acoustic methods, visual inspection, sampling and sieving, grain probes, insect traps and heat extraction methods (Thanushree *et al.*, 2018).

The odor detection techniques are used to detect insect infestation during the storage of food material by way of identifying volatile compounds released by the insects (Olsson *et al.*, 2002) [11]. The compounds at lower

concentration have to be extracted by distillation and headspace techniques and can be detected by using GC-mass spectroscopy. The E-nose can also be used to detect the insect infestation. A collection of chemical arrays containing in e-nose is used to detect odor compounds from the infested samples (Paollesse *et al.*, 2006) [12].

Kumari *et al.*, (2011) [6] reported that insect produce quinone, uric acid, inoculate bacteria and fungi, also leaves fecal materials and cast off skin that give unpleasant odour. The *T. castaneum* secretes uric acid and it leads to spoil the food materials and it also causes carcinogens (Mehmood *et al.* 2018) [8]. The major insect infesting in food processing facilities, mostly rice and wheat mill is confused flour beetle, *T. confusum*. The infestation leads to contamination in food products due to uric acid, quinone, and fragments of insects. The larva and adult stages of *T. confusum* causes damage to the processed food products. The uric acid can serve as a good index of infestation and unhygienic conditions in infested food grains (Randy *et al.*, 1984). The contamination of uric acid depends on the level of infestation, host / food material and also duration of storage of food material. Hence, a study was undertaken to find out the influence of host and duration storage on uric acid contamination in wheat products infested with confused flour beetle (*T. confusum*) using a spectrophotometric method.

Materials and Methods

Insect culture

The confused flour beetle, *T. confusum* was cultured in the glass container with wheat flour as food. The freshly emerged adults of *T. confusum* (50 numbers) were collected

from the stock culture, released in the glass container containing 300g of wheat flour and covered with the muslin cloth. It was kept at ambient temperature ($34\pm 2^{\circ}\text{C}$) for the egg laying. The adults were removed after 24 hrs of egg laying. The eggs grown into larvae, pupae and emerged as uniform aged adults for further studies (Negi *et al.*, 2021) [9].

Infestation of food matrices

The freshly emerged adults of *T. confusum* were separated from culture and released 20 adults each in seven glass containers containing the wheat flour, maida, and rava for infestation and covered with the muslin cloth. The infested food materials were kept at ambient temperature ($34\pm 2^{\circ}\text{C}$) for four weeks. The samples of infested wheat flour, maida, and rava were subjected to extraction of uric acid every week and the quantity of uric acid was estimated (Negi *et al.*, 2021) [9].

Extraction of Uric acid

One gram of infested product (wheat flour, rava, maida) with 7mL of sodium borate was taken in centrifuge tubes, mixed well in vortex and adjusted the pH to 8.7 using 0.01NHCl. The samples were centrifuged (REMI: model: C- 30BL) at 5000rpm for 15 minutes. The supernatant was collected, filtered using Whatman No.1 filter paper and stored the filtrate in vials for further spectrophotometric analysis (Dey & Bhattacharya, 2017) [11].

Estimation of uric acid in Spectrophotometric method

One mL of extracted sample was diluted five times with distilled water in a test tube. Then one mL of potassium ferricyanide and ferric chloride each were added and kept for 5 minutes. The spectrophotometric readings were taken in a UV-visible spectrophotometer (Shimadzu; model: UV-1800) at the absorbance of 520nm (Teepoo *et al.*, 2012) [15] were represented in Fig 1.

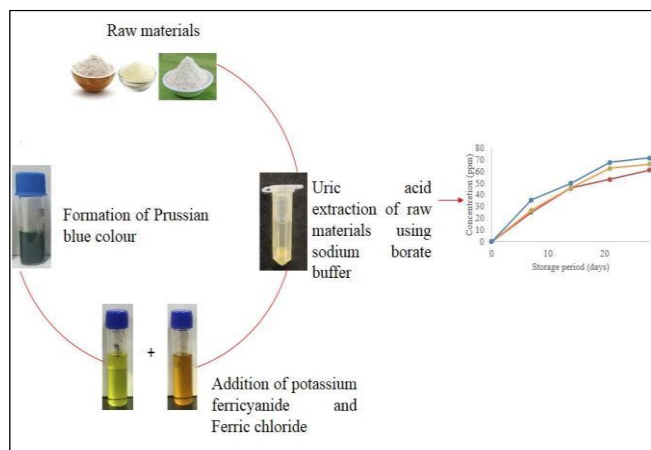


Fig 1: Flowchart for detection of uric acid contamination in food samples

Statistical analysis using Minitab software

The statistical analysis (One-way ANOVA) was carried out using Minitab® 20.4 software. In one-way ANOVA, the major factor is p-value (Tutorial *et al.*, 2015) [17]. The probability that measure the evidence against null hypothesis. The lesser probability affords null hypothesis towards the strong evidence. R² is defined as the percentage of variation in response is explained by the model. The higher R² shows the better model fit (Bower 2000) [2].

Result and Discussion

The uric acid content in insect infested wheat flour, maida, and rava were extracted and estimated using spectrophotometric method in weekly interval for 4 weeks. It was observed that the larvae contaminated the food material with uric acid ranged from 25.03 to 35.39 ppb within a week. The results showed a gradual significant increase in uric acid content in all wheat products (Table 1). The uric acid content in wheat flour was found to be 35.39, 49.63, 67.71 and 71.43 ppb on 7, 14, 21 and 28 days respectively. An increase in uric acid was due to increase in release by the larval stage as reported by Holmes, (1980) [3]. But the uric acid level was comparatively less in rava throughout the period when compared to maida and wheat flour which may be due to the variation in preference of food products by *T. confusum* beetle (Ojumoola *et al.* 2020) [10].

Table 1: Influence of storage period on uric acid content in wheat products

Storage period (days)	Uric acid concentration (ppm)*		
	Rava	Maida flour	Wheat flour
0	0.00 ^e	0.00 ^e	0.00 ^e
7	25.03 ^d	26.69 ^d	35.39 ^d
14	45.54 ^c	45.78 ^c	49.63 ^c
21	53.3 ^b	62.53 ^b	67.71 ^b
28	61.20 ^a	66.01 ^a	71.43 ^a

* Values with different letters in the same column differs significantly (p<0.05)

The uric acid content in maida flour was found to be 26.69, 45.78, 62.53 and 66.01ppb on 7, 14, 21 and 28 days respectively. The uric acid content in rava recorded lesser quantity with 25.03, 45.54, 53.31 and 61.20 ppb on 7, 14, 21 and 28 days respectively when compared to maida and wheat flour. An increase in uric acid in the wheat products may be due to increase in release rate of uric acid by late instar larvae. Similarly, the results showed that there is an increase in uric acid in all wheat products as the storage days' increases. The uric acid concentration of all wheat products still 4th weeks of storage shows significantly difference from each other (p<0.05). Pixton (1965) [13] reported that an increase in uric acid level in infested wheat flour which was related with an increase in larvae production. In their study, 32 number of adult showed an increase in uric acid content during larval stage within 14 days and also showed gradual increase in uric acid level while pupae turns into adult. The gradual increase of uric acid in the present study confirmed that increase in the release of uric acid by the late instar larvae.

The concentration of uric acid in infested rava sample increases from 0 to 61.20 ppb still 4th weeks of storage period, whereas for infested maida and wheat flour shows increase in uric acid concentration from 0 to 66.01 ppb and from 0 to 71.43 ppb till storage period of 4th weeks. Similarly Bhattacharya *et al.* (2017) [1] has reported a significant rise of uric acid in three different types of grains like sorghum, pennisetum and eleusine. The infested sorghum grains showed an increase in uric acid as well as weight loss. Stathers *et al.*(2020) [14] was reported that an increase in protein content also lead to cause contamination in maize samples with the presence of insect body parts and also immature stages of insect in the kernel and excretory wastes like uric acid. Another report showed an increase in density of infestation by rice weevil in wheat flour

correspond to the concentration of uric acid (Zakladnoy and Yaitskikh, 2020) [20]. The results of present study and earlier studies supported to conclude that the uric acid concentration increases when the storage period increases which leads to spoilage of food products in addition to weight loss.

Acknowledgements

The authors are thankful to the Indian Institute of Food Processing Technology for the facility provided for conducting the experiments.

Conflict of interest

The authors have no conflict of interest to declare.

References

- Bhattacharya Nilanjan Dey, Santanu. Nanomolar Level Detection of Uric Acid in Blood Serum and Pest-Infested Grain Samples by an Amphiphilic Probe. *Analytical Chemistry*,2017:89(19):10376-10383 doi: 10.1021/acs.analchem.7b02344.
- Bower, Keith M. Analysis of Variance (ANOVA) Using MINITAB. *Scientific Computing and Instrumentation*,2000:17(3)64-65.
- Holmes LG. Note on fluorometric method for determination of uric acid in flour, *Cereal Chem*,1980:57(5):371-372.
- Indumathi C, Manoj D, Loganathan M, Shanmugasundaram S. Impact of Radiofrequency Disinfestation on *Tribolium Castaneum* (Herbst) in Wheat Flour and Its Influence on the Functional Characteristics of Wheat Flour. *Journal of Food Processing and Preservation*,2021:45(10):1-14. doi: 10.1111/jfpp.15770.
- Johnson, J. *Pest Control in Postharvest Nuts*. Woodhead Publishing Limited, 2013, 56-87.
- Kumari, Prabha, Rekha Sivadasan, Anitha Jose. Microflora Associated with the Red Flour Beetle, *Tribolium Castaneum* (Coleoptera: Tenebrionidae). *Journal of Agricultural Technology*,2011:7(6):1625-31.
- Larsen, Torben, and Kasey M. Moyes. Fluorometric Determination of Uric Acid in Bovine Milk. *Journal of Dairy Research*,2010:77(4):438-444. doi: 10.1017/S0022029910000580.
- Mehmood, Khalid, Mureed Husain, Muhammad Aslam, Muhammad Shoaib Ahmedani, Azhar Mehmood Aulakh *et al.* Changes in the Nutritional Composition of Maize Flour Due to *Tribolium Castaneum* Infestation and Application of Carbon Dioxide to Manage This Pest. *Environmental Science and Pollution Research*,2018:25(19):18540-47. doi: 10.1007/s11356-018-2063-6.
- Negi, Aditi, Akash Pare, Loganathan Manickam, Meenatchi Rajamani. Effects of Defect Action Level of *Tribolium Castaneum* (Herbst) (Coleoptera: Tenebrionidae) Fragments on Quality of Wheat Flour. *Journal of the Science of Food and Agriculture*, 2021. doi: 10.1002/jsfa.11349.
- Ojumoola AO, Obikwe E, Oladigbolu AA, Adesiyun AA. Influence of Prior Feeding Experience and Food Deprivation on Flour Selection and Utilization by the Red Flour Beetle, *Tribolium Castaneum* (Herbst). *Agro-Science*,2020:19(2):41-47. doi: 10.4314/as.v19i2. 7.
- Olsson J, Börjesson T, Lundstedt T, Schnürer J. Detection and Quantification of Ochratoxin A and Deoxynivalenol in Barley Grains by GC-MS and Electronic Nose. *International Journal of Food Microbiology*,2002:72(3):203-14. doi: 10.1016/S0168-1605(01)00685-7.
- Paollesse, Roberto, Adriano Alimelli, Eugenio Martinelli, Corrado Di Natale, Arnaldo D'Amico, Maria Grazia D'Egidio, Gabriella Aureli, Alessandra Ricelli, and Corrado Fanelli. Detection of Fungal Contamination of Cereal Grain Samples by an Electronic Nose. *Sensors and Actuators, B:Chemical*,2006:119(2):425–30. doi: 10.1016/j.snb.2005.12.047.
- Pixton S.W. Detection of Insect Infestations in Cereals by Measurement of Uric Acid. *Cereal Chem*,1965:85(42):315-22.
- Stathers, Tanya E, Sarah EJ Arnold, Corinne J Rumney, Clare Hopson. Measuring the Nutritional Cost of Insect Infestation of Stored Maize and Cowpea. *Food Security*,2020:12(2):285-308. doi: 10.1007/s12571-019-00997-w.
- Teepoo S, Chumsaeng P, Jongjinako S, Chantu K, Nolykad W. A New Simple and Rapid Colorimetric Screening Test for Semi-Qualitative Analysis of Vitamin C in Fruit Juices Based on Prussian Blue. *Journal of Applied Sciences*,2012:12(6):568-74. doi: 10.3923/jas.2012.568.574.
- Thanushree MP, Vimala BSK, Moses JA, Anandharamakrishnan C. Detection Techniques for Insect Infestation in Stored Grains. *Agriculture Engineering Today*,2018:42(4):48-56.
- Tutorial, Minitab, Carpenter Review Source, Example Data Source, One-way Analysis, and Balanced Analysis. *Introduction to One-Way ANOVA*,2015:1:1- 18
- Vimala Bharathi SK, Vishnu Priya V, Vishnu Eswaran, Moses JA, Alice RP. Sujeetha. Insect Infestation and Losses in Stored Food Grains. *Ecology, Environment and Conservation*,2017:23(1):286-91.
- Wehling RL, Wetzel DL, Pedersen JR. Stored Wheat Insect Infestation Related to Uric Acid as Determined by Liquid Chromatography. *Journal - Association of Official Analytical Chemists*,1984:67(3):644-47. doi: 10.1093/jaoac/67.3.644.
- Zakladnoya GF, Yaitskikha AV. Dependence of Uric Acid Content in Stored Grain on the Population Density of the Rice Weevil *Sitophilus Oryzae* (L.) (Coleoptera, Dryophthoridae). *Entomological Review*. 2020:100:170-172. doi: 10.1134/S0013873820020049.



Development Of A Simple Rapid Method For Determination Of Uric Acid Using UV-Visible Spectroscopy

Induja C¹, Loganathan M²* and Shanmugasundaram S¹

¹National Institute of Food Technology, Entrepreneurship and Management (Formerly IIFPT), Thanjavur, Tamil Nadu, India

²Affiliated by Bharathidasan University, Tiruchirappalli, Tamil Nadu, India

Abstract: Insect infestation is a major problem in the storage of food products and causes quality and quantity loss. The total weight loss of food products is about 10 per cent which occurs due to moisture loss, insect infestation, rodents, microorganism and birds during transportation and storage period. The insect infestation can be identified by detecting the presence of insect fragments, uric acid contamination, and quinone contamination. The uric acid can be determined by various instrumental methods but requires longer duration and high-tech equipment. The major objective of our study is to develop a simple rapid method to determine the uric acid content using UV-visible spectroscopy in the insect infested food materials. The rapid method is required for the food processing industries. A rapid method was developed to determine the uric acid with lesser time and accuracy. In the present study, a preceding method forms an unstable chromophore, whereas in case of a rapid method with UV-visible spectrophotometer, it was based on the formation of Prussian blue colour. The rapid method was validated with the preceding method. The R, R², standard error and Durbin- Watson test values of preceding method were 0.996, 0.991, 0.000572 and 1.103 respectively, whereas the values for rapid method were 0.997, 0.994, 0.024806 and 1.713 respectively. The results of the analysis showed that, the rapid spectrophotometric method required less time of 20 minutes for analysis, whereas the preceding method required 40 minutes. The results of the study concluded that, the new rapid method is a simple and easy method to determine the uric acid content in a lesser time. The outcome of the result will help the food processing industries to utilize this simple rapid method for testing the uric acid analysis in the food products in a lesser time.

Keywords: Uric acid, insect infestation, UV-visible spectrophotometer, rapid method, validation.

*Corresponding Author

Loganathan M , National Institute of Food Technology, Entrepreneurship and Management (Formerly IIFPT), Thanjavur, Tamil Nadu, India



Received On 9 November, 2021

Revised On 13 January, 2022

Accepted On 17 January, 2022

Published On 24 January, 2022

Funding This research did not receive any specific grant from any funding agencies in the public, commercial or not for profit sectors.

Citation Induja C, , Loganathan M, And Shanmugasundaram S , Development Of A Simple Rapid Method For Determination Of Uric Acid Using UV-Visible Spectroscopy.(2022).Int. J. Life Sci. Pharma Res.12(1), L200-205
<http://dx.doi.org/10.22376/ijpbs/lpr.2022.12.1.L200-205>

This article is under the CC BY- NC-ND Licence (<https://creativecommons.org/licenses/by-nc-nd/4.0>)



Copyright @ International Journal of Life Science and Pharma Research, available at www.ijlpr.com

1. INTRODUCTION

Insect infestation is the most vital problem in the storage of grains and flours; which results in contamination of uric acid and exuviae in stored food materials. These contaminations reduces the quality of the product and its market value. The periodical monitoring of infestation will help to assess the quality of the grains and flours and to take necessary control measures. The infestation can be monitored by visual inspection, but the contamination in grains has to be detected by insect fragment counts and uric acid estimation. Most of the methods of uric acid detection were based on chemicals, enzymatic, fluorescence and biosensors.¹The important structural components of insect cuticle are chitin, but it cannot be used as a sign of infestation or contamination. The presence of fungi in stored food products may also indicate insect infestation.² But the microbial growth will occur only when the grain or flour stored with high moisture content.³ It was reported that the major end product of nitrogen metabolism in insect is uric acid and 80 percent of nitrogen from faeces was released by insects.⁴ Hence measuring uric acid with accurate and rapid method will help to follow disinfestation method in the food storage system. A colorimetric method was used to measure the uric acid content in infested food samples.⁵ A large number of food samples can be analyzed rapidly by this colorimetric method using phosphotungstic acid. The turbidity in food samples (flours and grains) can be avoided by using phosphotungstic acid. It was reported that, the method based on arsenal phosphotungstic acid gave a practically good correlation between uric acid concentration and insect number exists in the grain samples.⁴ It had been enhanced by a fusion of uricase enzyme and by use of paper chromatography. An enzyme- based colorimetric method was simpler than an enzymatic- ultraviolet method to determine uric acid in flour. This method is more susceptible and uricase enzyme action can be destroyed by adding hydrochloric acid to the sample. This procedure had not been widely used because of the time required for analysis is too long.⁶ The liquid chromatography was used to find out the uric acid content of internally infested wheat kernels by various life stages of granary weevil (*Sitophilus granarius*), rice weevil (*Sitophilus oryzae*) and lesser grain borer (*Rhyzopertha dominica*).⁷ It was reported that the correlation exists between insect population and uric acid content of infested grain by a particular stage of an internally infesting stored product insect, with correlation coefficients ranging from 0.970 to 0.998. They also found a detection limit for the analytical procedure of less than 1.0 ppm uric acid for late instar granary weevil larvae. But it is difficult to analyse a large number of samples in these methods in a shorter period. Based on the literature review for determination of uric acid in the food materials, the aim of the present study is to develop a rapid method to determine uric

acid contamination due to insect infestation in food products. The major objective of our study is to develop a simple rapid method, to determine the uric acid content using UV-visible spectroscopy in the insect infested food materials during processing, storage and validation of the developed method.

2. MATERIALS AND METHODS

A simple rapid method for uric acid determination was developed with standard uric acid at different concentrations and validated using the colorimetric method (Preceding method). It was also validated statistically.

2.1 Standard Preparation

A stock solution of uric acid was prepared by weighing 100mg of uric acid and 900mL of distilled water and made up to 1litre in volumetric flask. From the stock solution, the working standard of different concentrations (20, 40, 60, 80 and 100 ppm) was prepared in a 50mL volumetric flask and made up to volume with distilled water. The working standard was allowed to stand for 10 days.

2.2 Determination The Uric Acid With Colorimetric Analysis Of Allantoin (Preceding Method)

The different concentration of uric acid (1mL) was taken in a boiling tube and 5mL of distilled water was added and 1mL of NaOH (0.05M) in the boiling tube. It was mixed well using a vortex (DLab; MX-S60HZ) and kept in a water bath at 100°C for 7 minutes. The tubes were cooled with water and adjusted the pH to 2.16 with 0.05M HCl. Then 1 mL of phenylhydrazine hydrochloride (0.023 M) was added and mixed with vortex. The tubes were again kept in a water bath at 100°C for 7 minutes and dumped it immediately into an icy alcohol bath (40% NaOH) for 7 minutes.⁸ Then 3 mL of concentrated HCl and 1 mL of potassium ferricyanide (0.05M) were added and kept for 20 minutes. The colour developed was recorded at 522 nm in a UV-visible spectrophotometer (Shimadzu; UV-1800).

2.3 Formation Of Chromophore Based On Reaction Mechanism In Preceding Method

In the preceding method, uric acid was hydrolyzed using weak alkaline (NaOH, 0.05M) at 100°C. The hydrolysed uric acid changed into allantoinic acid by the activity of allantoinase enzyme. The allantoinic acid degrades into urea and glyoxylic acid in acid solution (HCl, 0.05M) (Fig.1).⁸ The phenyl hydrazine hydrochloride reacts with glyoxylic acid to form phenyl hydrazone. The potassium ferricyanide reacts with phenyl hydrazone to form an unstable chromophore.

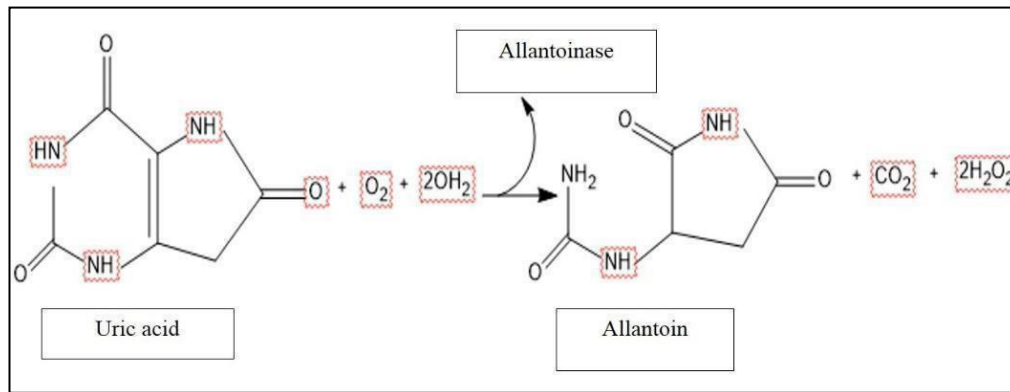


Fig.1.The oxidation reaction of uric acid to allantoin

2.4 Rapid spectrophotometric method to determine uric acid

2.4.1 Developing a simple rapid spectrophotometric method to determine uric acid

A rapid method was developed to reduce the duration of analysis and also to get accuracy. In this method, different concentrations (1mL) of uric acid was diluted five times with distilled water and then 1mL of potassium ferricyanide and ferric chloride (1mL) were added. It was mixed well and kept for 5 minutes.⁹ The spectrophotometric readings were taken in a UV-visible spectrophotometer (Shimadzu; model: UV- 1800) at the absorbance of 520 nm .

2.4.2 Formation of Prussian blue colour based on reaction mechanism (Rapid method)

The reaction mechanism of uric acid was studied for the simple rapid method to determine the uric acid content using UV-visible spectroscopy. The potassium ferricyanide reacts with the uric acid in infested samples and converts into potassium ferrocyanide (Fig.2). Ferric chloride reacts with potassium ferrocyanide to produce Prussian blue color.¹⁰ The principle of the present rapid method was based on the formation of Prussian blue. The potassium ferricyanide acts with the ferric or ferrous solution to form Prussian blue. The thermal equilibrium occurs between the two solutions and the colour intensity will increase based on the heating process at 25°C.

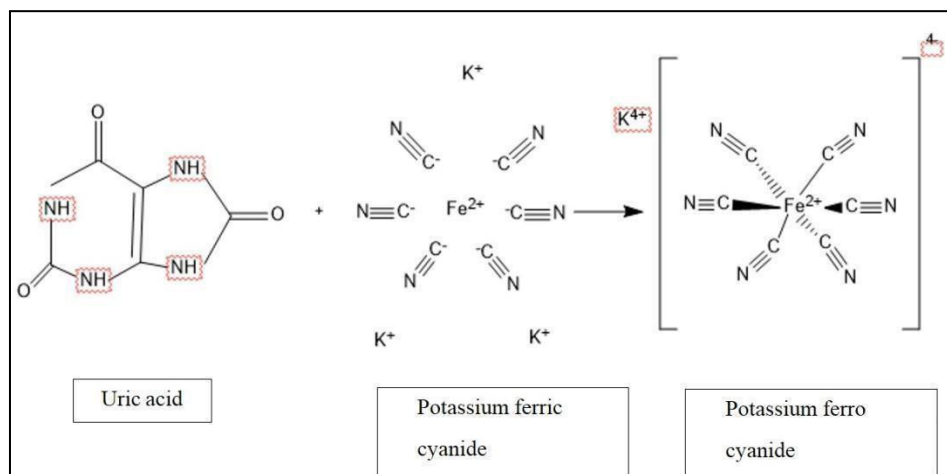


Fig.2.The mechanism of Prussian blue colour formation

2.4.3 Validation Of Rapid Method With The Preceding Method Using Regression Model

A multiple linear regression involves fitting a model for a dependent variable involving more than one independent variable, which is linear in its parameters. The model summary describes R , R^2 , Adjusted R^2 and standard error of dependent value (OD) of both the methods. The R value is considered as a measure of quality of prediction of dependent variable (OD). The R^2 ranges from 0 to 1 that represents the proportion of variation in the dependent variable that can be explained by the model explanatory variable. The R^2 represents the coefficient of correlation between dependent and independent variables in the linear regression.¹¹ The R^2 increases whereas the model is better. The adjusted R^2 is the correction for the number of x variables involved in the

the large proportion of variability in the dependent variable that has been explained by the regression model. The adjusted R^2 number which is nearer to 0 indicates that it did not show much variations in the dependent variable. The Durbin- Watson (DW) test is used to test the hypothesis with autocorrelation. If the DW value lies from 0 to 2, it indicates positive autocorrelation. The standard error (SE) represents the average distance that the observed values fall in the regression line. The smaller value of SE indicates that the observation is closer to the fitted line.¹² In case both preceding and rapid methods can be evaluated based on parameters of the regression model.

3. STATISTICAL ANALYSIS

The data obtained were analyzed using XLSTAT software

predictive model. The adjusted R is close to 1 that indicates

(Version 2021.2.2.1137). A multiple linear regression model was used to compare the both methods to determine uric acid level based on goodness of fit. The probability value less than 0.05 was assumed in ANOVA.¹³

4. RESULTS AND DISCUSSION

The determination of uric acid in a shorter time is important for analyzing large numbers of food samples. In the present study, a rapid UV-spectrophotometric method was developed to reduce the determination time with more accuracy and validated with the calorimetric method.

4.1 Efficiency of uric acid determination methods

A study using the nanostructured sensor, based on gold nanoparticles and nafion for uric acid determination found that the accuracy and reliability of results have good correlation with the enzymatic spectrophotometric analysis ($R^2 = 0.9938$).^{14,15} Earlier reports on rapid determination of uric acid using electrochemically activated glassy carbon electrode showed a linear range from 0.04 to $2\mu\text{M}$ with slope of 55.6 A M^{-1} , R^2 of 0.99 and limit of detection of 9 nM.¹⁶⁻¹⁸ In the present study, the correlation coefficient (R^2) of the rapid method using UV-visible spectrophotometer showed 0.994 (Fig.4) and preceding method showed 0.991 (Fig.5) which showed the similar accuracy of both the methods. Earlier, the sensors for detecting infestation were used and found that hybrid adapted Neuro-Fuzzy Inference System models (ANFIS) were the best fit to optimize the sensor array detecting infestation and to predict the number of insects ($R = 0.999$) and uric acid ($R = 0.985$).¹⁹ A pyrene based amphiphilic receptor was utilized in the nanomolar detection of uric acid content of the aqueous extracts of infested stored grain samples which was used to measure the uric acid at physiological pH in water.²⁰ A fast method to determine uric

acid in milk samples with R^2 value of 0.98 and p value of less than 0.001 was reported.²¹ The results of the present study showed that the rapid UV-spectrophotometric method required lesser time of 20 minutes for analysis whereas the preceding method required 40 minutes which explained that the new method required only half of the time to determine uric acid compared to the preceding method. The results revealed that the simple rapid UV-spectrophotometric method is having good accuracy and correlation coefficient with lesser time for determination of uric acid in food samples.

4.2 Validation of rapid method and preceding method using regression model

4.2.1 Comparison of linear regression for preceding and rapid method

The linear regression is normally used for the comparison of analytical methods. It was reported that aromatic characteristics of 2-cyano-N-(3-cyano-7-tetrahydrobenzo[b]thiophen-2-yl)-acetamide using multiple linear regression models showed an R value of 0.754. Whereas in present research work, the model outline of linear regression describes about the R value of 0.996 and 0.997 for preceding and rapid method respectively which showed the R value of both methods indicates good sign of prediction in regression model.²² The purine derivatives against c-Src tyrosine kinase showed best fit with R^2 of 0.802 was explained by earlier workers.²³ Similarly, the present study showed the R^2 of 0.991 and 0.994 for preceding and rapid method respectively (Fig 3 and 4). These results revealed that the R^2 value of 0.994 is more accurate and the rapid method is more fit in the regression model. The adjusted R^2 of 0.990 and 0.994 were found for preceding and rapid method respectively.

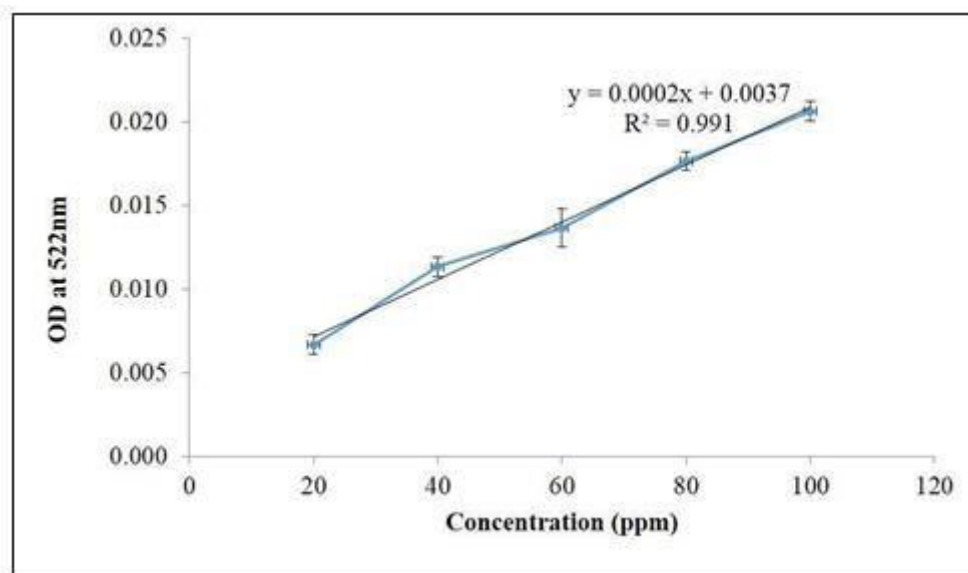


Fig.3. Calibration curve of the preceding method

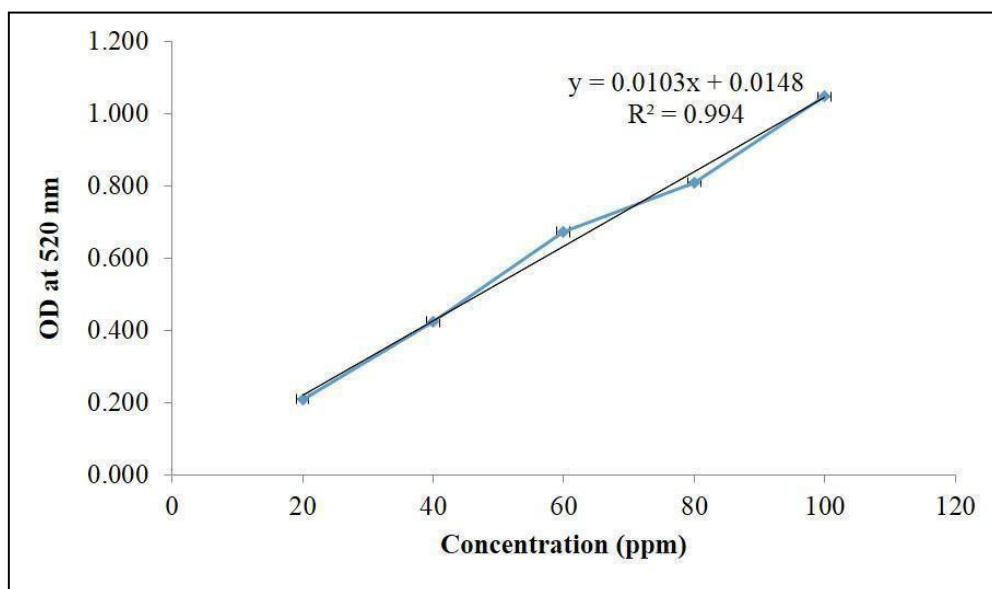


Fig.4. Calibration curve of the rapid method

The SE of model fit is a measure of precision. The SE of preceding and rapid method are 0.000572 and 0.024806 which are less than 2 as reported earlier.²⁴ The DW test

indicated the autocorrelation of preceding and rapid method were 1.103 and 1.713 respectively which are less than 2 (Table 1).

Table 1. Validation of preceding and rapid method		
Parameters	Preceding method	Rapid method*
R	0.996	0.997
R ²	0.991	0.997
Adjusted R ²	0.990	0.994
SE of the estimate	0.000572	0.024806
DW test	1.103	1.713
Time required per sample (min)	40	20

*Rapid method showed good fit with lesser time for each sample

The accuracy of the methods were predicted using multiple linear regression model with R, R² and SE in the present study (Table 1) which is similar to that the prediction of imidazo[1,2-a]pyrazine derivatives against cancer cell lines Log HepG-2 using multiple linear regression model with the terms of R, R², SE value.^{25,26} The results of the present study support the earlier report of uric acid detection can be used as an index of insect infestation.²⁷ It also demonstrated a positive linear correlation between the amount of uric acid and the density of rice weevil, *S. oryzae* in wheat grain.^{28,29}

5. CONCLUSION

The preceding method is used to detect the uric acid indirectly by converting the uric acid to allantoin. The uric acid was treated with a weak alkaline solution to convert uric acid to allantoic acid by the activity of allantoinase enzyme. The extraction procedure and colorimetric analysis also required more time (40 minutes) for each sample. But the rapid method is a direct method to determine the uric acid by the formation of Prussian blue colour. This method required less time (20 minutes) compared with the preceding method. The rapid method and preceding method were accurate whereas the R² of rapid method is 0.997 showed good fit compared with the preceding method. The results concluded that, the rapid

method is a simple and easy method to determine the uric acid content in a lesser time. The method can be very useful for the food processing industries to monitor the infestation of raw materials and food products.

6. ACKNOWLEDGEMENTS

The authors are thankful to the National Institute of Food Technology, Entrepreneurship and Management-Thanjavur (NIFTEM-T) for the facility provided for conducting the experiments.

7. AUTHORS CONTRIBUTION STATEMENT

Induja, C did this research work under the guidance of Dr. M. Loganathan. Dr. Shanmugasundaram S helped in analysis and drafting of the paper. All the authors read and approved the final version of the manuscript.

8. CONFLICT OF INTEREST

Conflict of interest declared none.

9. REFERENCES

- Lamkin WM, Unruh NC and Pomeranz Y. Use of fluorometry for the determination of uric acid in grain. Elimination of interfering fluorescence. *Cereal Chem.* 1991;68(1):81-86.
- Hackman RH and Goldberg M. A method for determinations of microgram amounts of chitin in arthropod cuticles. *Anal Biochem.* 1981; 110(2):277-280.
- Mirocha CJ and Donald WW. Chitin as a Measure of Fungal Growth in Stored Corn and Soybean Seed. *Cereal Chem.* 1977; 54:466-474.
- VenkatRao S and Nuggehalli RN, Pingale SV, Swaminathan M and Subrahmanyam V. The relation between the uric acid content and the extent of kernel damage in insect-infested grain. *Food Sci.* 1957 ;(6):273.
- Franke E and Benedict S. A method for the direct determination of uric acid in urine. *JBiolChem.* 1922; 52:387-391.
- Gin Farn and Smith DM. Rate of Excretion of Uric Acid by the Rust-Red Flour Beetle. *J AOAC Int.* 1963; 46(3):517-521.
- Wehling RL, Wetzel DL and Pedersen JR. Stored wheat insect infestation related to uric acid as determined by liquid chromatography. *J Assoc off Anal Chem.* 1984; 67(3):644-647.
- Young EG and Conway CF. On the estimation of allantoin by the Rimini-Schryver's reaction. *J Biol Chem.* 1942; 114:243-248.
- Teepoo S, Chumsaeng P, Jongjinakool S, Chantukand Nolykad W. A New Simple and Rapid Colorimetric Screening Test for Semi-qualitative Analysis of Vitamin C in Fruit Juices Based on Prussian blue. *J Appl Sci.* 2012; 12(6):568-574.
- Izatt RM, Watt GD, Bartholomew CH and Christensen JJ. A Calorimetric Study of Prussian Blue and Turnbull's Blue Formation. *Inorg Chem.* 1970; 9(9):2019-2021.
- Dhakal CP. Interpreting the Basic Outputs (SPSS) of Multiple Linear Regression. 2019 ;(January 2018); 8(6):1448-1452.
- Stellefson ML, Hanik BW, Chaney BH, Chaney JD. A Tutorial on Calculating and Interpreting Regression Coefficients in Health Behavior Research. 2008; 40(1):12-20.
- Dhakal CP. Multiple Regression Model Fitted for Rice Production Forecasting in Nepal: A Case of Time Series Data. 2018; 2:89-98.
- Natalia Stozhko, Maria Bukharinova, Leonid Galperin and KheinaBrainina. A nanostructured sensor based on gold nanoparticles and nafion for determination of uric acid. *Biosensors.* 2018; 8(21):1-13.
- Kudo H, Takagi Y. Electrochemical biosensor for simplified determination of salivary uric acid. *Sensors Mater.* 2018; 30(5):1187-95.
- Shi K, Shiu KK. Determination of uric acid at electrochemically activated glassy carbon electrode. *Electroanalysis.* 2001; 13(16):1319-1325.
- Inoue K, Namiki T, Iwasaki Y, Yoshimura Y, Nakazawa H. Determination of uric acid in human saliva by high-performance liquid chromatography with amperometric electrochemical detection. *J Chromatogr B Anal Technol Biomed Life Sci.* 2003; 785(1):57-63.
- Fujita K, Yamada H, Iijima M, Ichida K. Electrochemical analysis of uric acid excretion to the intestinal lumen: Effect of serum uric acid-lowering drugs and 5/6 nephrectomy on intestinal uric acid levels. *PLoS One.* 2019; 14(12):1-11.
- Gayatri M, Shubhangi S, Panda BK and Mishra HN. Sensor array optimization and determination of *Rhyzopertha Dominica* infestation in wheat using hybrid neuro-fuzzy-assisted electronic nose analysis. *Anal Methods.* 2018; 10(47):5687-5695.
- Dey N, Bhattacharya S. Nanomolar Level Detection of Uric Acid in Blood Serum and Pest-Infested Grain Samples by an Amphiphilic Probe. *Anal Chem.* 2017; 89(19):10376-83.
- Larsen T, Moyes KM. Fluorometric determination of uric acid in bovine milk. *J Dairy Res.* 2010;77(4):438-444.
- El-chokrafi FZ, Khalil F, Bouachrine M. QSAR studies of the antiproliferative activity of heterocyclic derivatives using topological descriptors. 2017; 4:590-9.
- Elbahi S, Koubi Y, Boutalaka M, Hajji H. Rhazes : Green and Applied Chemistry The c-Src kinase inhibitors: 2D-QSAR study by Multiple Linear Regression method. 2021; 13:29-42.
- Wuttichaikitcharoen P, Babel MS. Principal Component and Multiple Regression Analyses for the Estimation of Suspended Sediment Yield in Ungauged Basins of Northern Thailand. 2014; 6(8):2412-2435.
- El Masaoudy Y, Aanouz I, Moukhliiss Y, Koubi Y, Maghat H, Lakhlifi T, Bouachrine M. 2D-QSAR study of the antimicrobial activity of a series of 5- (substituted benzaldehyde) thiazolidine-2, 4-dione derivatives against *Staphylococcus aureus* by Multiple Linear Regression method. 2020; 11(11):1914-27.
- Chtita S, Ghamali M, Larif M, Adad A, Rachid H, Bouachrine M, Lakhlifi T. Prediction of biological activity of imidazo[1,2-a]pyrazine derivatives by combining DFT and QSAR results. *Int J Innov Res SciEngTechnol (An ISO Certif Organ [Internet].* 2007; 2(12):7951-62.
- Rajendran.S S. Detection of Insect Infestation in Stored Foods. *Adv Food Nutr Res.* 2005; 49(4):163- 232.
- Zakladnoy GF, Yaitskikh A V. Dependence of Uric Acid Content in Stored Grain on the Population Density of the Rice Weevil, *Sitophilus oryzae* (L.) (Coleoptera, Dryophthoridae). *Entomol Rev.* 2020; 100(2):170-172.
- Induja C, Loganathan M. Influence of host and duration of storage on uric acid contamination in wheatproducts infested with confused flour beetle, *Triboliumconfusum*. *International Journal of Entomology research,* 2021; 6(6):84-86.